ASIAC
Flight Dynamics Directorate
Aerospace Structures Information and Analysis Center
Operated by CSA Engineering, Inc.

TR-91-5

Air Force Office of Scientific Research

PANEL DISCUSSION

ON

ORIGIN OF IMPERFECTIONS

1 November 1991
Holiday Inn, Dayton Ohio

Approved for public release; distribution unlimited

REPORT DOCUMENTATION PAGE

Form Approved
OMB No. 0704-0188

1. AGENCY USE ONLY *(Leave blank)*

2. REPORT DATE
1 November 1991

3. REPORT TYPE AND DATES COVERED

4. TITLE AND SUBTITLE
Panel Discussion on Origin of Imperfections

5. FUNDING NUMBERS

6. AUTHOR(S)
George Sendeckyj
Spencer Wu

7. PERFORMING ORGANIZATION NAME(S) AND ADDRESS(ES)
Air Force Office of Scientific Research
Building 410
Bolling AFB, DC 20332-6448

8. PERFORMING ORGANIZATION REPORT NUMBER
ASIAC-TR-91-5

9. SPONSORING/MONITORING AGENCY NAME(S) AND ADDRESS(ES)
Air Force Office of Scientific Research
Building 410
Bolling AFB, DC. 20332-6448

10. SPONSORING/MONITORING AGENCY REPORT NUMBER

11. SUPPLEMENTARY NOTES

12a. DISTRIBUTION/AVAILABILITY STATEMENT
Approved for Public Release: Distribution Unlimited

12b. DISTRIBUTION CODE

13. ABSTRACT *(Maximum 200 words)*

This report is a summary of a panel discussion on Origin of Imperfections, and the presentations that were included. This meeting was sponsored by AFOSR and was held at Wright-Patterson AFB, Ohio on 9 October 1991.

The panel discussion had two major objectives. The first objective was to present current research activities under the AFOSR Initiative on the "Origin of Imperfections." The second objective was to obtain a consensus on science issues in this critical research area and to identify topics for future research efforts.

14. SUBJECT TERMS
Acoustic Microscopy, Imperfections, Acoustic, Emission, Non-destructive Evaluation, NDE, Defects, Failure, Materials, Composites, Microplasticity, Micro-Fracture, Micro-cracks, Damage Accumulation

15. NUMBER OF PAGES
134

16. PRICE CODE

17. SECURITY CLASSIFICATION OF REPORT	18. SECURITY CLASSIFICATION OF THIS PAGE	19. SECURITY CLASSIFICATION OF ABSTRACT	20. LIMITATION OF ABSTRACT
Unclassified	Unclassified	Unclassified	Unlimited

NSN 7540-01-280-5500

Standard Form 298 (Rev. 2-89)
Prescribed by ANSI Std. Z39-18
298-102

FOREWORD

The Air Force Office of Scientific Research (AFOSR) sponsored two contractor meetings on the "Mechanics of Materials" and "Structural Dynamics" at the Holiday Inn in Fairborn, Ohio during the week of 7 October 1991. The meetings were hosted by Mr. Robert M. Bader, Chief of the Structures Division, Flight Dynamics Directorate, Wright Laboratory at Wright-Patterson Air Force Base. The technical sessions were organized and coordinated by Dr. Spencer Wu, AFOSR Program Manager for Aerospace Sciences. A panel discussion on the Origin of Imperfections was conducted in conjunction with these meetings on Wednesday, 9 October. This panel session was chaired by Dr. George Sendeckyj, of the Structural Integrity Branch of the Structures Division.

This report includes a summary of the panel discussion and the six technical presentations that were part of the program.

The administrative arrangements for the AFOSR meetings and panel discussions were conducted by the Aerospace Structures Information and Analysis Center (ASIAC), which is operated for the Flight Dynamics Directorate, Wright Laboratory by CSA Engineering, Inc. The efforts of Mr. Gordon R. Negaard, ASIAC Technical Manager, and all the ASIAC staff for coordinating and arranging the meeting details are greatly acknowledged.

TABLE OF CONTENTS

Section — Page

I Panel Discussion Summary - Dr. George Sendeckyj, Wright- Laboratory 1

1. Introduction 2

2. Summary of Formal Presentations 3

2.1 Introductory Comments by Sprncer Wu, AFOSR/NA 3
2.2 "The Microscopic Origin of Inelastic Behavior" 3
2.3 "Quantitative Non-Destructive Evaluation of Fatigue- Induced Surface Damage by Line-Focus" 3
2.4 "Origins of Imperfections in Composites" 5
2.5 "Examination of Precursors to Fracture" 5
2.6 "Hysteresis and Incremental Collapse of Structures, A Paradigm for the Strength of Metals" 6

3. Summary of General Discussion 7
4. Conclusion 10

II Technical Presentations: 11

Dr. Spencer T. Wu, AFOSR 12

Prof. J. D. Achenbach, Northwestern 17

Prof. D. E. Chimenti, John Hopkins University 33

Prof. J. T. Dickinson, Washington State University 46

Prof. S. A. Guralnick, IIT 78

Dr. Harold Weinstock, Bolling AFOSR 125

SECTION I

ORIGIN OF IMPERFECTIONS PANEL

DISCUSSION SUMMARY

Dr. George P. Sendeckyj
Aerospace Research Scientist

Fatigue, Fracture & Reliability Group
Structural Integrity Branch
Structures Division
Flight Dynamics Directorate
Wright Laboratory
United States Air Force
Wright-Patterson Air Force Base, Ohio

1. INTRODUCTION

A panel discussion on the "Origin of Imperfections" was held in Dayton OH on 9 October 1991 as part of the Air Force Office of Scientific Research (AFOSR) Contractors Review. The discussion consisted of brief introductory remarks by Dr Spencer Wu, AFOSR/NA, five (5) formal presentations by panel members, and a general discussion on the origin of imperfections. The presentation material is reproduced in the Appendix, with some minor editing to correct obvious typographical errors.

To put the panel discussion in proper perspective, it is necessary to define what is meant by an imperfection. With this in mind, an imperfection is defined as a shortcoming, defect, fault or blemish that has a detrimental effect on the performance of a structural material system for a particular application. Imperfections can occur on different scales in structural materials. At the macro or structural scale, the nature of imperfections in materials is well understood and their effect on structural performance can be predicted with a high degree of accuracy. Our understanding of the nature of imperfections and their consequences on structural performance is relatively poor at the mini- and micro-scales, and almost non-existent at the nano-scale.

The Aerospace Sciences Directorate of the Air Force Office of Scientific Research has a small research initiative to develop a fundamental understanding of the origin of imperfections. The objectives of the initiative are to develop experimental tools for observing the origin of imperfections at the micro- and nano-scale and their evolution to the macro-scale in structural materials, and to formulate theoretical models of the damage evolution process.

The panel discussion had two major objectives. The first objective was to present current research results obtained under the AFOSR Initiative on the "Origin of Imperfections." The second objective was to obtain a consensus on science issues in this critical research area and to identify topics for future research activities.

2. SUMMARY OF FORMAL PRESENTATIONS

2.1 Introductory Comments by Dr Spencer Wu, AFOSR/NA.

Dr Spencer Wu, AFOSR/NA, opened the panel discussion with a short introductory presentation. He introduced the panel members, indicated the objectives and funding level of the AFOSR Initiative on the Origin of Imperfections and stated the objectives to be achieved during the panel discussion.

2.2 "The Microscopic Origin of Inelastic Behavior" by Dr Harold Weinstock, AFOSR/NE

Dr Weinstock presented some research results on the use of the Barkhausen effect to study the onset of hysteresis and changes in surface residual compressive stresses in ferromagnetic materials. He became interested in this area when he saw some results on the Kaiser effect in acoustic emission monitoring. He decided to determine whether the Kaiser effect also occurs in the magnetic field induced in ferromagnetic materials under mechanical loading. He performed some experiments and observed that induced magnetization undergoes a jump at approximately 60% of elastic limit strain. This jump has been interpreted as an indication of the occurrence micro-plasticity, which can be interpreted as the onset of hysteresis. He is pursuing further research in this area. A practical application of the Barkhausen effect is in inspection of surface hardened steel structures, which rely on residual compressive surface stresses to achieve required performance.

2.3 "Quantitative Non-Destructive Evaluation of Fatigue-Induced Surface Damage by Line-Focus Acoustic Microscopy" by J. D. Achenbach, M. E. Fine, J. O. Kim and S. M. McGuire, Northwestern University

Dr Achenbach presented results of an experimental investigation of surface micro-cracking in SiC whisker reinforced aluminum alloys using scanning acoustic microscopy. He indicated that Dr Fine, one of his colleagues, had performed some tedious experiments on the evolution of surface micro-cracking in SiC whisker reinforced aluminum alloys. He presented some of those result on the surface crack length distributions as a

function of number of fatigue cycles for whisker reinforced aluminum composites by way of an introduction of their current research on the application of line-focus acoustic microscopy to damage detection and quantification. He described the operation of the scanning acoustic microscope and discussed how data on the state of near surface imperfections are generated. He presented some results on the variation of surface wave speed with anisotropy and number of fatigue cycles. He indicated that the missing link is the correlation of surface wave speed data with the actual damage state. He believes that this correlation can only be obtained by analyzing wave propagation in a half-space with a random distribution of surface cracks. He and his colleagues are working this problem.

2.4 "Origins of Imperfections in Composites" by D. E. Chimenti, Johns Hopkins University

Dr Chimenti discussed the application of scanning electron thermal microscopy (SETM) to the detection of imperfections in composite materials. The SETM process consists of inducing thermal waves in a sample inside a scanning electron microscope (SEM). The thermal waves are due to localized periodic heating of the surface and they can be used to image subsurface features. The SETM has high spatial resolution that is limited by the elastic wave length. He also described their acoustic microscope. Finally, he presented the goals of the funded research work.

2.5 "Examination of Precursors to Fracture" by J. T. Dickinson, Washington State University

Dr Dickenson discussed his research on the examination of precursors to fracture. By way of a general introduction, he made some general comments on the failure process and sources of pre-existing and grown-in defects. He also discussed some work on the simulation of the damage evolution process. After the introductory comments, he described his research work on fracto-emission during the failure process. He presented results on the emission of argon during tensile fracture of argon sorbed polystyrene. The results indicate that argon emission correlates with craze volume evolution during the fracture process. He also presented results on electron emission during fracture of polycarbonate, alkali emission from NaCl, and O_2 emission during microcracking in single crystal MgO. The results indicate that there are many different precursors to failure that have not been fully exploited by the research community. Dr Dickinson concluded his presentation with the following list of research issues:

a. Detection and characterization of defects
b. Description and kinetics of evolution of damage
c. Materials design to control degradation
d. Statistical physics concepts (fractals, self-organized criticality, scaling phenomena)
e. Experimental advances

i. sensitivity to differences (i.e., perfect versus flawed, defects as a function of time)

ii. surface versus interior phenomena

iii. probes in hostile environments (temperature, atmoshere/chemical, radiation)

f. Modeling efforts (global, atomic, etc.)

2.6 "Hysteresis and Incremental Collapse of Structures, A Paradigm for the Fatigue Strength of Metals" by S. A. Guralnick and T. Erber, Illinois Institute of Technology

Dr Guralnick presented results of a research program with the objectives to (a) correlate fatigue and hysteresis by recognizing the processes which begin with micro-imperfections, progress through macro-imperfections and culminate in fatigue rupture and (b) correlate acoustic emission phenomena with the inception of the damage growth process which ultimately results in fatigue rupture. He began the presentation discussing possible defects in metal crystals and polycrystals, and possible micromechanical responses of metals to cyclically-varying loads. He then presented various experimental evidence to support the concept that microplasticity is a precursor to fatigue crack initiation, and outlined two scenarios for the progression of the fatigue process. His model of the fatigue processes consists of the following steps:

a. Inception of microplasticity
b. Cooperative organization of zones of microplasticity
c. Damage growth and accumulation leading to micro-fracture
d. Macro-crack initiation
e. Crack propagation and organization leading to rupture of the material.

Dr Guralnick outlined a number of diagnostic techniques for studying the damage evolution process in metals. In addition to those discussed by the previous speakers, he mentioned acoustic emission monitoring as a viable damage documentation technique. He also presented some acoustic emission results for aluminum. Finally, he indicated directions for future research that he plans to pursue.

3. SUMMARY OF GENERAL DISCUSSION

The formal presentations described a number of experimental tools for observing microscopic imperfections in materials and their evolution into macroscopic defects that lead to structural failure. The experimental tools addressed by the presenters include acoustic emission monitoring, acoustic microscopy, scanning electron thermal microscopy, fracto-emission monitoring, and magnetic effect monitoring. They permit the observation of surface or near surface imperfections and their evolution. Since x-ray techniques can easily image interior defects in solids, Dr. T. Moran of the Materials Directorate of the Wright Laboratory was asked to briefly indicate the capabilities of their micro-focus computer-aided tomography (CAT) scanner. He indicated that their unit has the capability to image defects and imperfections with dimensions on the order of 250 micro-meters. The CAT scanner has another unique capability in that it can be used to experimentally determine internal strain distributions in materials with texture. By imaging the texture in the material under different loads and superimposing the images, interference patterns related to relative displacement are formed. The patterns can be analyzed to determine strain distributions. Dr Moran indicated that their CAT scanner does not possess the required resolution for this purpose, but other CAT scanners with the required resolution are available within the research community.

After the comments on the CAT scanner, the discussion was opened for general comments and questions from the audience. Dr Chimenti was asked how severe the localized heating could get in the SETM. He indicated that local temperatures can be very high (on the order of thousands of degrees Centigrade). This led to a discussion of how to determine that the SETM gives a true indication of the local subsurface features. A procedure for establishing the electron beam modulation parameters was suggested. This indicated a set of experiments that should be performed in the SETM.

The discussion then turned to where the new experimental tools were leading the research community and whether the study of the origin of imperfections was necessary. It was pointed out that new research tools for documenting imperfections and their evolution have better resolution than previously available tools and that the resolution continues to be improved. The question was asked when this will stop. By way of a response, the analogy

between the development of medical and materials diagnostic tools was made. In the early days of medicine, section of cadavers was used to infer information about the human body. The counterpart of this is the use of sectioning to study damage in composite materials, which is tedious. Then the stethoscope was developed as means of diagnosing living organisms. The conventional ultrasonic techniques are the counterpart of the stethoscope. They provide much useful information on the nature of the damage evolution process in composite materials, but at present do not have the required resolution to guide the formulation of models of the damage evolution process at the lamina level. The x-ray techniques, including CAT scanning, were developed for the medical profession to provide improve diagnostic information. They were adapted to damage documentation in composite materials. As a result, physically realistic models of the damage accumulation process are being developed. These models are sufficiently accurate for engineering simulation of the damage accumulation process in composite materials, but they do not provide adequate information on the imperfections that lead to the damage observed by the x-ray techniques. Thus, better research tools are required to identify the imperfections that lead to the damage. Such tools are the acoustic microscope, the scanning electron thermal microscope, and fracto-emission monitoring. Whether these research tools are adequate to determine the origins of imperfections is not clear at present, but their use is a step in the right direction. It was the consensus of the panel and audience that research to develop experimental tools with still better resolution will improve the understanding of the behavior of materials and should be pursued. The concern was raised about reaching the point when the observation tools affect the observations, that is, reaching an uncertainty point. This was not fully addressed during the discussion.

The question was raised about what kind of defects are detectable with field instrumentation. This is an important consideration since it addresses the practical problem faced by the materials user community. The materials user is only interested in when the material develops defects that threaten safety and affect durability of the structure. He is also interested in how often the structure must be inspected using the available inspection tools and how fast can the inspections be performed. It is doubtful that inspection tools with higher resolution will impact the damage tolerance philosophy and design criteria. It is

expected that inspection tools with higher resolution will impact the durability design procedures, since they are based on the ability to model the growth and find small imperfections. As a consequence. it is important to be able to correlate the amount of initial imperfections with the resulting defects and to determine how soon the imperfections evolve into defects that lead to eventual failure of the structure.

It became obvious during the discussions that the primary reason for studying the origin of imperfections is to develop the necessary understanding to design better materials for structural applications. This requires an in-depth understanding of imperfections and how they evolve into defects, such as cracks, that finally lead to structural failure. This requires the use of modern experimental tools to observe the origin of imperfections and their evolution into structural defects. At the very least this research will lead to a better understanding of the behavior of structural materials. It may also lead to a breakthrough in materials design once the defect causing imperfections are understood and means for eliminating them are developed.

Finally, the research on the origin of imperfections is an excellent example of natural philosophy. The term natural philosophy is used for the scientific process of observing and developing theories to explain phenomena. In the present case the phenomenon of interest is the evolution of structural defects from material imperfections. Experimental observations are necessary to guide the formulation of models and simulations of the damage evolution process. The models and simulations must capture the salient features of the damage accumulation process. Moreover, experiments must be designed to determine the accuracy and soundness of the models and simulations. If successful, this will lead to a better understanding of the behavior of structural materials. Moreover, this understanding can be used to design improved structural materials.

4. CONCLUSIONS

The major conclusions of the panel discussion on the origin of imperfections are:

1. Understanding of imperfections and their evolution into defects that eventually lead to structural failure is necessary. This will not only lead to a better understanding of material behavior, but will also provide guidelines for the design of better structural materials.

2. The research tools being developed for studying the origin of imperfections include acoustic microscopy, scanning electron thermal microscopy, micro-focus tomography, etc. With the exception of acoustic emission monitoring and micro-focus tomography, these tools only permit of observation of the evolution of damage from near surface imperfections.

3. It is unlikely that an understanding of the origin of imperfections will impact the damage tolerance design philosophy. It will have an eventual impact on the durability design philosophy.

SECTION II

PANEL DISCUSSION

ON

ORIGINS OF IMPERFECTIONS

TECHNICAL PRESENTATIONS

Dr. Spencer T. Wu
Program Manager, Aerospace Sciences
Bolling Air Force Base
"Introduction and Overview"

Professor J. D. Achenbach
Northwestern University
"Quantitative Non-Destructive Evaluation of
Fatigue-Induced Surface Damage"

Professor D. E. Chimenti
John Hopkins University
"Origins of Imperfections in Composites"

Professor J. T. Dickinson
Washington State University
"Examination of Precursors to Fracture"

Professor S. A. Guralnick
Illinois Institute of Technology
"Hysteresis and Incremental Collapse of Structures"

Dr. Harold Weinstock
Bolling Air Force Base
"The Microscopic Origin of Inelastic Behavior"

TECHNICAL PRESENTATION

"Panel Discussion on Origin of Imperfection"

BY

Dr. Spencer T. Wu

AFOSR

Bolling Air Force Base

PANEL DISCUSSION ON ORIGIN OF IMPERFECTION --- S. WU

PANELISTS

J. D. ACHENBACH, NORTHWESTERN UNIVERSITY

D. E. CHIMENTI, JOHNS HOPKINS UNIVERSITY

J. T. DICKINSON, WASHINGTON STATE UNIVERSITY

S. A. GURALNICK, ILLINOIS INSTITUTE OF TECHNOLOGY

G. P. SENDECKYJ, WRIGHT LABORATORY

H. WEINSTOCK, AFOSR

ORIGIN OF IMPERFECTION INITIATIVE

- THE INITIATIVE IS TO UNDERSTAND THE PHENOMENA RELATED TO THE ORIGIN OF IMPERFECTIONS AT BOTH THE MICROSCOPIC AND MACROSCOPIC LEVELS, AND TO BE ABLE TO FIND THE FUNDAMENTAL CORRELATIONS BETWEEN THESE PHENOMENA.

RESEARCH ISSUES

- DEVELOP MEASUREMENT TECHNIQUES TO CHARACTERIZE THE NATURE OF IMPERFECTIONS

- UNDERSTAND THE RELATED PHYSICAL/CHEMICAL PROCESSES

- CORRELATE THE MICRO- AND MACRO- IMPERFECTIONS

- DEVELOP THEORETICAL MODEL TO QUANTIFY THE IMPERFECTION PHENOMENA

AFOSR'S CURRENT EFFORTS

- DETECTION/EXAMINATION OF PRECURSOR BEHAVIOR TO FAILURE
- COMPLEMENTARY DIAGNOSIS/CHARACTERIZATION DEVICES
- INTEGRATED NDE THEORY AND EXPERIMENT DEVELOPMENT
- FATIGUE AND HYSTERESIS CORRELATION

TECHNICAL PRESENTATION

"Quantitative Non-Destructive Evaluation of Fatigue-Induced Surface Damage"

BY

Professor J. D. Achenbach

Center for Quality Engineering and Failure Prevention

Northwestern University

Material :

Silag SiC (20 vol.% whisker) / Al (2124-T4)

whiskers : diameter ~ 1 μm, length ~ 10 μm

rolled (tends to align whiskers at surface ⇒ surface anisotropy)

Loading :

cyclic (0.5 Hz)

tension (stress range 222 MPa)

QNDE technique :

line-focus acoustic microscope

225 MHz

V(z) curves at increasing numbers of cycles (N)

surface wave speed vs. angle (anisotropy) for increasing N

surface wave speed vs. N for various angles

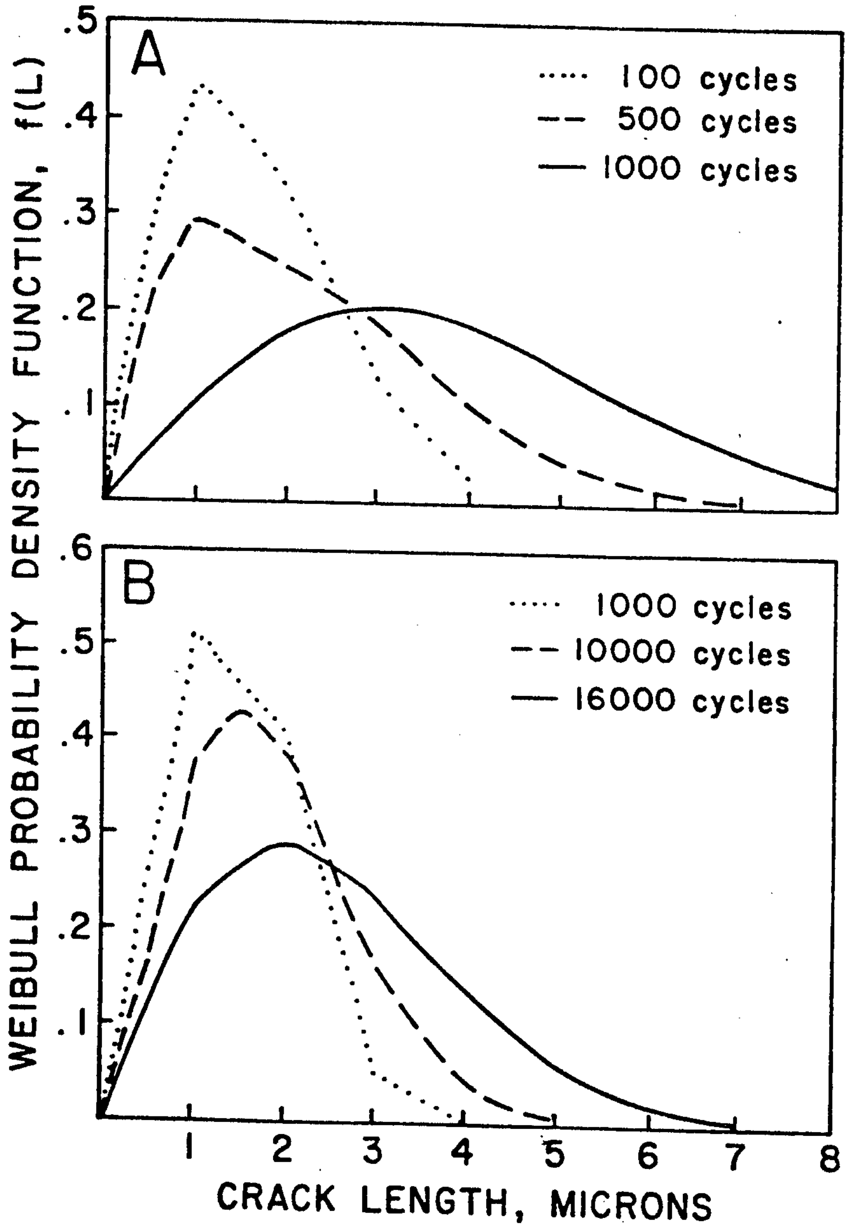

The Weibull probability density function as a function of crack length. A: Silag SiC (20 vol. pct. whisker)/Al (2124-T4), Heat #A6104Z-2A, at 100, 500 and 1000 cycles, 300 MPa. B: Silag SiC (20 vol. pct. whisker)/ Heat #A2038Z-C at 4000, 10000 and 16000 cycles, 300 MPa.

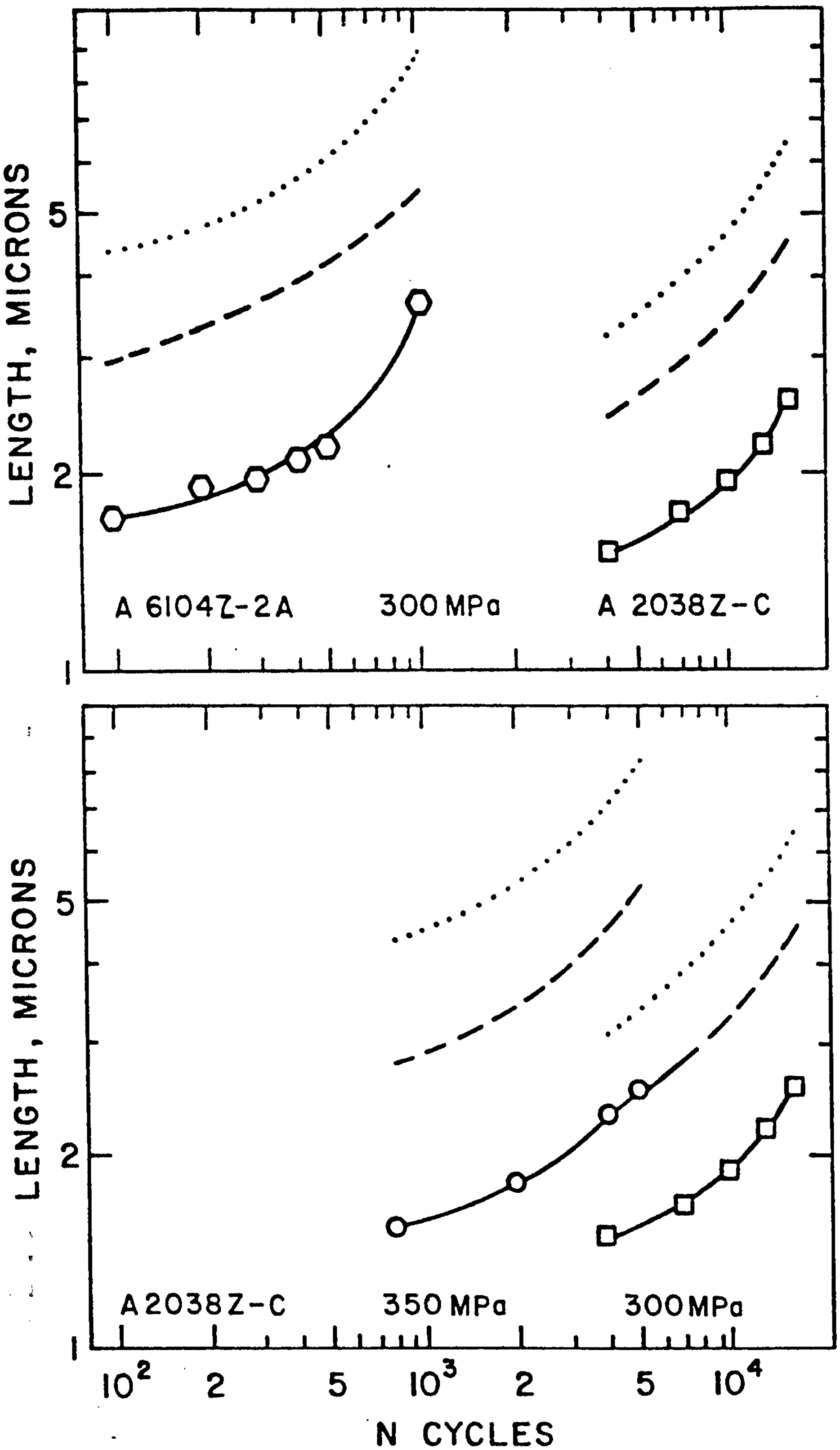

Crack lengths corresponding to 99% (dotted curves) and 90% (dashed curves) of the Weibull cumulative distribution function, and average crack length (solid curves with data points) as a function of number of cycles. A: Silag SiC (20 vol. pct. whisker)/Al (2124-T4), Heat #A6104Z-2A, vs. Silag SiC (20 vol. pct. whisker)/Al (2124-T6), Heat #A2038Z-C, both at 300 MPa. B: Silag SiC (20 vol. pct. whisker)/Al (2124-T6), Heat #A2038Z-C, at 300 and 350 MPa.

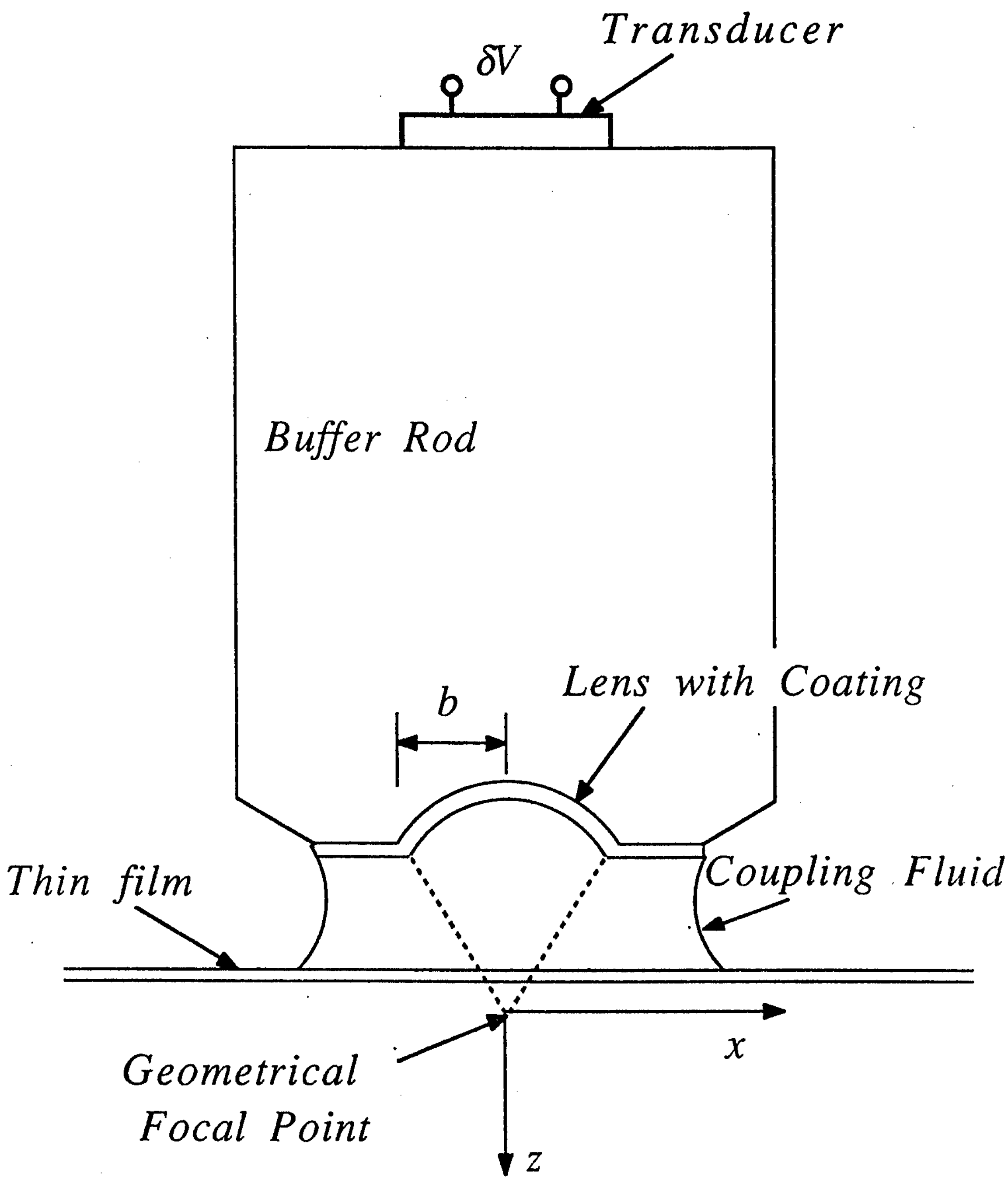

Figure 1 Geometry of the line-focus acoustic microscope.

The Scanning Acoustic Microscope

The focused beam is scanned mechanically and an image is built up from the beams scattered from objects in the focal region of each point of the scan. The frequency of operation can range from 100 MHz to 1 GHz. At 200 MHz the wavelength in water is 7.5 μm and the compressional wavelength in aluminium is 32 μm.

When the focal point lies below the interface a leaky Rayleigh wave is excited. At 200 MHz the Rayleigh wavelength in aluminium is 14 μm. This wave participates in the imaging, making vertical features particularly distinct.

In an alternative mode, the lens assembly is lowered so that the focal point lies well below the interface and then the assembly is raised. Both the reflected and leaky Rayleigh waves are collected by the lens and added vectorially by the transducer. The resulting interference pattern is called the acoustic material signature or V(z) effect.

The purpose of the present work is to extract quantitative information from the acoustic microscope by relating the voltage from the microscope to the mechanical properties of the insonified material.

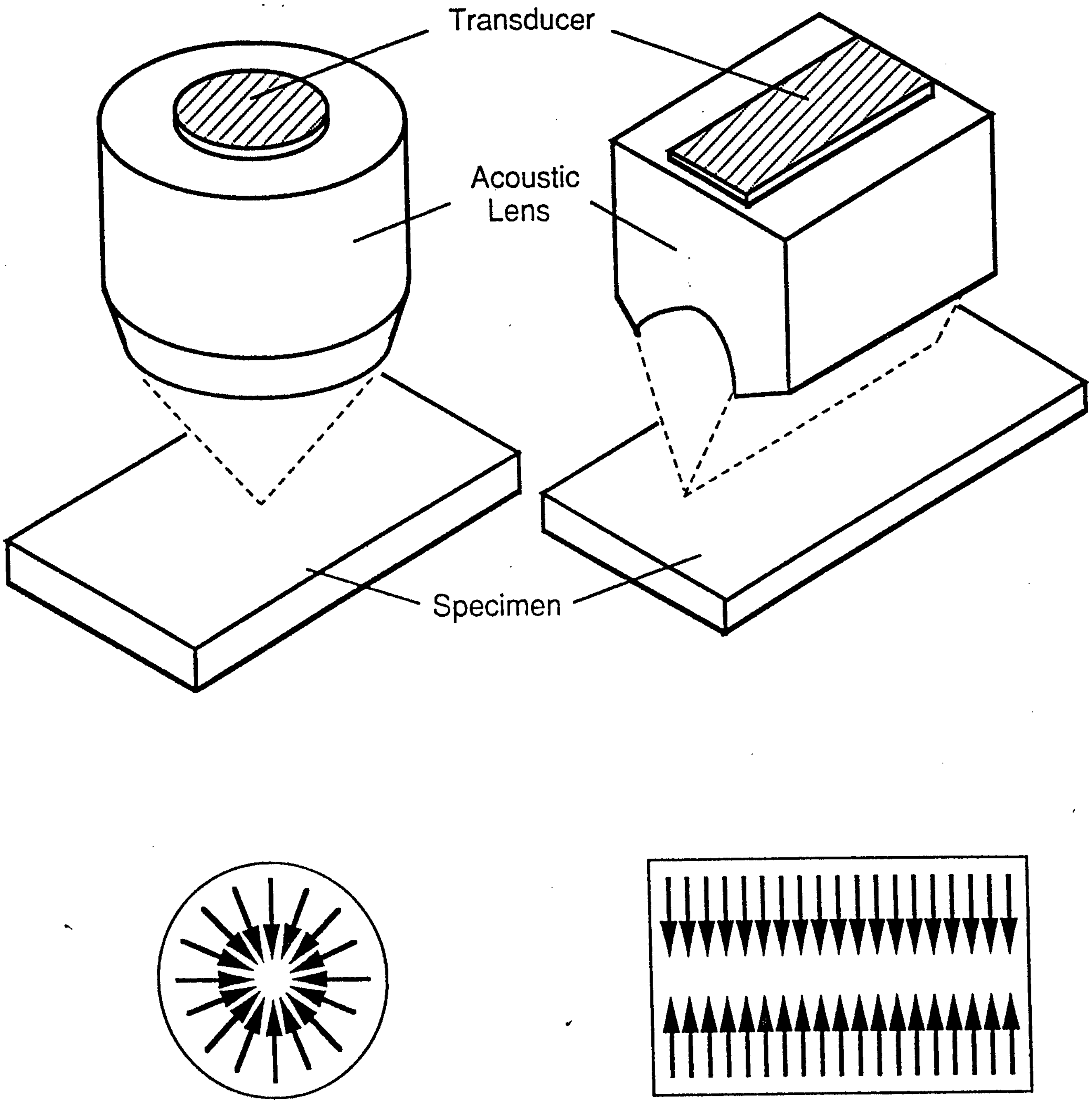

Point-Focus-Beam Lens **Line-Focus-Beam Lens**

METAL MATRIX COMPOSITE

Silicon Coated Carbon Fibers in Titanium

1.6 GHz, 200 μm

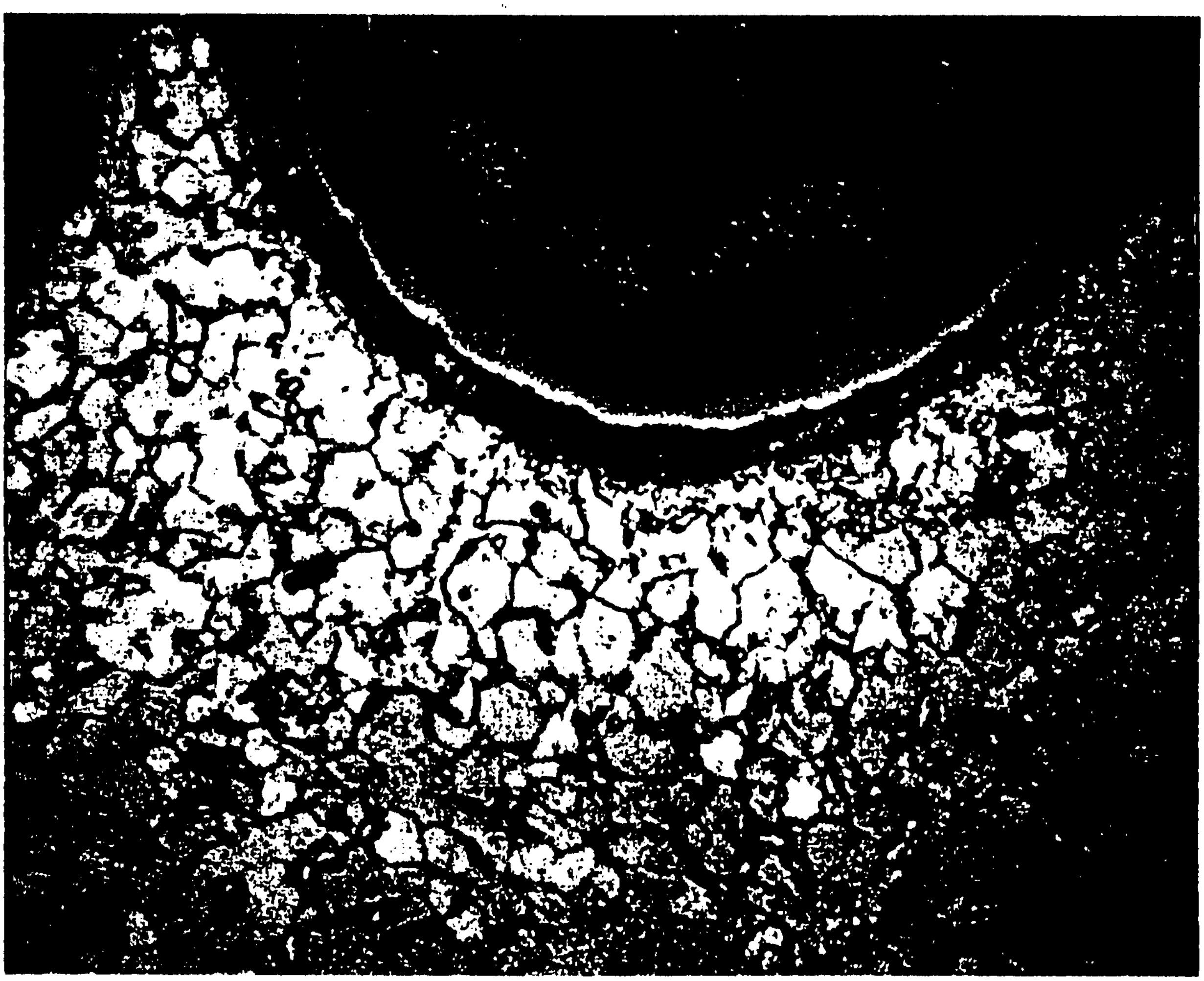

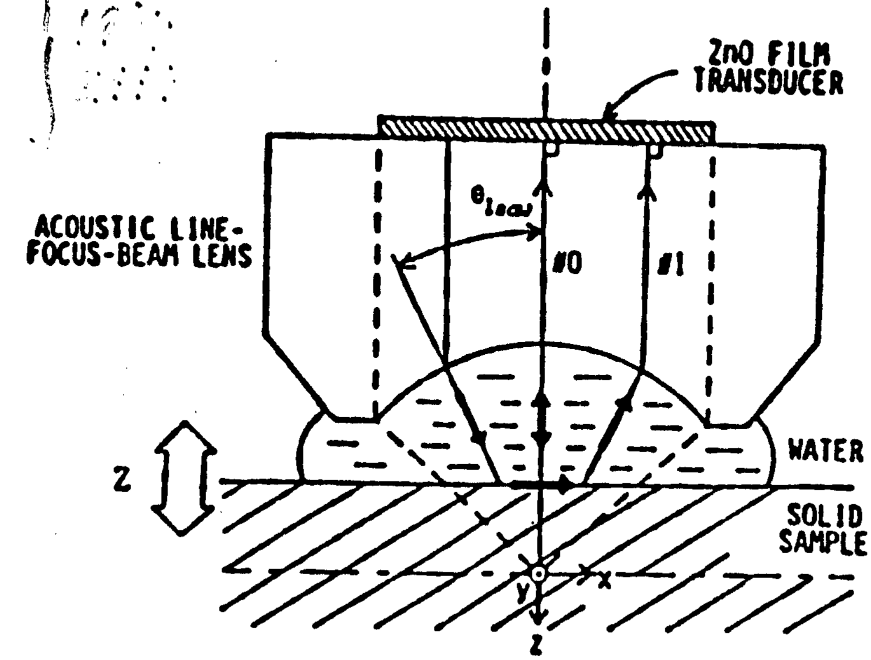

Fig. 4. Cross-sectional geometry of LFB acoustic lens to show V(z) curve measurements.

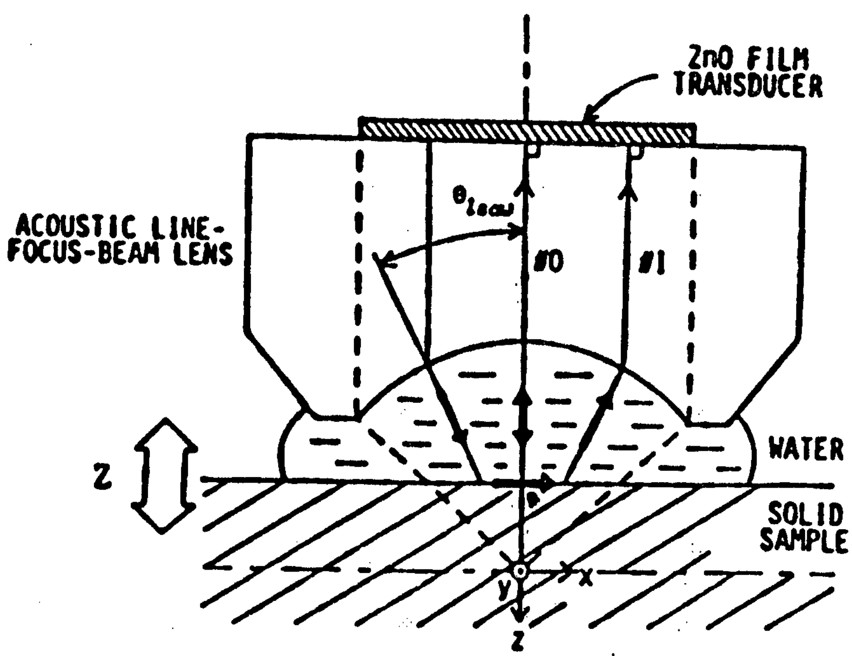

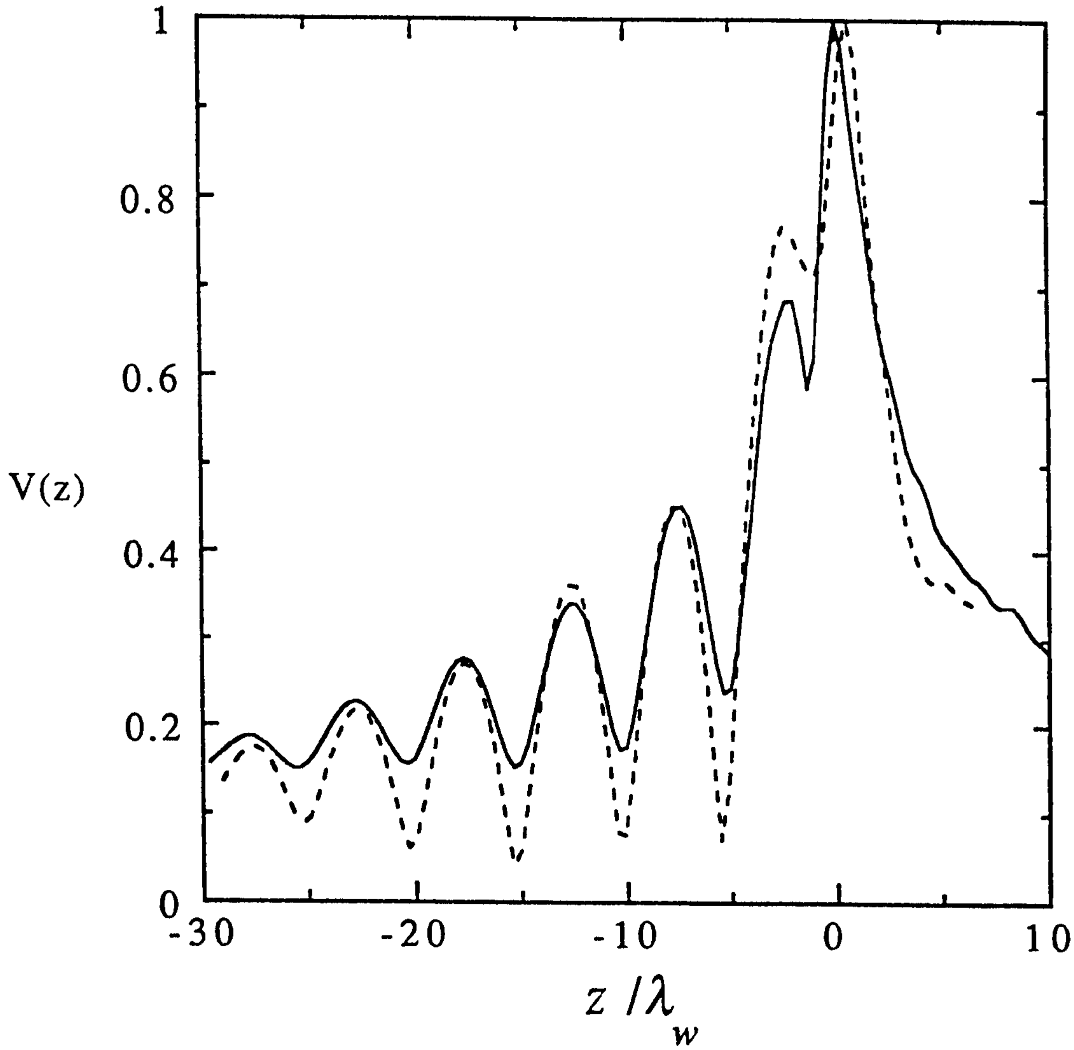

The magnitude of V as a function of z/λ_w for fused quartz. Solid BEM calculation and dashes experimental result.

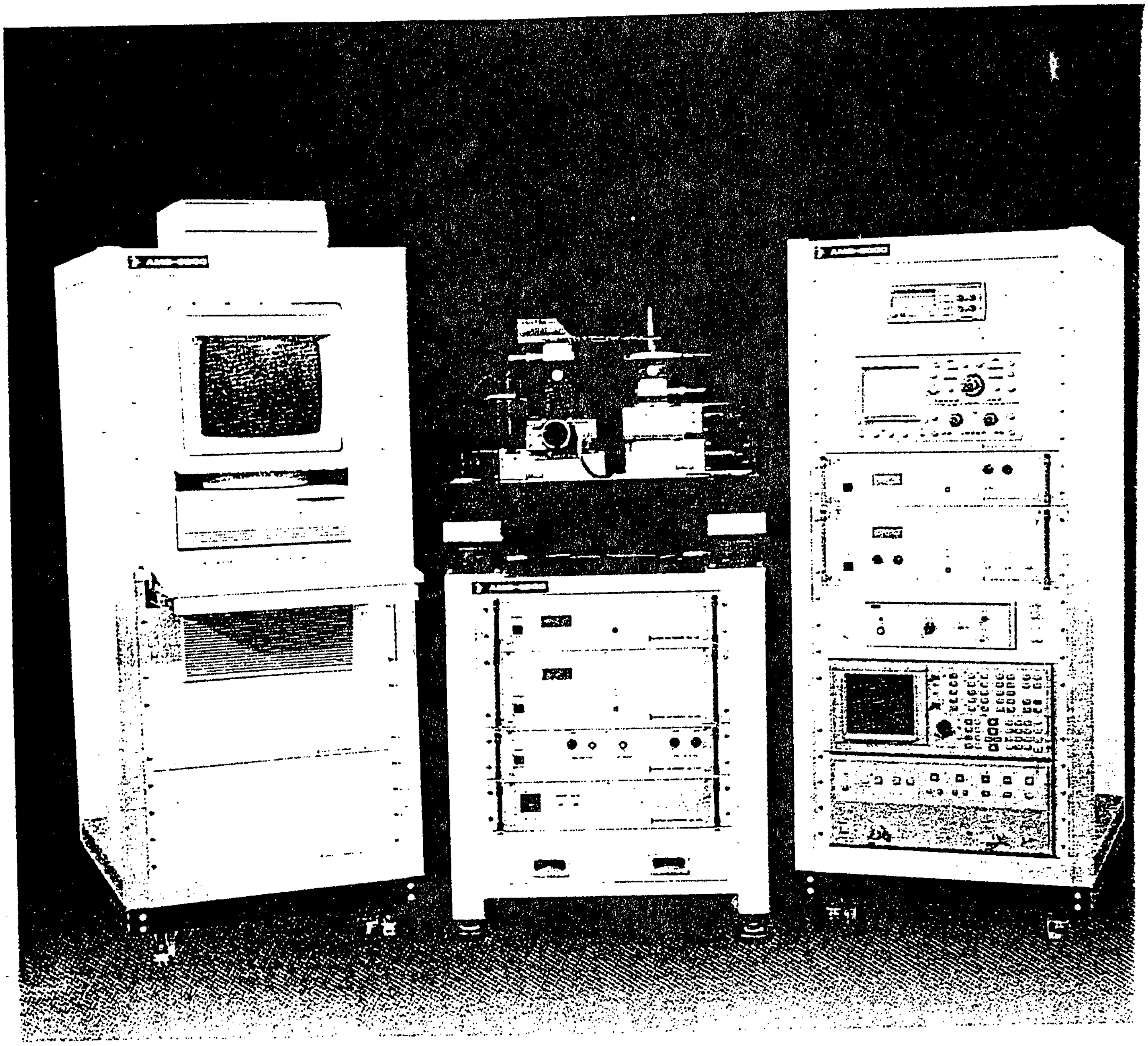

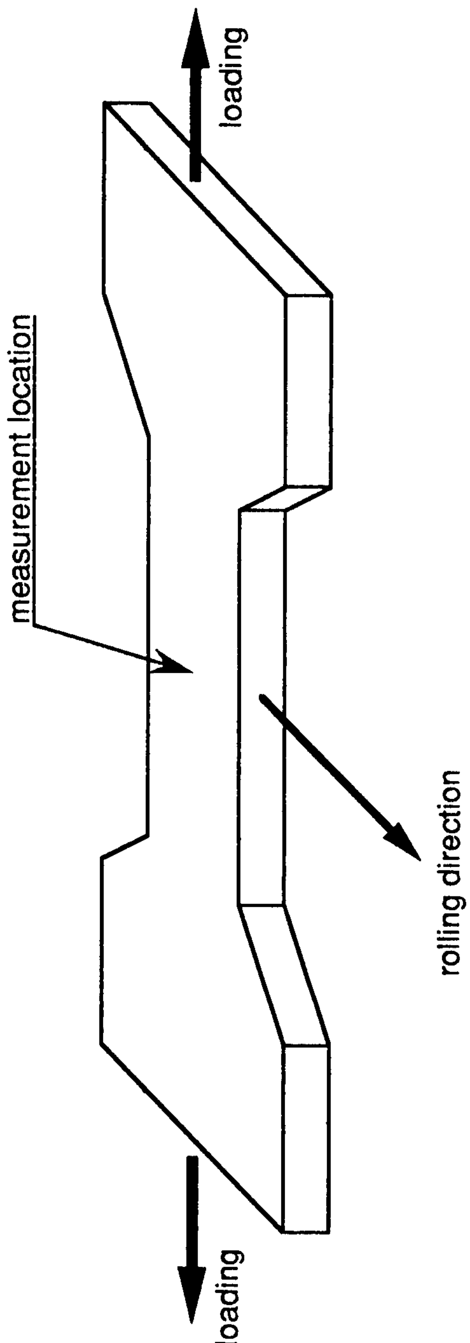
loading
measurement location
rolling direction
loading

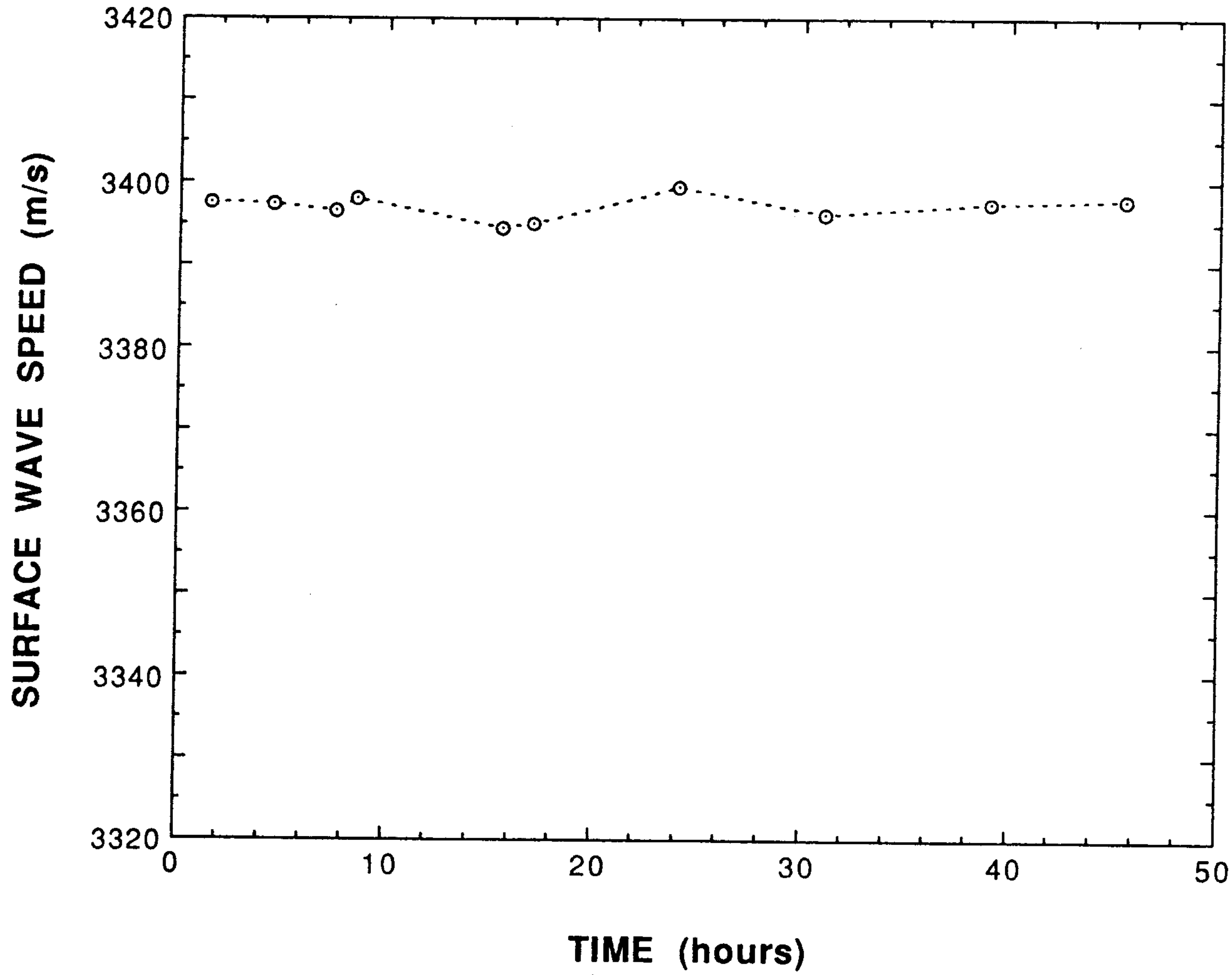

Water loading effect on the surface wave speed.

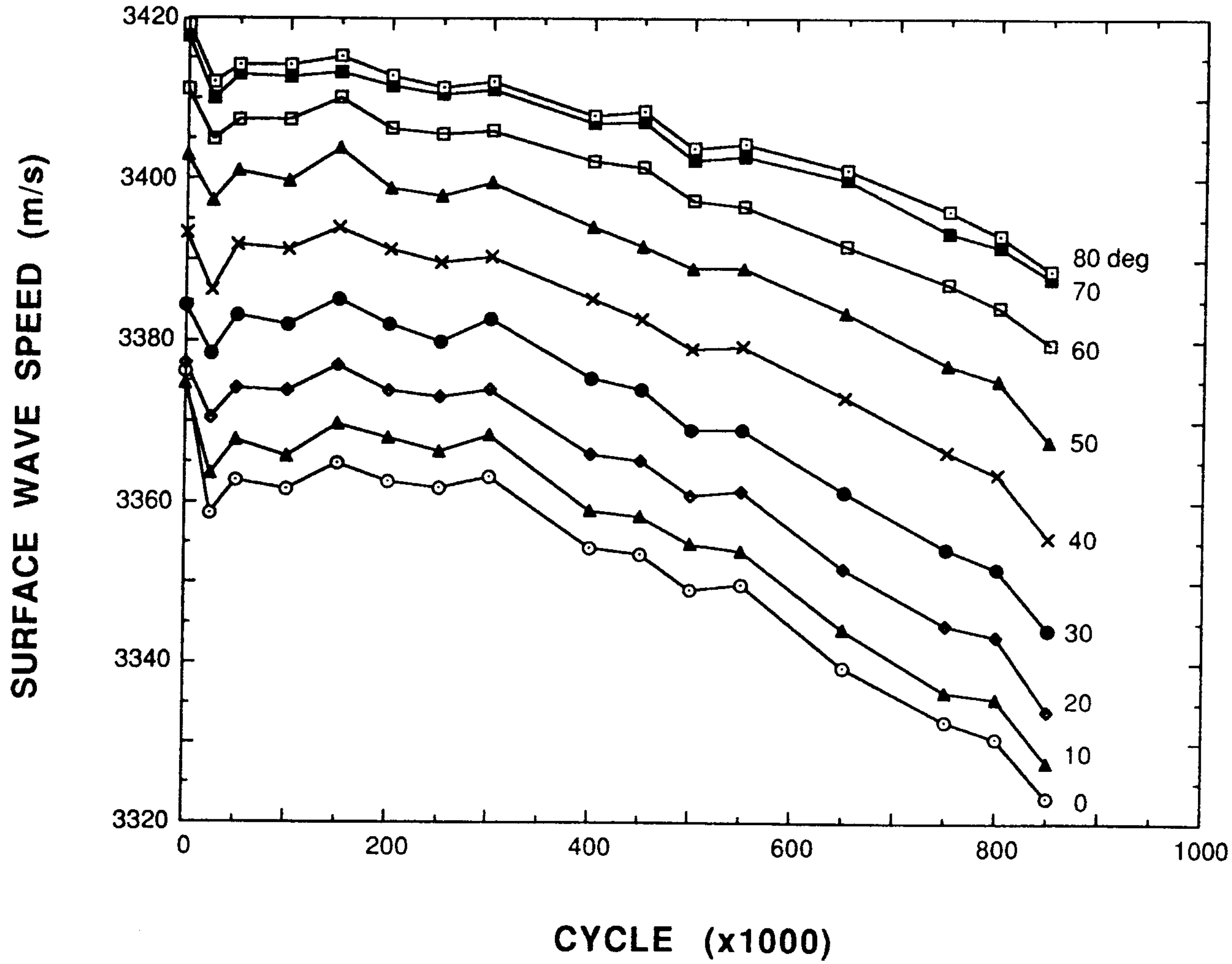

Surface wave speed variation on SiC/Al composite under cyclic loading.

$$v = v_w\left[1 - (v_w/2f\Delta z)^2\right]^{-1/2} \approx \left[v_w \cdot f \cdot \Delta z\right]^{1/2}$$

v : surface wave speed
v_w : wave speed in water
f : wave frequency
Δz : dip interval

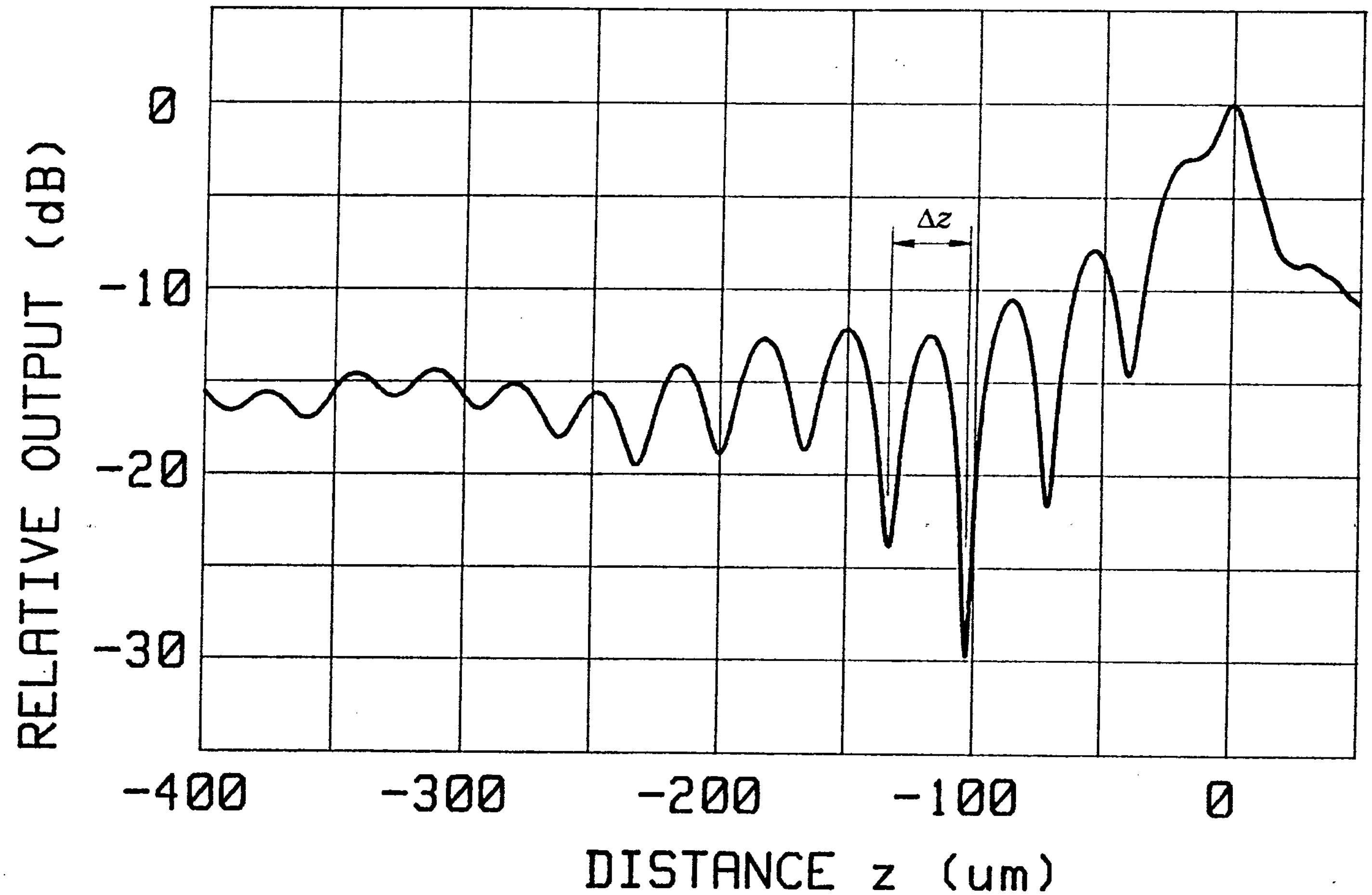

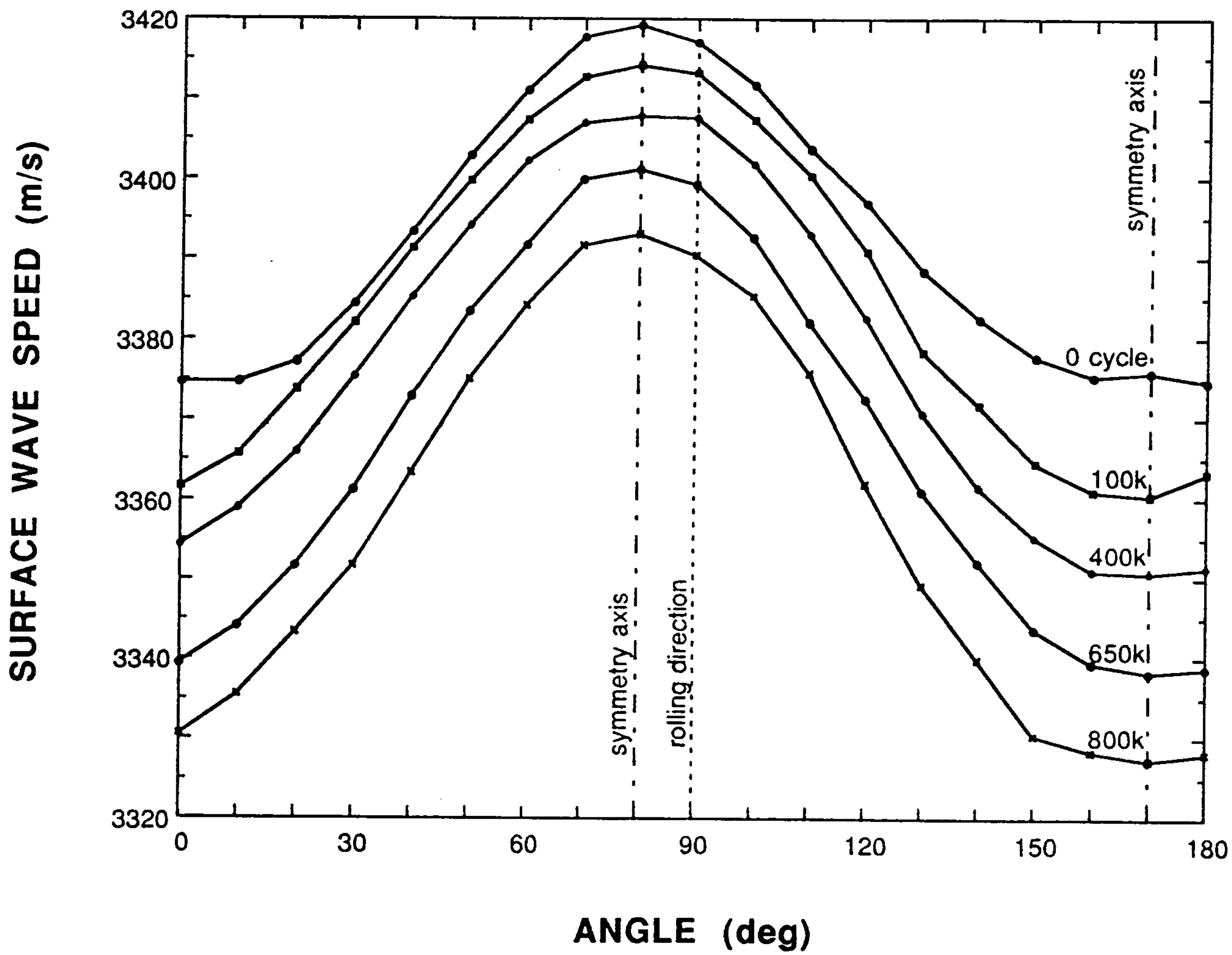

Acoustic anisotropy of SiC/Al composite.

TECHNICAL PRESENTATION

"Origins of Imperfections in Composites"

BY

Professor D. E. Chimenti
John Hopkins University

Objectives

- Conduct research leading to the identification and characterization of origins of imperfections in advanced composite materials.
- Demonstrate optimum characterization methods for the defects to which the imperfections lead.
- Detect and characterize incipient damage in composites that have been mechanically, thermally, and environmentally stressed.
- Examine occurrence, development, and growth of imperfections such as matrix plastic deformation, microcracking, fiber fracture, fiber/matrix debonding, and other potential failure modes.

Incipient Damage

As-fabricated It has been demonstrated that origins of future damage are often introduced into the material in the fabrication stage

Mechanical Loading *in situ* static and cyclic stress to induce the nucleation and development of mechanical damage

Thermal Loading Electron beam energy deposited in the SETM causes large rise in local temperature ($\sim 10^3$ °C)

Environmental Degradation Electrochemical or corrosive action in MMC's to nucleate imperfection sites leading to damage

Approach to Microscopic Characterization

Scanning Electron Thermal Microscopy Performed in an electron microscope and detected by delicately sensing the minute bending moments thermally induced in the sample

Acoustic Microscopy A derivative of an established method, but performed at intermediate frequencies and with an advanced lens design to permit critical study of subsurface material properties

Scanning Electron Thermal Microscopy

- Based on thermal wave imaging

- Performed in SEM by injecting heat (and electrons) with E-beam

- Modulated E-beam gives periodic heat source

- Functions over broad frequency range (10 - 1000 kHz)

- Thermal energy deposited below the surface (dependent on accelerating potential, target density)

Scanning Electron Thermal Microscopy, cont

- Extremely high spatial resolution (like SEM)

- Detected by observing thermoelastic signal generated within sample

- Periodic sample deformations detected phase-sensitively by piezoelectric element

- Very large local temperature excursions can be produced with E-beam

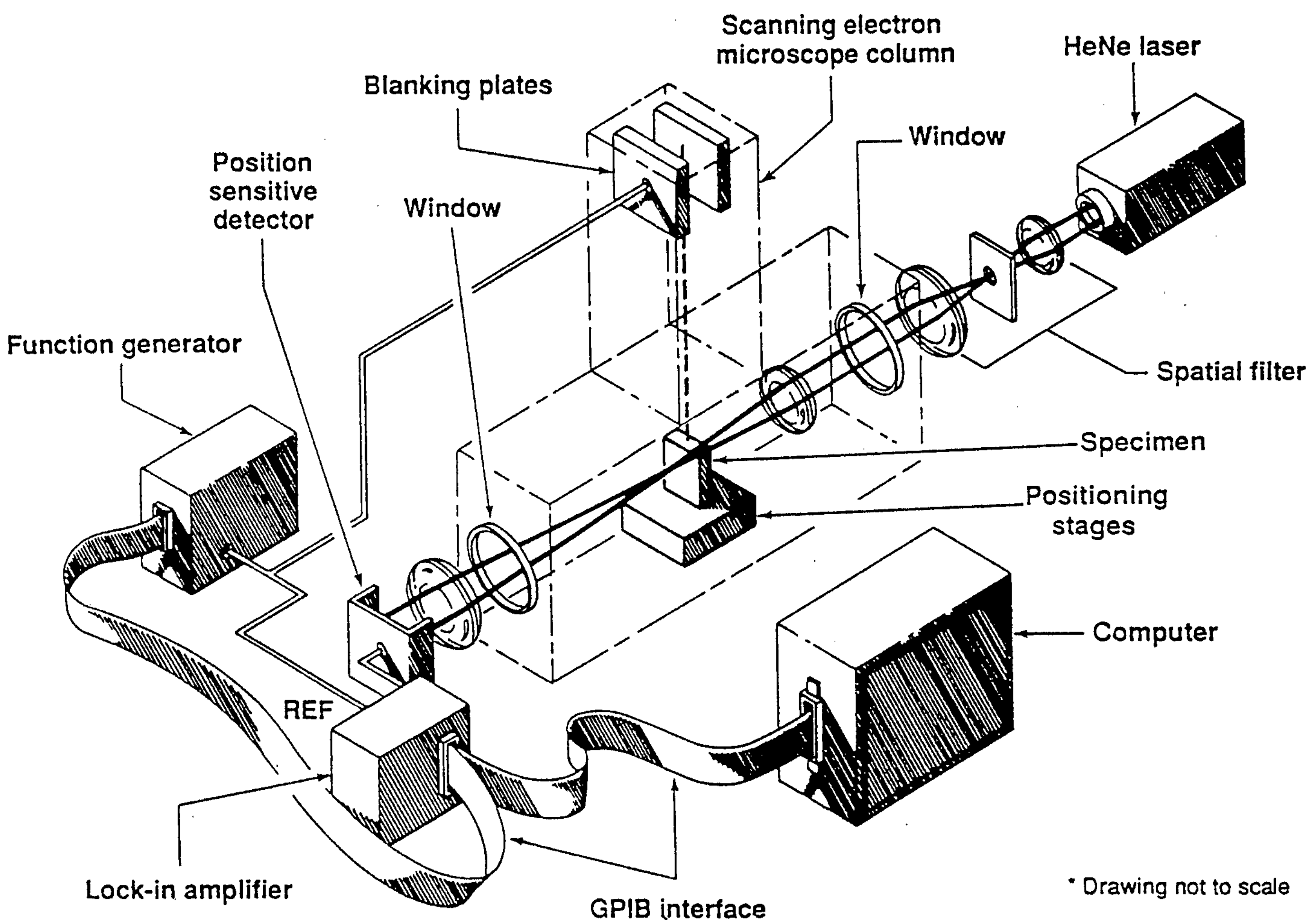

Scanning electron
microscope column
HeNe laser
Blanking plates
Window
Position
sensitive
detector
Window
Function generator
Spatial filter
Specimen
Positioning
stages
Computer
REF
Lock-in amplifier
GPIB interface
* Drawing not to scale

Analysis of SETM signals

Coupled acoustic field equations and thermal diffusion equation

$$\mu\nabla^2\mathbf{u} + (\lambda+\mu)\nabla(\nabla\cdot\mathbf{u}) - \rho\frac{\partial^2\mathbf{u}}{\partial t^2} = \alpha_T(3\lambda+2\mu)\nabla T$$

$$\nabla^2 T - \frac{1}{\alpha}\frac{\partial T}{\partial t} = -\frac{1}{\kappa}H(\mathbf{x},t)\,,$$

λ, μ	Lame elastic constants
$\mathbf{u}$	particle displacement
ρ	mass density
α_T	coefficient of thermal expansion
α	thermal diffusivity
κ	thermal conductivity
$H(\mathbf{x},t)$	power density of the heat source, a tabulated function for a circular source.

Analysis of SETM signals

Voltage induced in a piezoelectric element is

$$V_{ac} \propto \frac{P_0 e^{-\beta R_s/2}[\gamma + \alpha_T(3\lambda + 2\mu)]}{\sqrt{\omega\rho\kappa C}}, \qquad (1)$$

P_0	incident power
β	electron attenuation coefficient
R_s	E-beam attenuation coefficient ($\propto$ beam energy)
γ	thermal stress constant
ω	modulation frequency
C	heat capacity

Acoustic Microscopy

- Can create images of surface or subsurface features
- Sensitive to weak, small scatterers and near-surface elastic property variations
- Large aperture lens permits Rayleigh wave imaging at intermediate wavelengths (2 – 10 μm)
- Spherical focus lens best for detecting, imaging small sample features
- Cylindrical focus lens best for quantitative property determination
- Can also map surface topography

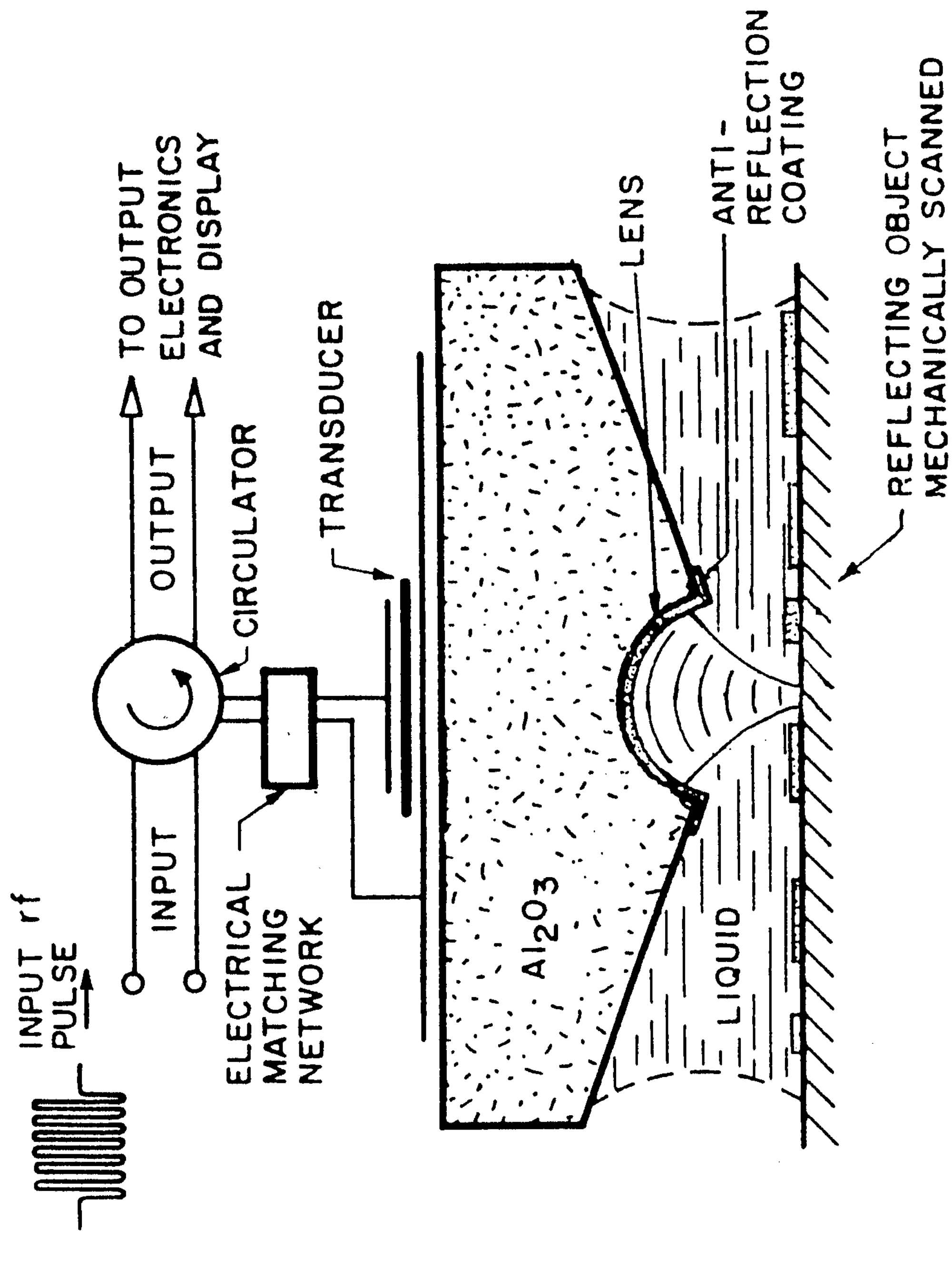

INPUT rf PULSE
INPUT
OUTPUT
TO OUTPUT ELECTRONICS AND DISPLAY
CIRCULATOR
ELECTRICAL MATCHING NETWORK
TRANSDUCER
Al_2O_3
LENS
ANTI-REFLECTION COATING
LIQUID
REFLECTING OBJECT MECHANICALLY SCANNED

Goals for first year

1.1 Phase I: Establishment of initial capability

Task 1: Scanning electron thermal microscopy

- Confirm operation of e-beam modulator on the Center SEM.

- Design and install mechanical load stage on SEM to perform SETM simultaneously with application of mechanical load.

- Setup and test and detection electronics and data acquisition system.

- Verify spatial resolution and operation over bandwidth of interest using calibration standards.

Goals for first year, cont

<u>Task 2: Acoustic microscopy</u>

- Construct scanning acoustic microscope system with computerized motion control and data acquisition; system to be capable of 2 μm spatial resolution.

- Build or procure cylindrical microscope lens for operation with wideband transducer in the frequency range 50 $\sim$ 100 MHz.

- Integrate system components and test operation on appropriate standard samples.

1.2 Phase II: Sample selection and defect initiation procedures

- Select specimen composite material systems of interest in consultation with sponsor or sponsor-related organizations.

TECHNICAL PRESENTATION

"Examination of Precursors to Fracture"

BY

Professor J. T. Dickinson

Dept. of Physics & Material Science Program

Washington State University

General Comments

Catastrophic failure initiates when the Griffith (defect size) criteria is exceeded either by:

(a) increasing the stress until the critical size equals the size of a preexisting defect, or

at lower stresses:

(b) increasing size of existing defects (subcritical crack growth) until a critical defect size(causing catastrophic crack growth) is reached

(c) nucleating defects (void formation, pile up of dislocations-crack formation, instabilities--e.g., necking) which then grow to critical size [in ceramics grain size

(d) linkage of defects to produce critical dimensions.

Service loads are typically well below the stress required for catastrophic failure ---> lifetime predictions require modelling of defect growth from assumed distributions of initial defects.

In many applications, most failures occur early in the expected life cycle (weak items–infant mortality) or late in the expected life cycle (defect growth–wear out, or induced failure).

<u>Sources of preexisting defects:</u>

inherent defects (impurities, inhomogeneities -- including fluctuations, dislocations)

processing defects

voids

occluded particles (composite fillers, dust in polymers)

design factors (stress concentrations, rivet holes, exposure to environment)

Sources of grown-in defects (usually requires preexisting defect such as above)

localized phases (e.g., glassy phase in polyxtal. ceramic-- secondary phases usually initiates cracks)

cracks (for materials without secondary phase -- subcritical crack growth)

shear bands (fracture of metallic glass often nucleates at surface step associated with shear band -- Koh cracks in inorganic crystals)

crazes (fracture of PS usually initiates at crazes)

synergisms with chemical effects (humidity, saltwater, fingerprints etc.)

residual stresses (tempered glass, interfaces)

EXAMPLE: GLASSES

flaws:
- surface flaw (often due to mechanical contact)
- devitrification at inhomogeneities (misfit stresses)
- atmospheric corrosion (pits)

subcritical crack growth

catastrophic crack growth

- Environmentally Induced Fracture of Glass--(Michalske, Freiman, Wiederhorn).

Glass = inorganic substance which is a non-crystalline fluid with extremely high viscosity--for all practical purposes it is a rigid solid

Silica glasses based on SiO_2 structure built from tetrahedra:

Metallic Glasses

surface steps formed by shear banding (concentrate stress)

cavitation within shear bands

devitrification (decohesion $\rightarrow$ void formation)

EXAMPLE: POLYCARBONATE

Typical path to failure:

processing defect--e.g., surface flaw, dust particles

initial craze growth (μm dimensions) [crazes -- thermal/stress activated in the presence of defects void formation + highly oriented bridging fibrils]

craze rupture (usually at craze boundary)

crack often halted by interaction with cold drawing

tearing of cold drawn material

catastrophic crack growth

In craze resistant polymers: shear bands form, followed by tearing. (crazing possible precursor).

The relation between crack velocity, v, and strain energy release rate, G, may be written (after Maugis)

$$G - 2\gamma = 2\gamma\, a(T)\, f(v)$$ [$G - 2\gamma$ is the dissipative part of the energy loss]

γ is the minimum energy required for surface formation

a(T), f(v) are functions which describe the temperature and velocity dependence of dissipative processes. At G_c (a critical value of G) crack velocity increases discontinuously.

Distributed Flaws : The Real World

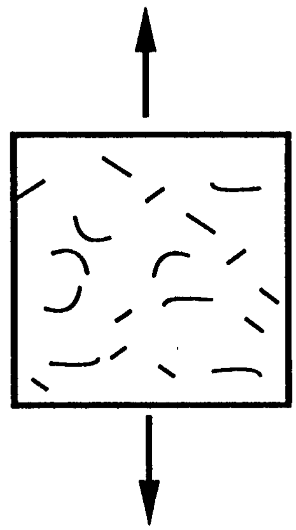

Distribution of flaws under stress -- changes with time.

For ith flaw:

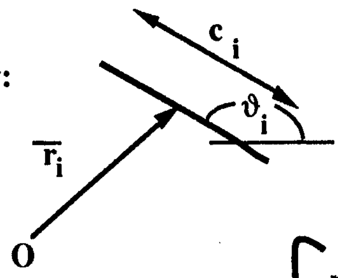

first region to fail determined by distribution of $\begin{cases} r_i \\ \vartheta_i \\ c_i \end{cases}$

damage zones evolve

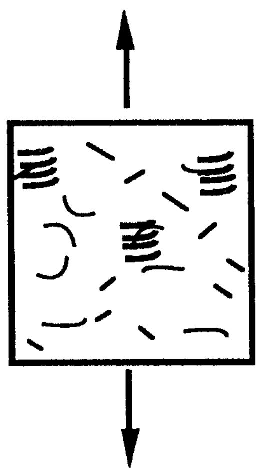

A zone that fails will tend to fail again.

When repeated failure starts, ~ at critical breaking point <---> damage zones compete - larger cracks grow fastest. Coalescence very effective in localization of failure zone.

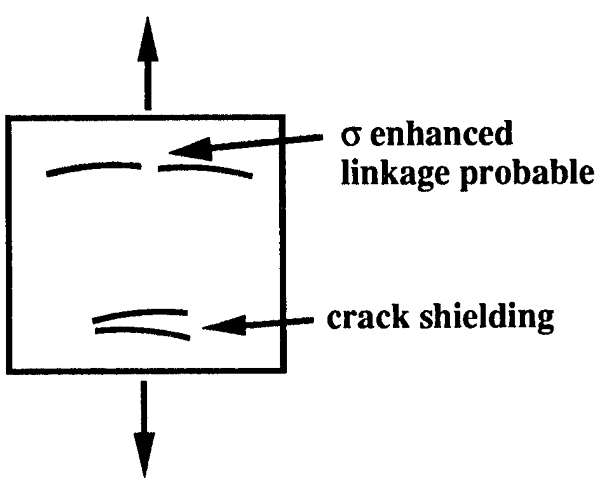

Monte Carlo Simulation of a "Brittle Polymer" Paul Meakin

Assume a bond breaking rate probability for the ith bond to be:

$$P_i \sim \exp(k_i \delta_i^2)/k_B T$$

where k_i is the force constant for the ith bond and δ_i is the elongation of the bond. Sample is stretched in one direction; Bonds are chosen by a Monte Carlo algorithm and tested for bond breaking by testing P_i.

At low forces (mostly small δ_i) bond breaking is random. At higher forces, cracks form that have very irregular shapes and small cracks resemble large cracks. Suggests fractal geometry of cracks = 1.27 - 1.31 depending on method.

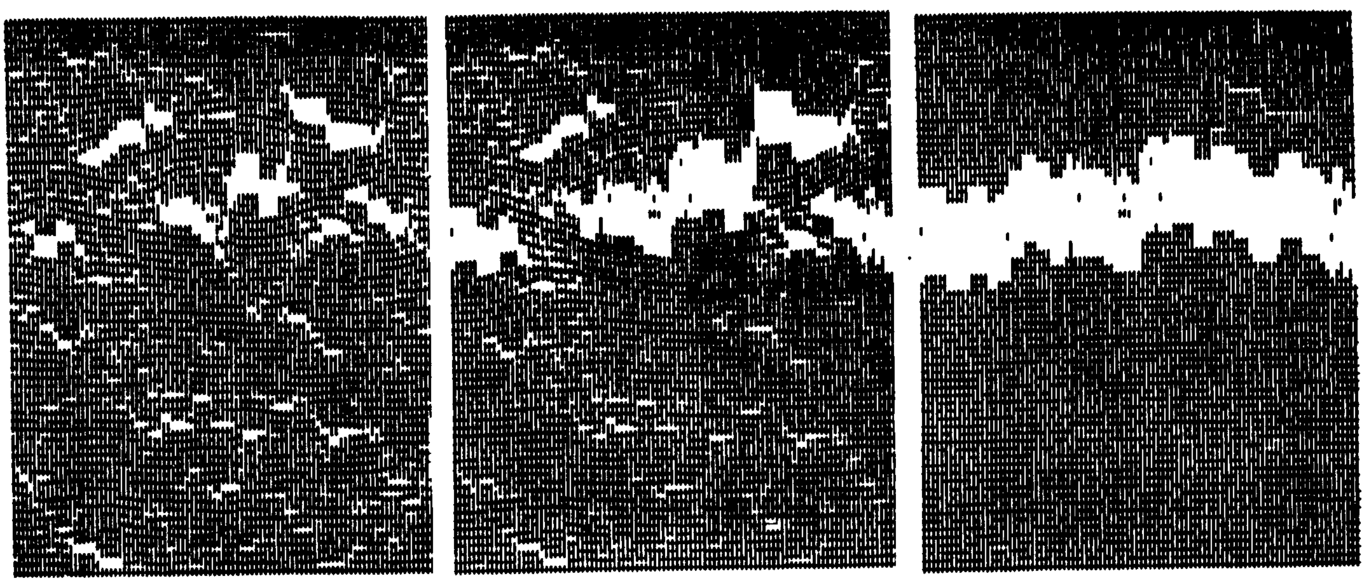

Figure 9.1 Results from a typical simulation carried out using the two dimensional model of Termonia and Meakin.[9] At the start of this simulation the network of nodes and bonds was stretched by 20% in the y direction (without allowing bond breaking to occur). The parameters used to obtain these results were $k_x = 20$, $k_y = 20$ and $k_B T = 1$. Figures a, b and c show three different stages well before failure, close to failure and at failure.

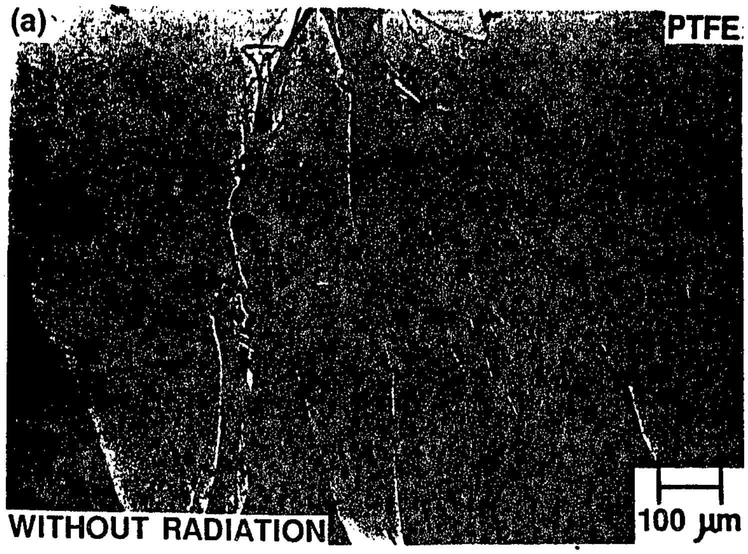

PTFE WITH ELECTRON BEAM

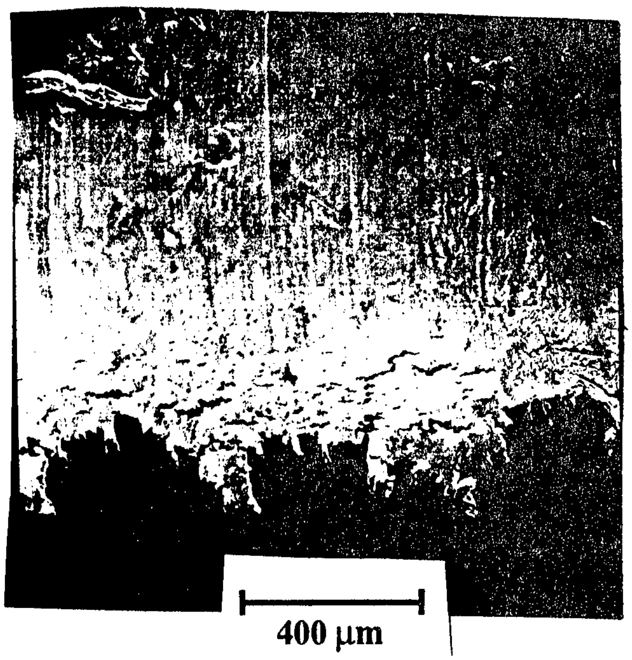

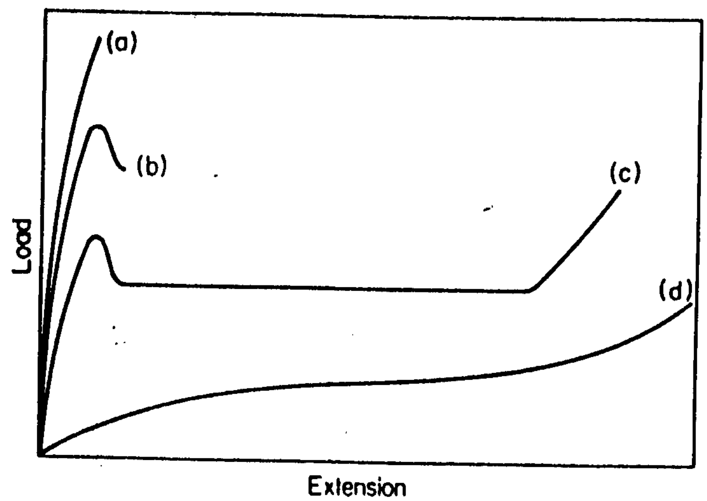

Figure 1.19 Breaking characteristics for a typical polymer tested at different temperatures: (a) brittle, (b) ductile, (c) necking and cold-drawing and (d) rubber-like behaviour.

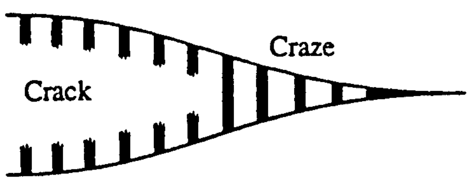

Figure 2.5.9 Cross-section of a polymer craze.

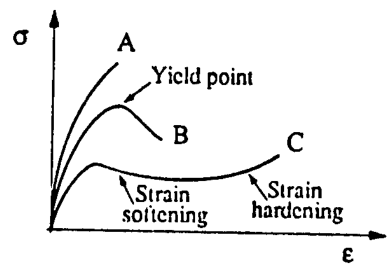

Figure 2.5.7 Typical stress-strain curves of polymers.

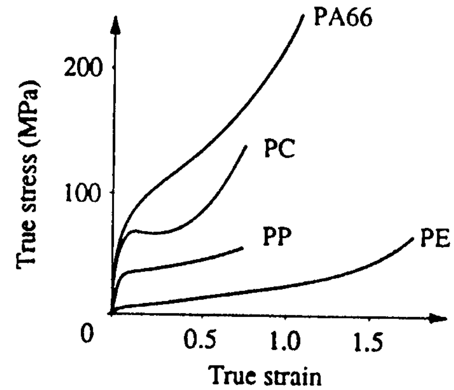

Figure 2.5.8 Examples of stress-strain curves.

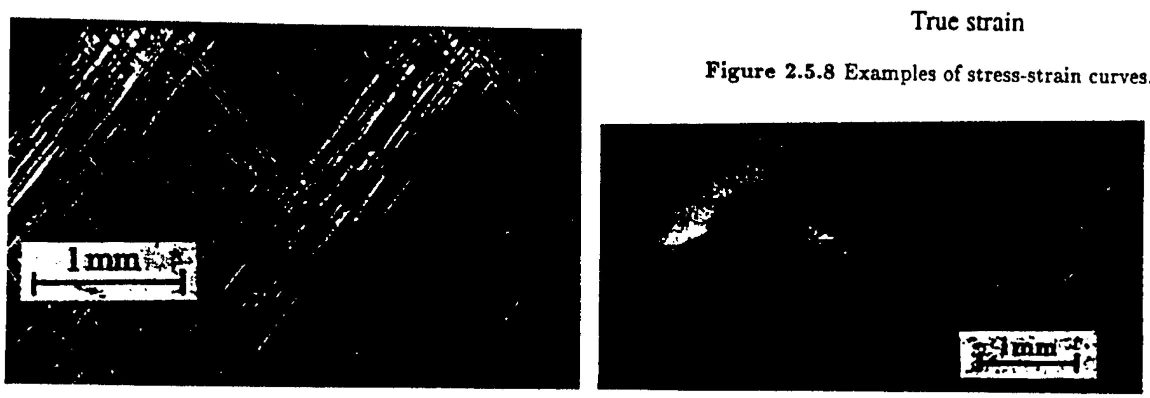

Figure 2.5.10 Types of shear bands observed between cross-polarizers.

SEM Micrographs of PS Fracture Surfaces

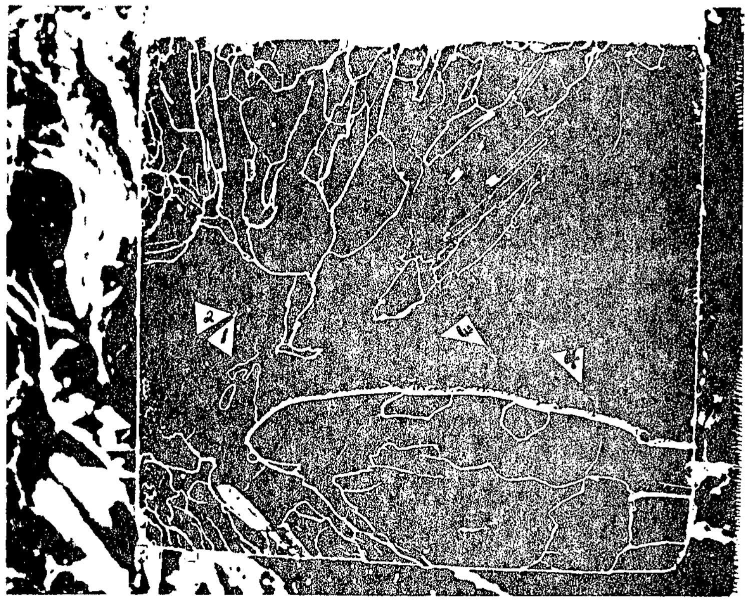

Heavily Crazed

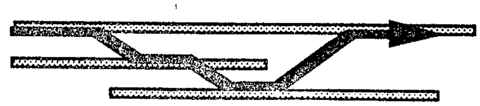

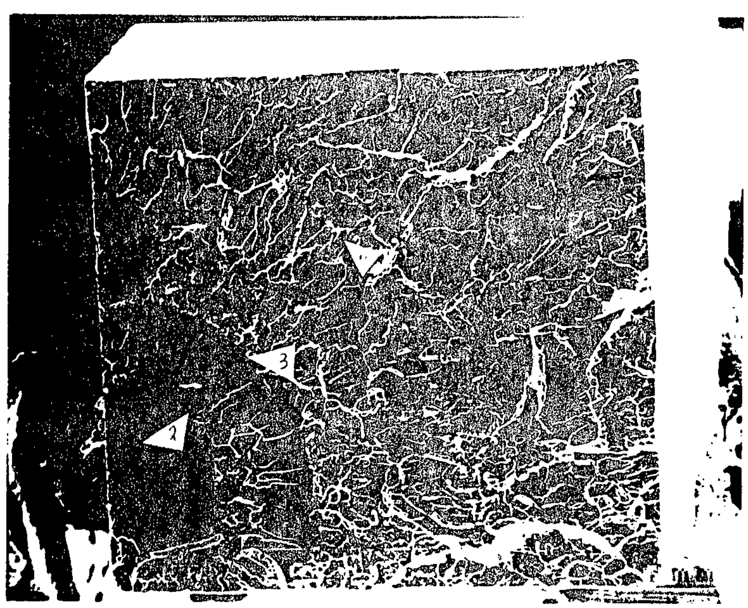

Lightly Crazed

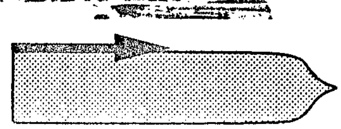

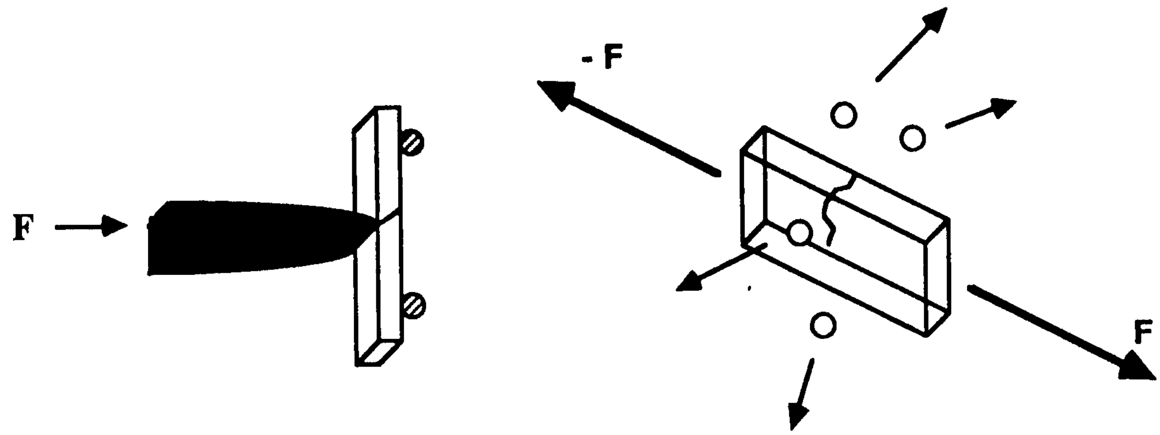

<u>FRACTO-EMISSION</u> (FE):

DURING AND FOLLOWING THE DEFORMATION AND FRACTURE OF MATERIALS: THE EMISSION OF ELECTRONS, IONS, NEUTRALS, AND PHOTONS (INCLUDING LONG WAVELENGTH ELECTROMAGNETIC RADIATION - RADIO WAVES).

<u>PROPERTIES WE MEASURE</u>:

- TYPE OF PARTICLE
- TIME DEPENDENCE (VS CRACK GROWTH)
- INTENSITIES
- ENERGIES (electrons, ions; photons [λ])
- MASS (neutrals, ions)
- TIME CORRELATIONS BETWEEN SPECIES

<u>FE DEPENDS ON</u>:

- MATERIAL
- LOCUS OF FRACTURE
- SAMPLE STRENGTH
- CRACK VELOCITY
- ENVIRONMENT (in some cases)

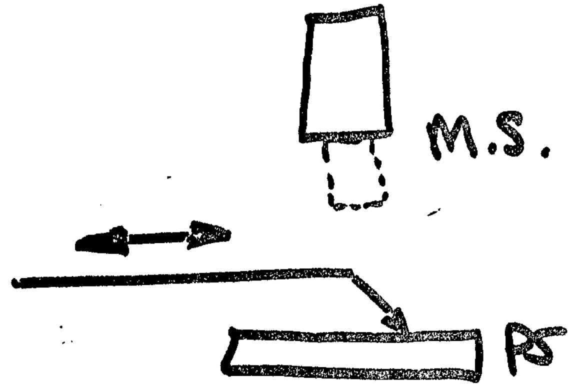

Mass Scan during Abrasion of Polystyrene (Styron 680)

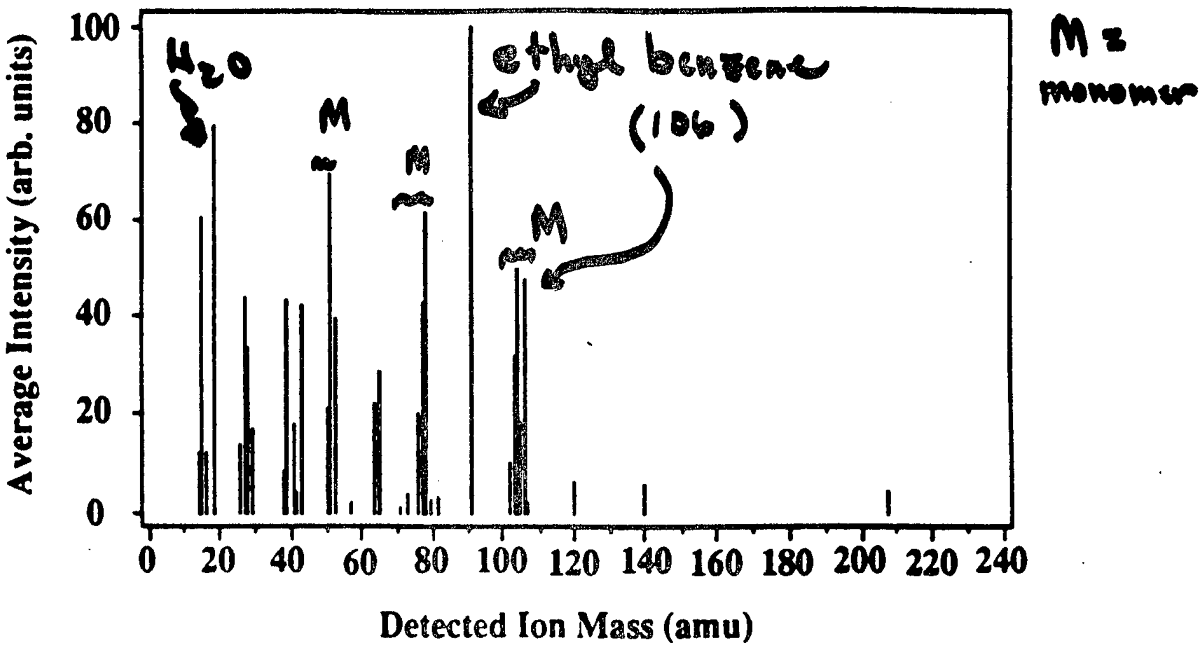

Primarily Occluded Gases.

Introduced Ar and D_2O by "soaking"

Mass 40 During the Tensile Fracture of Argon Sorbed Polystyrene

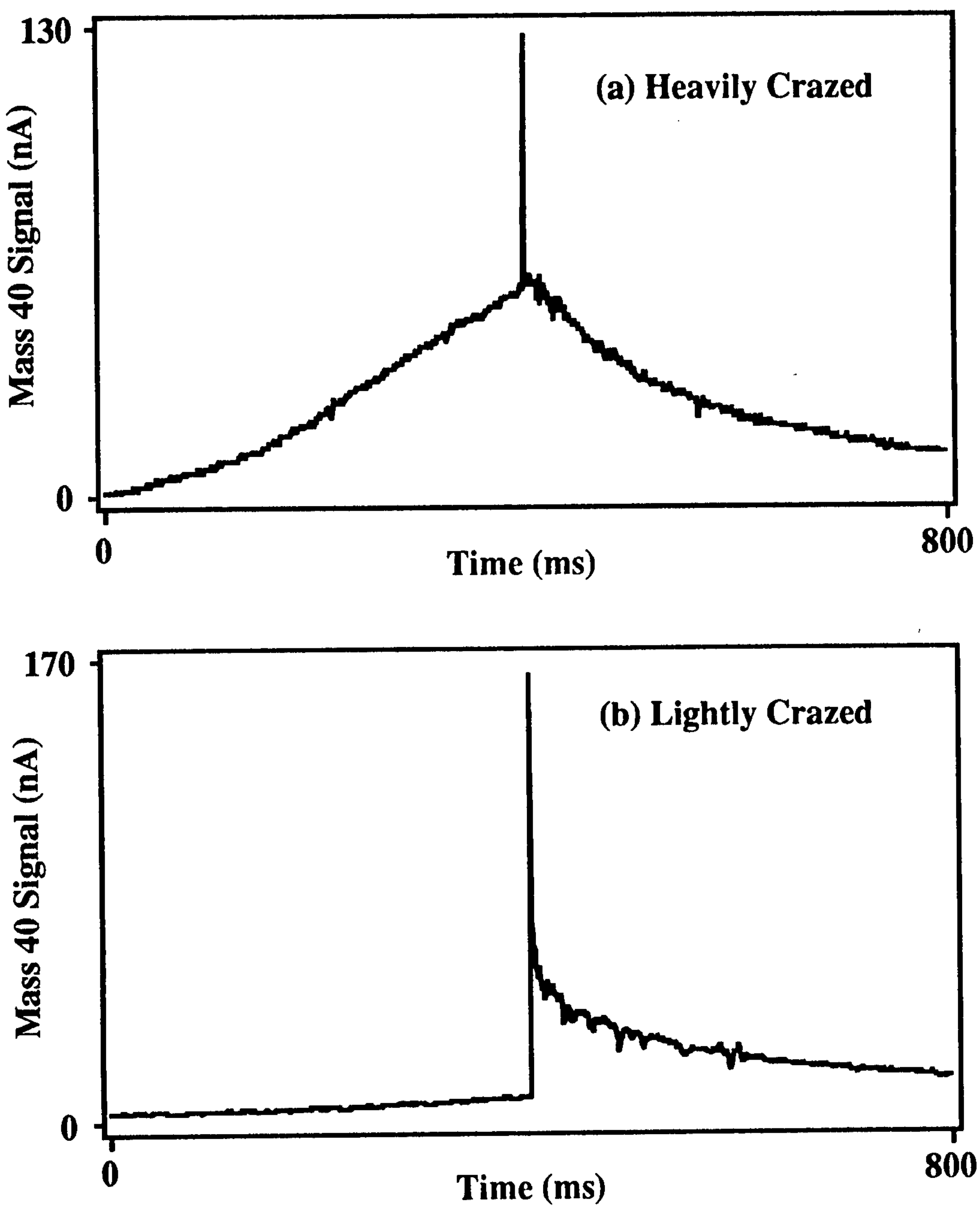

91-461 & 462 Mass 40 (Argon) during the tensile fracture, 461 (top) shows a lot of crazing and the final fracture surface is smooth. 462 (bottom) does not show as much crazing and has a more classic fracture (mirror, mist, hackle zone) appearance. Strain rate is 0.07 mm/s for each.

Ar Emission and Craze Volume in Polystyrene

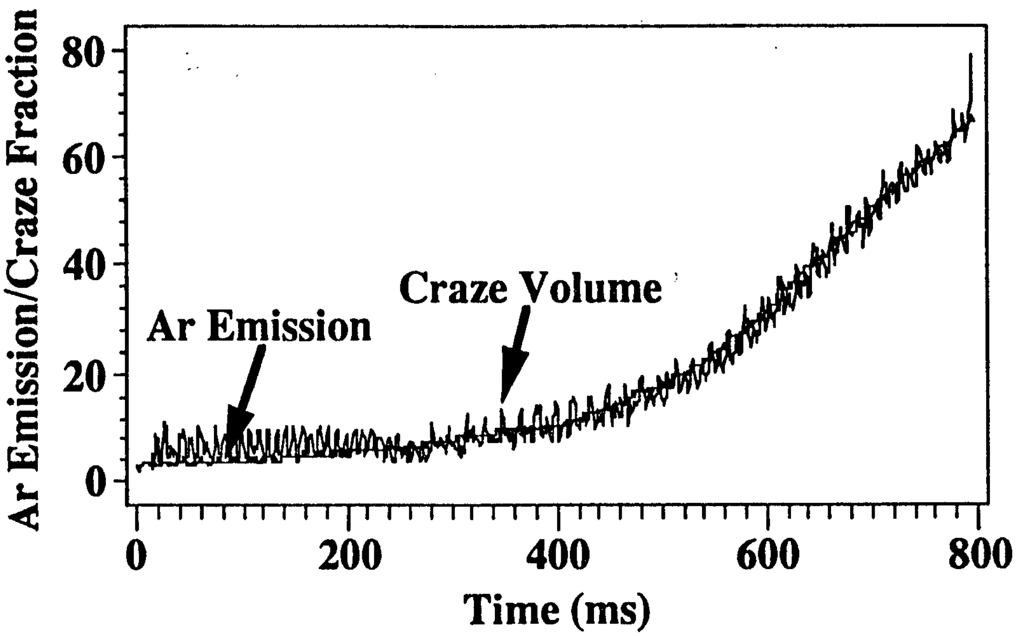

Craze volume estimate at constant strain rate:

Assume all deviations from elastic behavior due to craze formation.

$$\text{Load} = E\,(\varepsilon_{\text{applied}} - \varepsilon_{\text{craze}})$$

where E is Young's modulus. The strain due to the craze is proportional to the craze volume, where

$$\varepsilon_{\text{craze}} = \frac{\text{Load}}{E} - \varepsilon_{\text{applied}}$$

The Ar emission intensity is proportional to the total craze volume.

High Impact Polystyrene

XL 8023 (Styron)

~8% BR

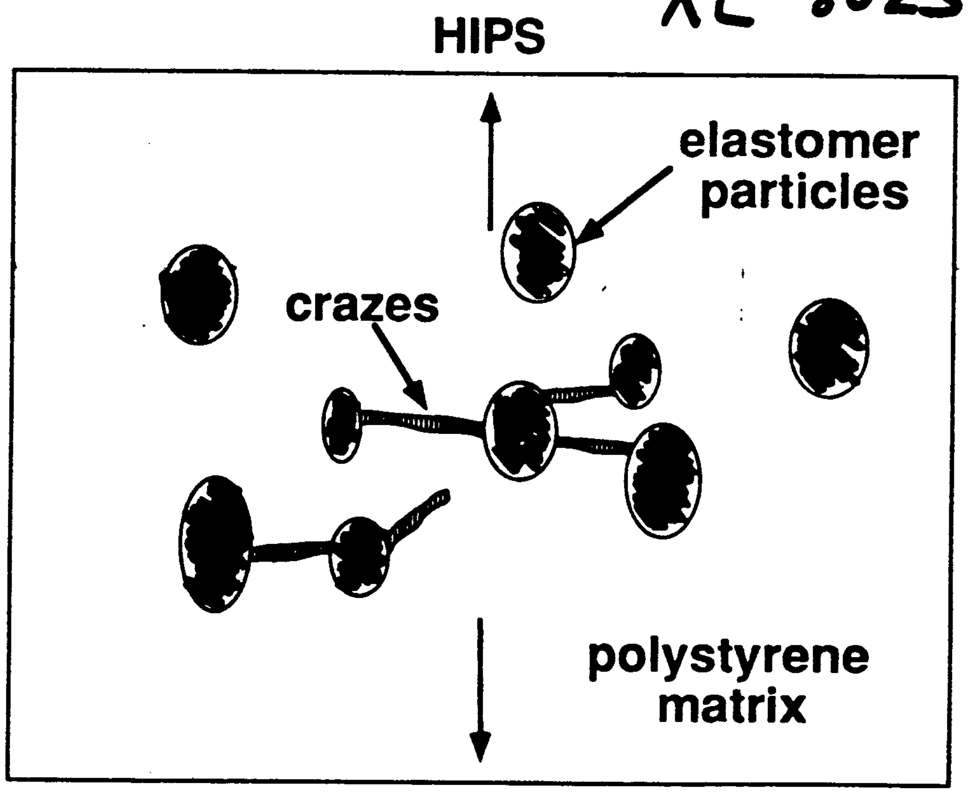

Ar Emission During the Deformation and Fracture of HIPS

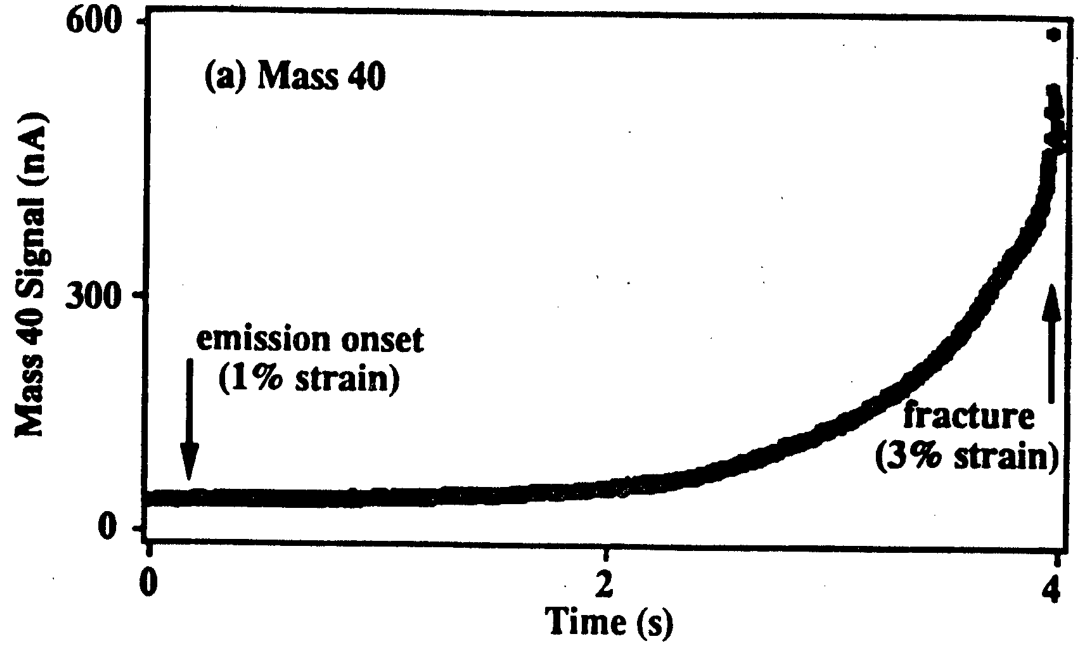

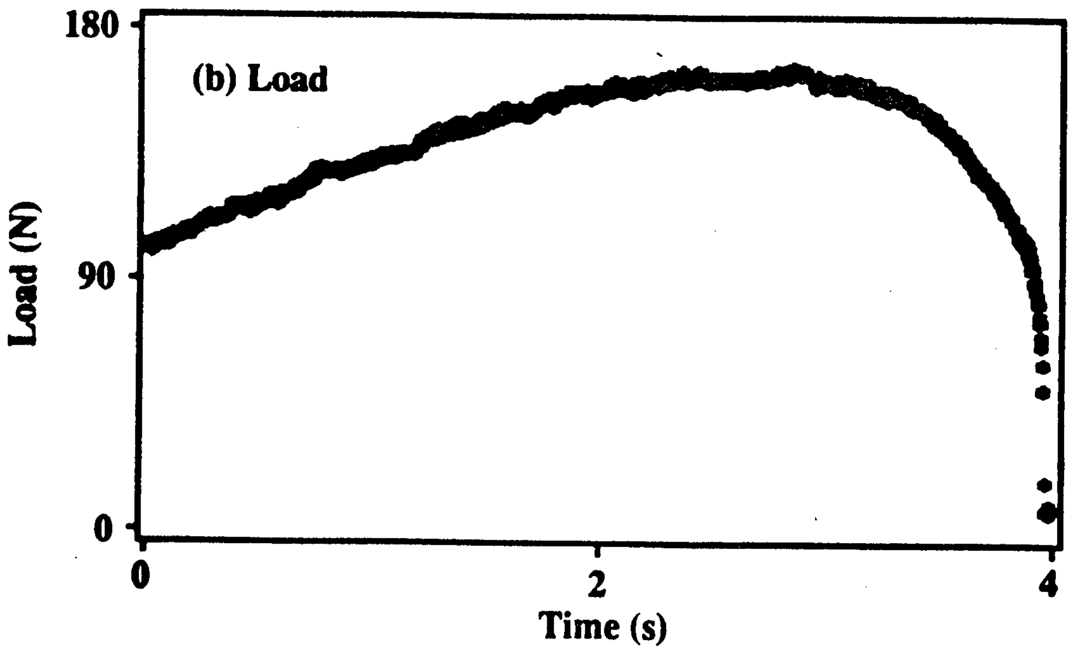

Craze Volume Fraction and Mass 40 Signal

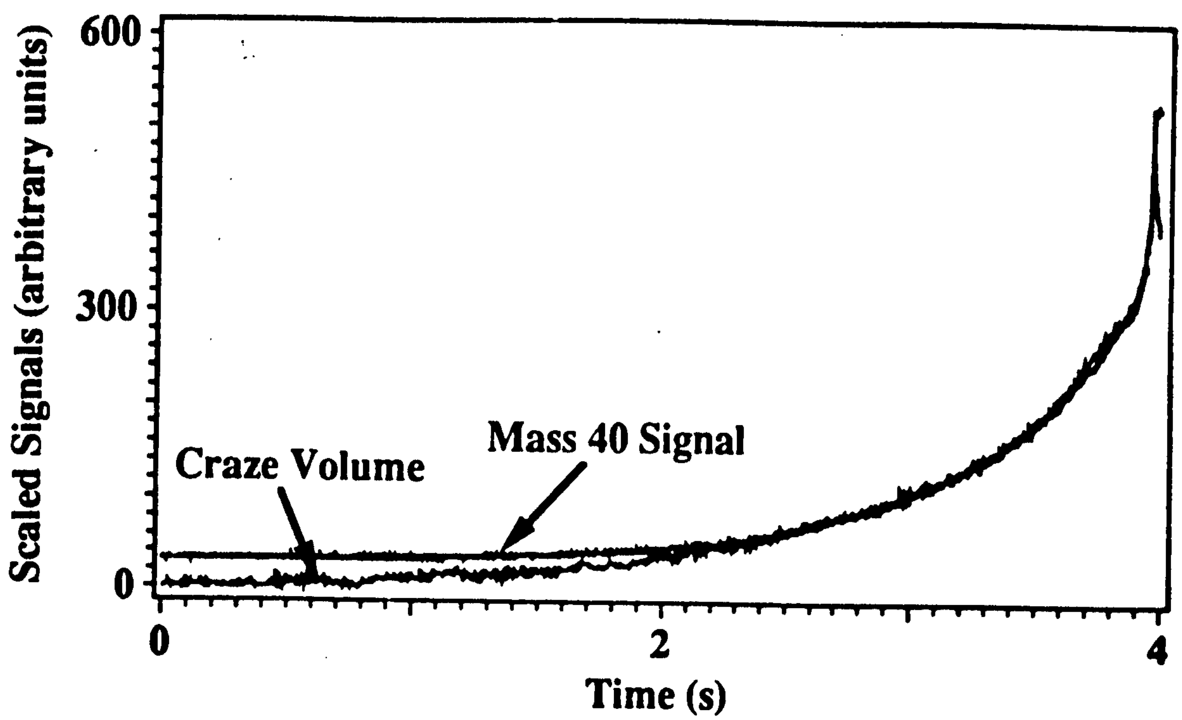

initial slope
(extrapolate)

$$\frac{V_{craze}}{V_{sample}} \propto \varepsilon_{craze} \propto \varepsilon_{total} - \varepsilon_{uncrazed}$$

elastic

$$\propto \dot{L}_{initial} \cdot t - L$$

ε_{total} : Total strain at constant strain rate.

ε_{craze} : "Plastic" strain in crazed material.

$\varepsilon_{uncrazed}$: Elastic strain in uncrazed material.

$\dot{L}_{initial}$: Initial slope of load curve.

L : Load.

Bond Energies of Various Bonds of Polycarbonate

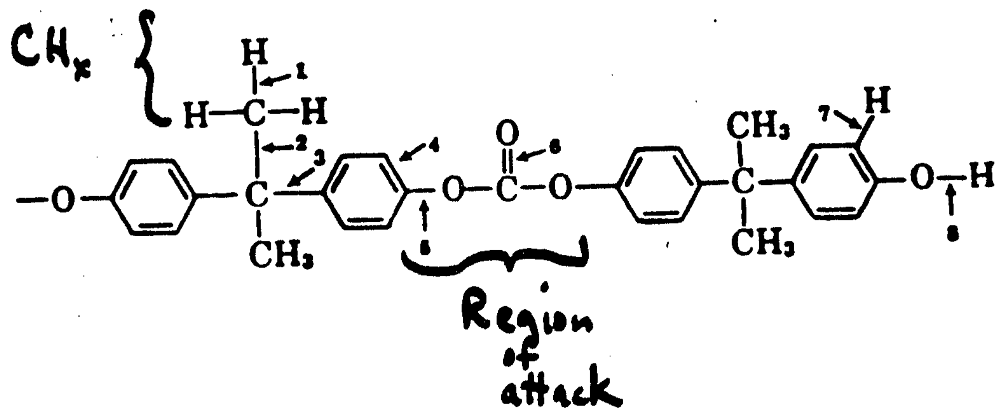

Polycarbonate Structure

No.	Bond	Bond energy, kcal./mole
1	C—H	98.7
2	$C—CH_3$	60.0
3	C—C	82.6
4	C=C	147.5
5	C—O	85.5
6	C=O	176.0–179.0
7	C=C—H	102.0
8	O—H	101.5

L. H. Lee, J. Poly. Sci. A 2, 2859 (1964) review paper.

Soaked in Liquid D_2O for 24 hr - 1 week, Rm T
In Vacuum 24 hr.

Mass 20 and Load During the Tensile Fracture of Polycarbonate

Exposure + heat

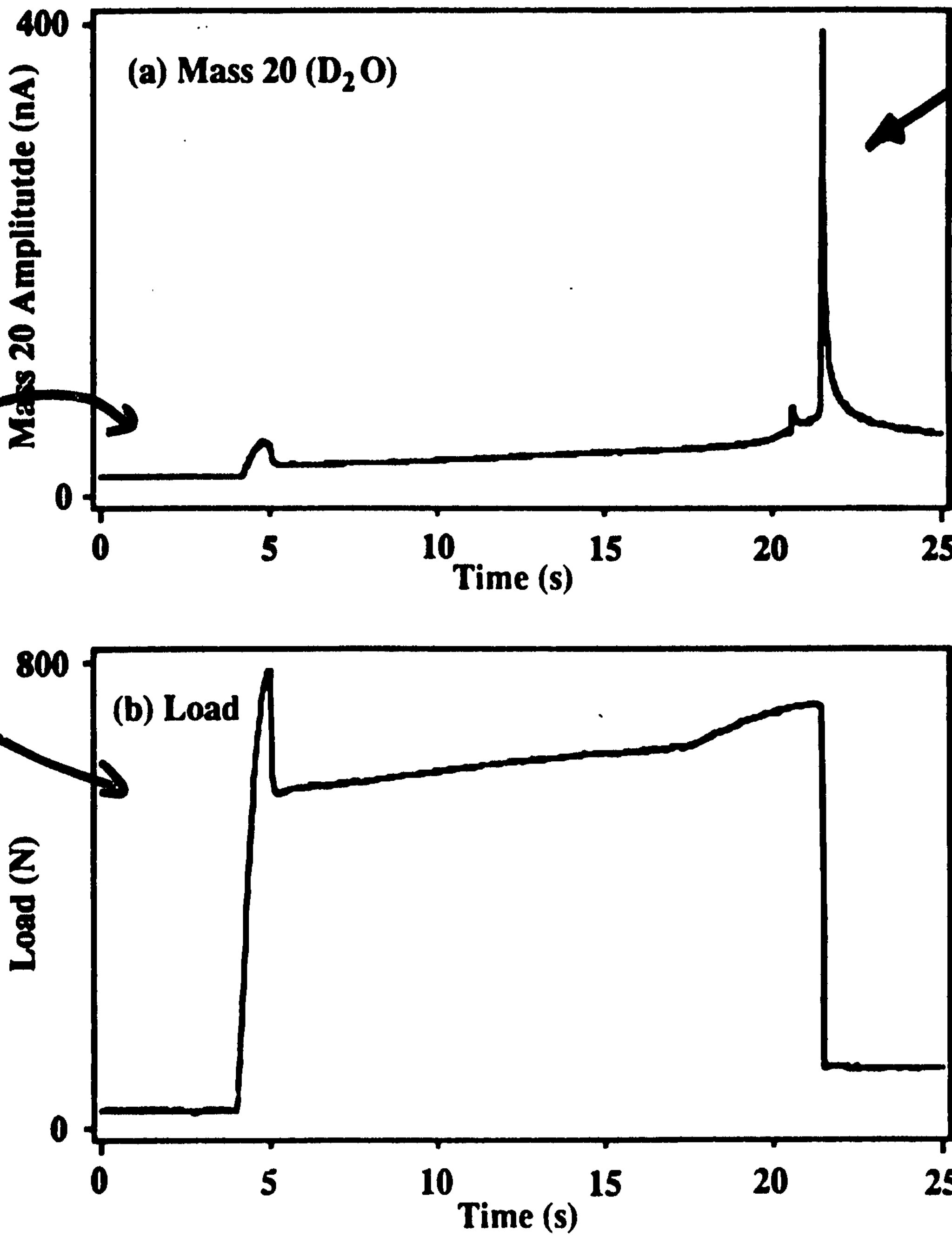

Smaller peak for Lower Y'

Mass 20 and Load During the Tensile Elongation of Polycarbonate

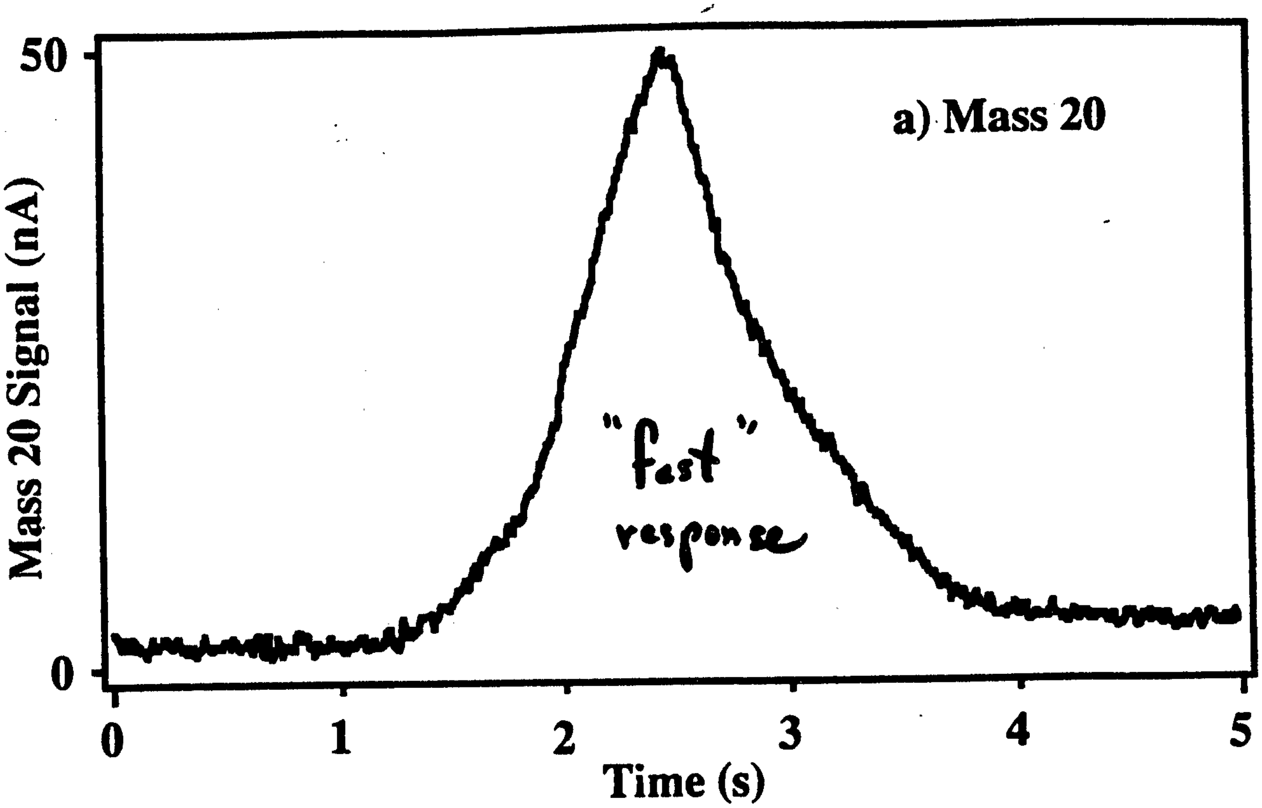

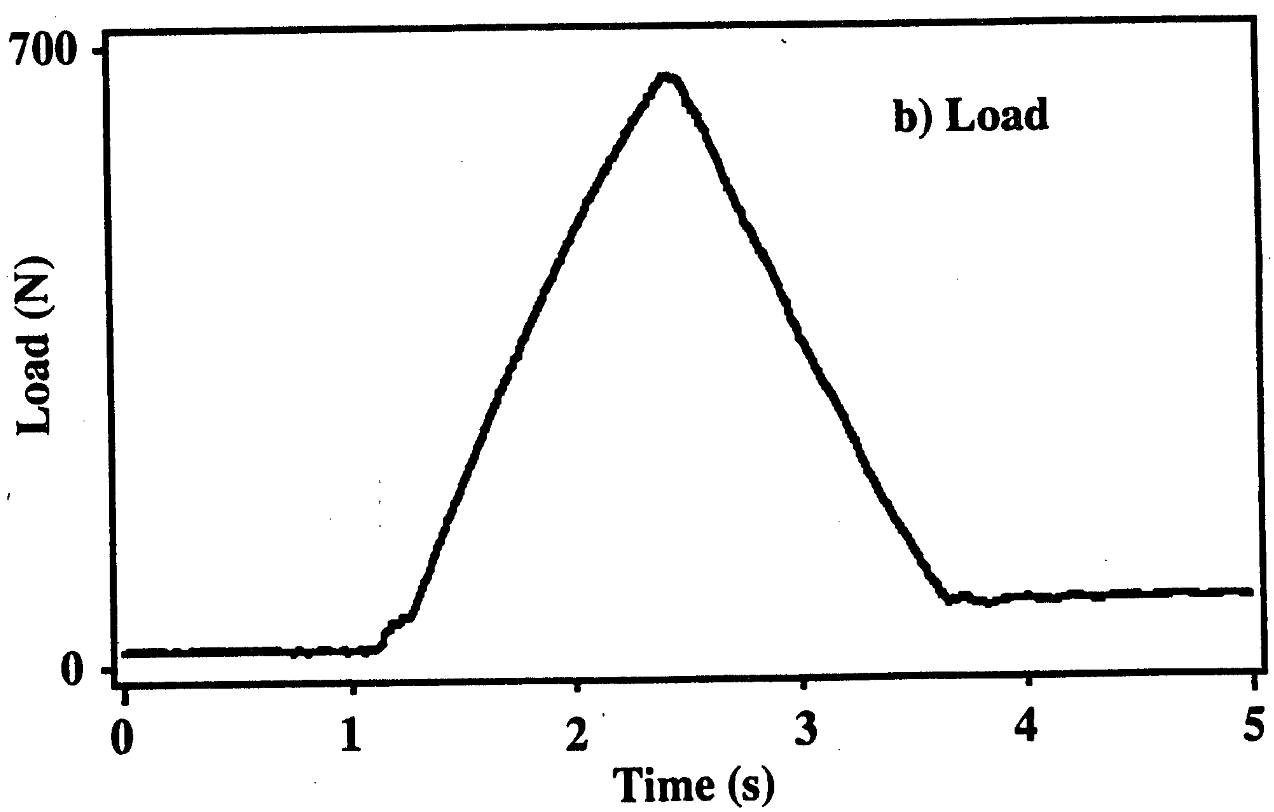

Mass 20 and Load During the Elongation of Polycarbonate

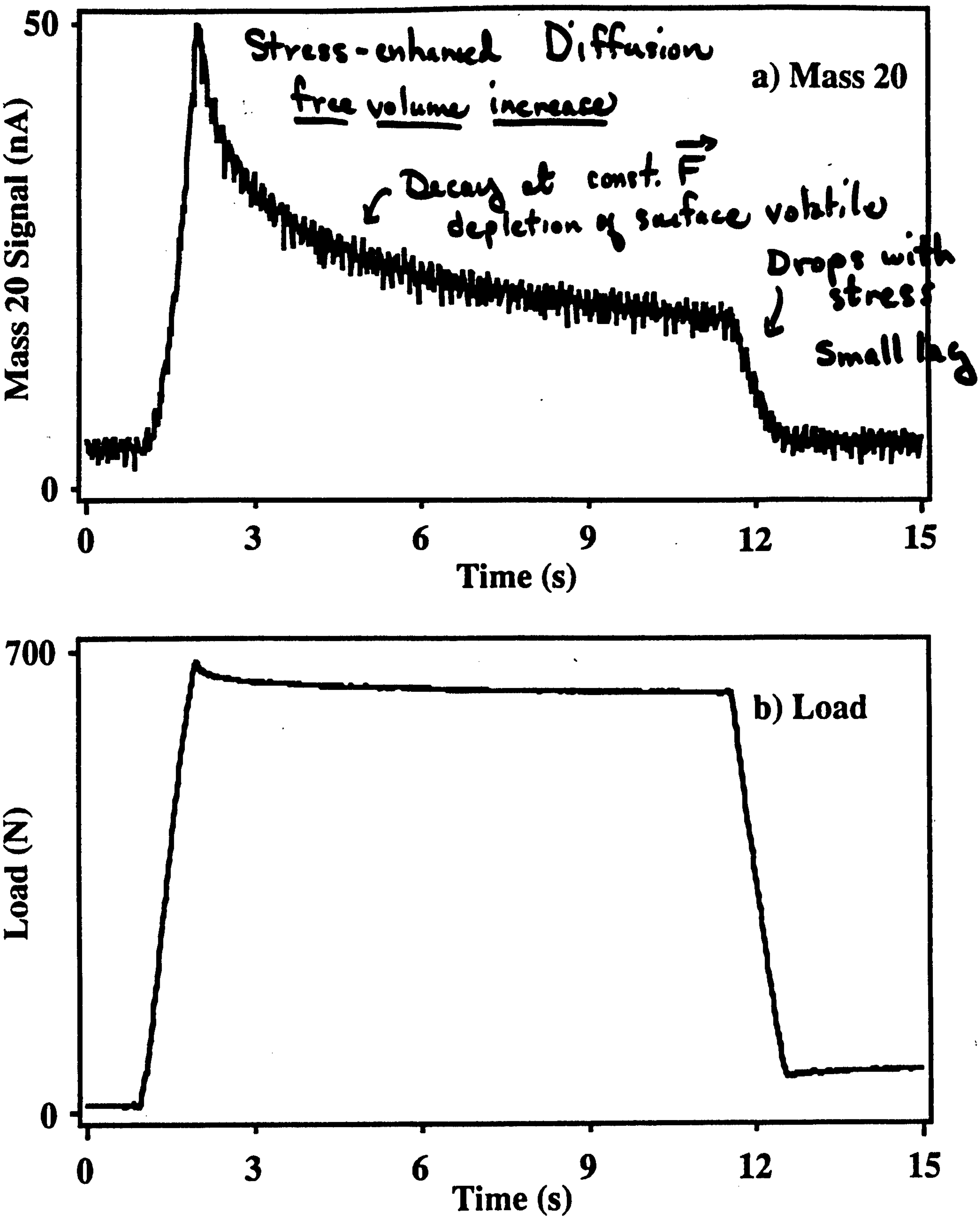

Mass 20 and Load During the Tensile Elongation of Polycarbonate

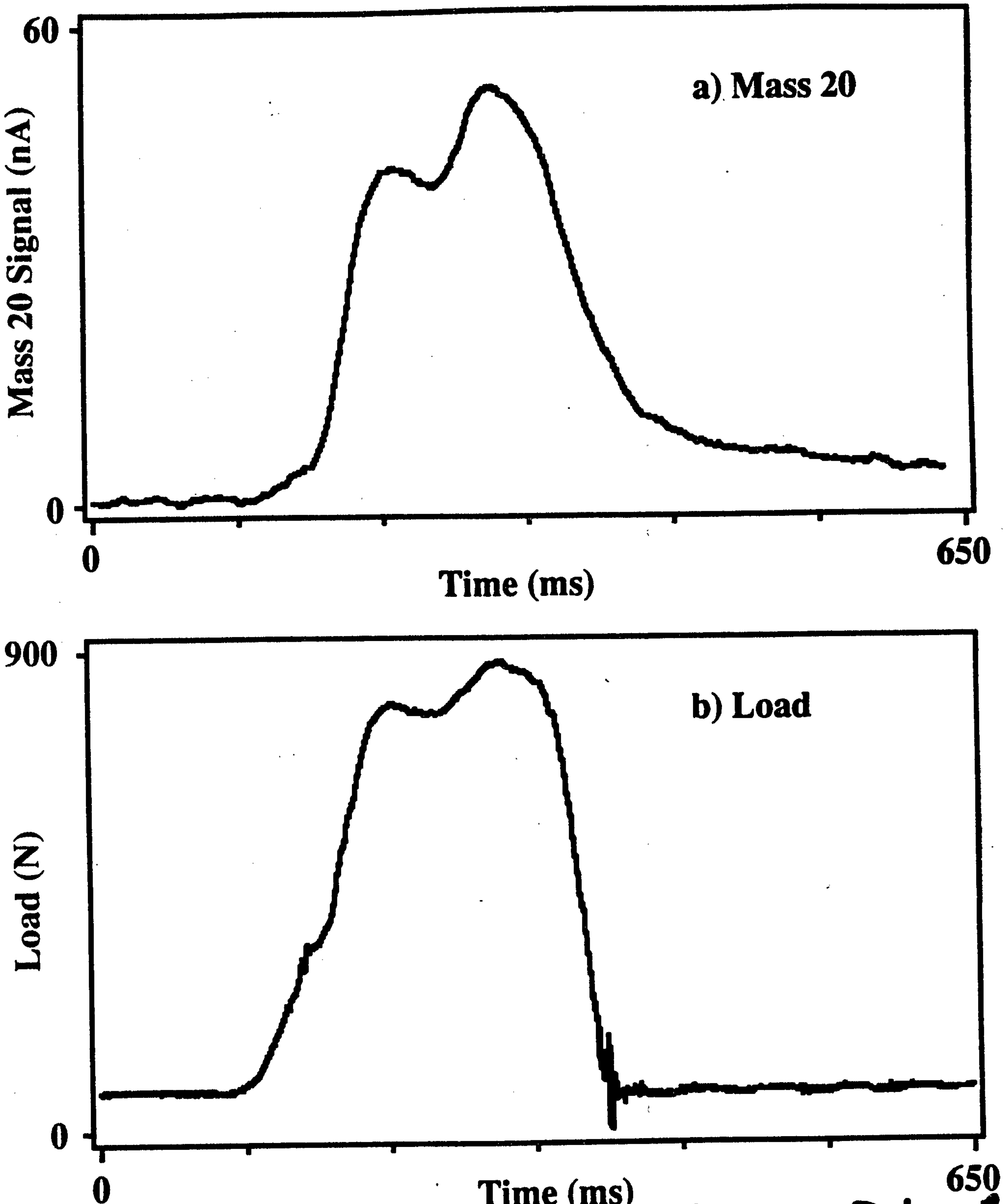

<u>NOT</u> <u>Heating</u> Induced. Matsuoka + Bair Report $\Delta T < 0$ as load reaches upper yield pt. (Near M20 peak; M20 drops as load drops due to plastic def.)

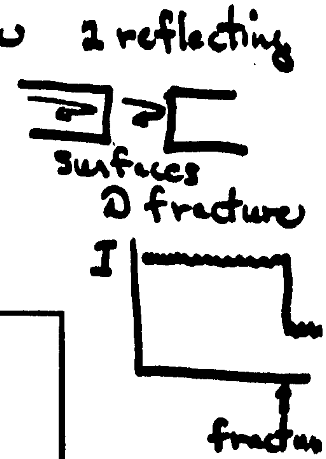

Timing Light and Load from Fracture of Polycarbonate

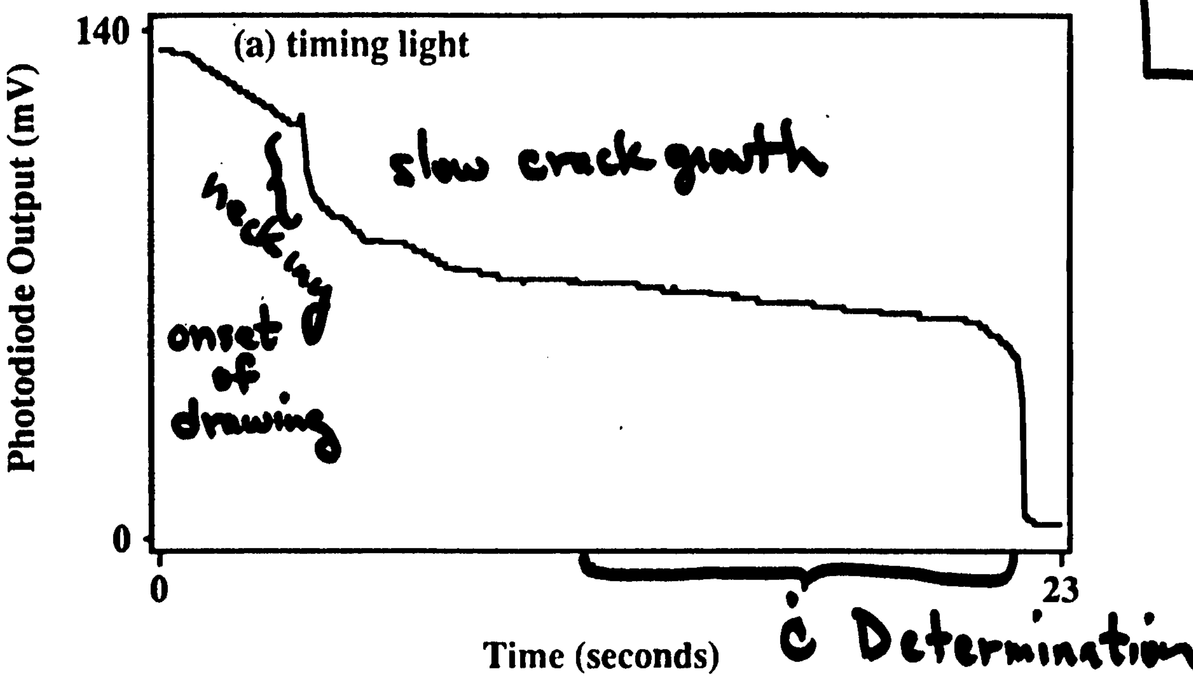

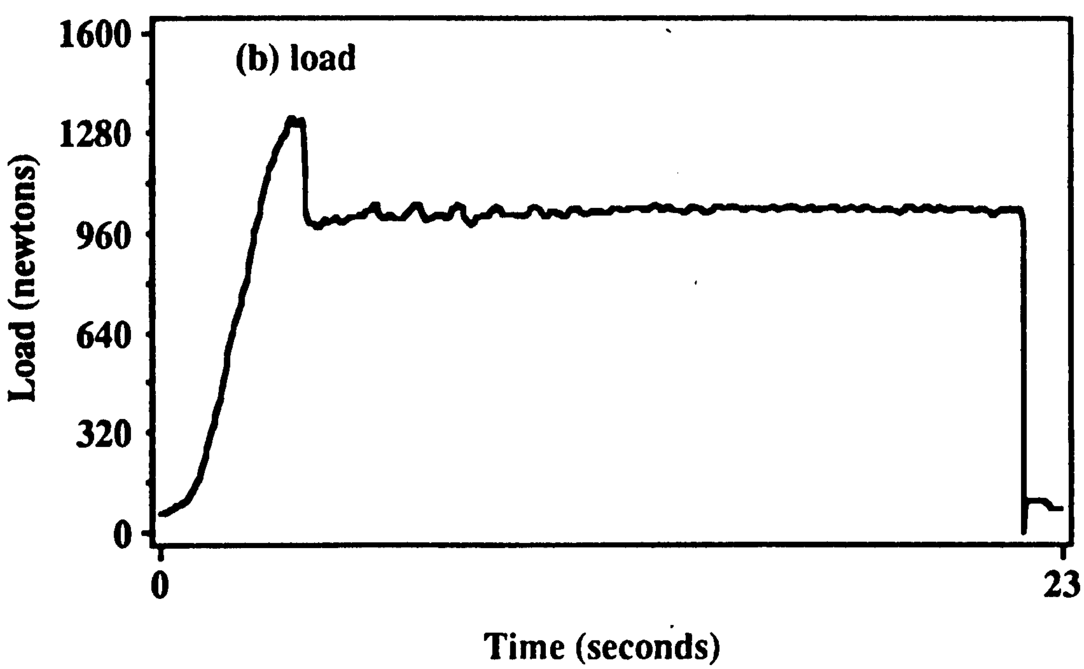

EE and Timing Light Signal from Fracture of Polycarbonate

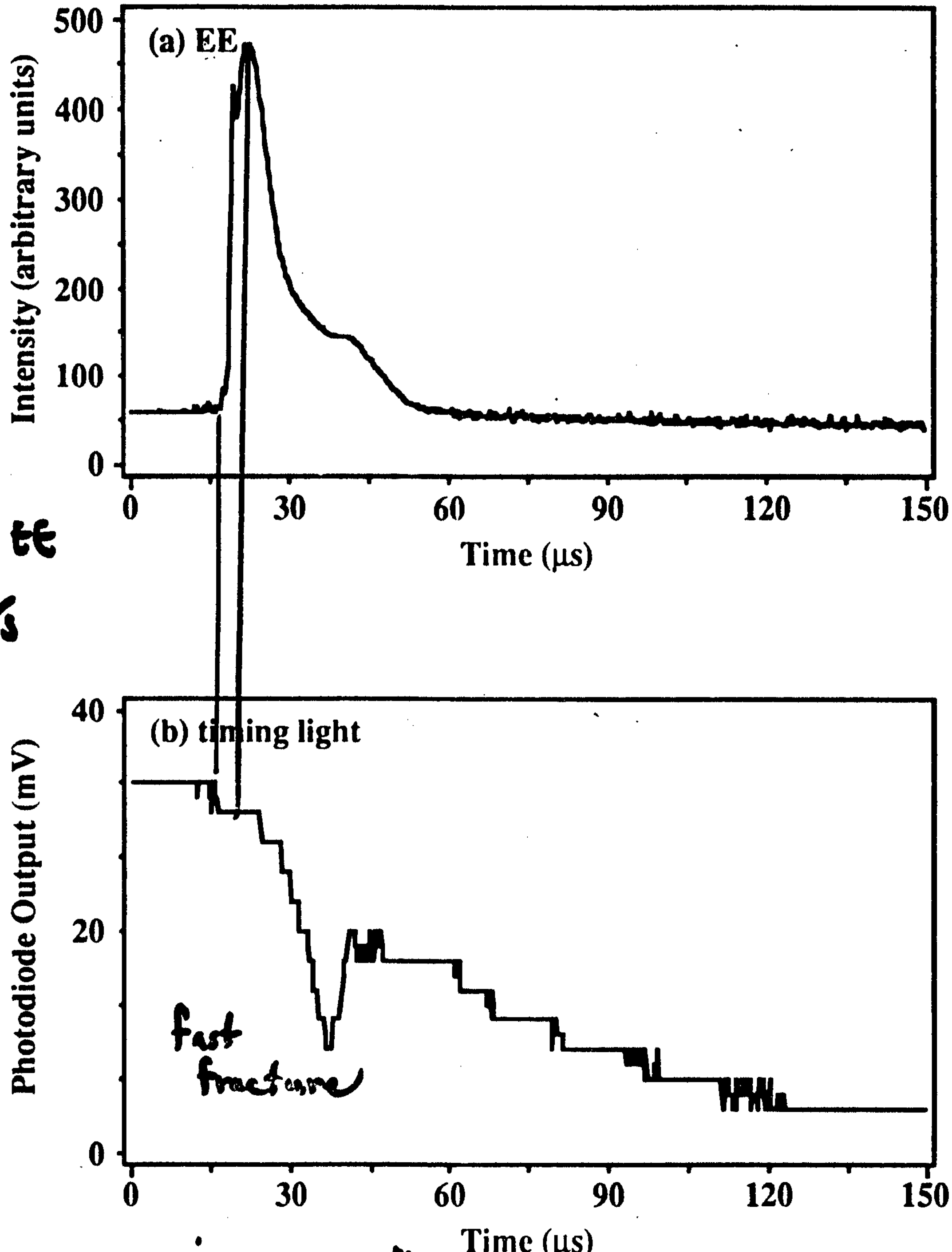

$\dot{C}_{onset\ EE}$ ~ 8 m/s

$\dot{C}_{max}$ ~ 150 m/s

901307

Crack Velocity during Tensile Loading of PC Inferred from Light Transmission Measurements (LED Source)

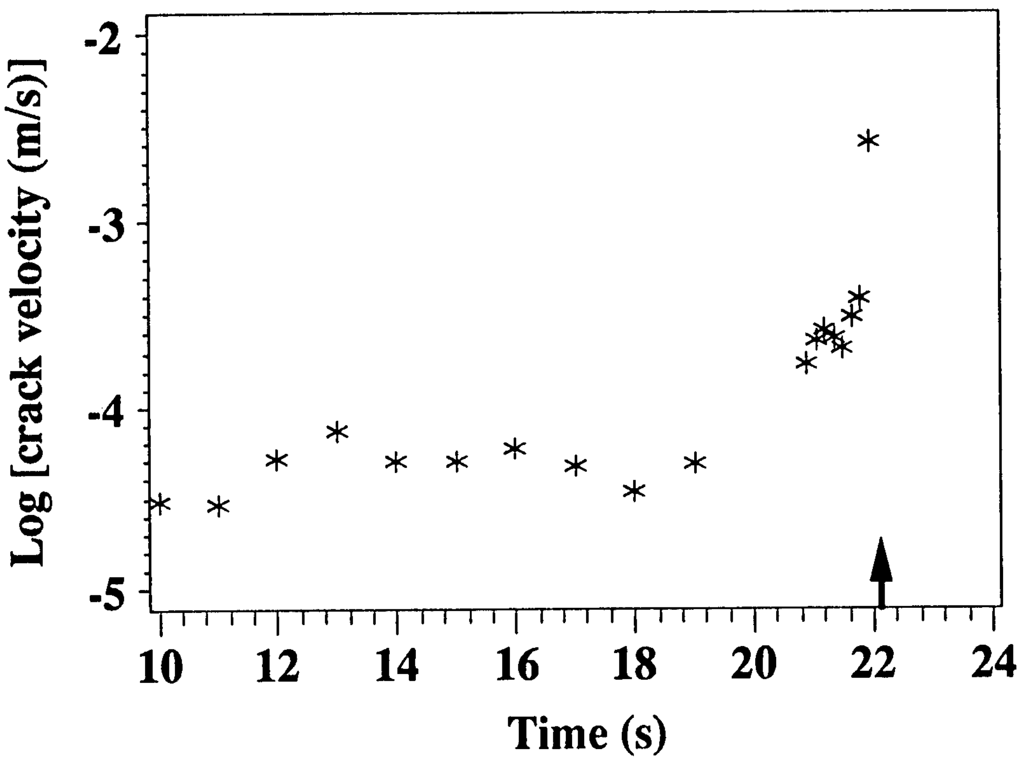

Geometry of Crack Growth

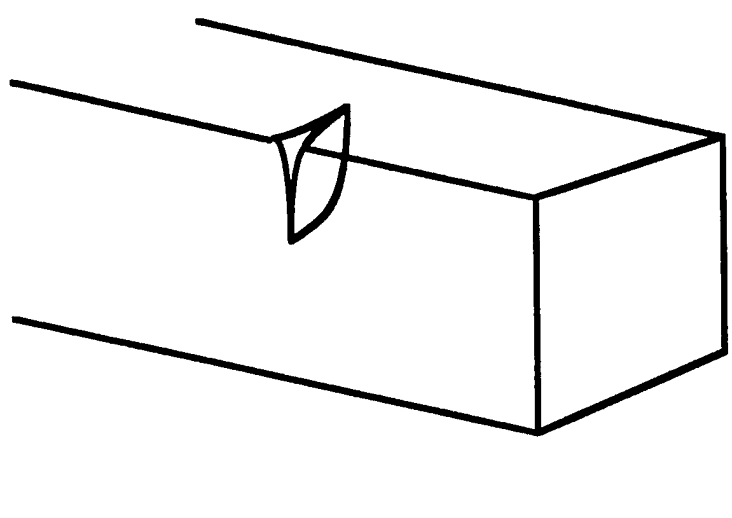

Small Bursts in Total Alkali Emission from NaCl

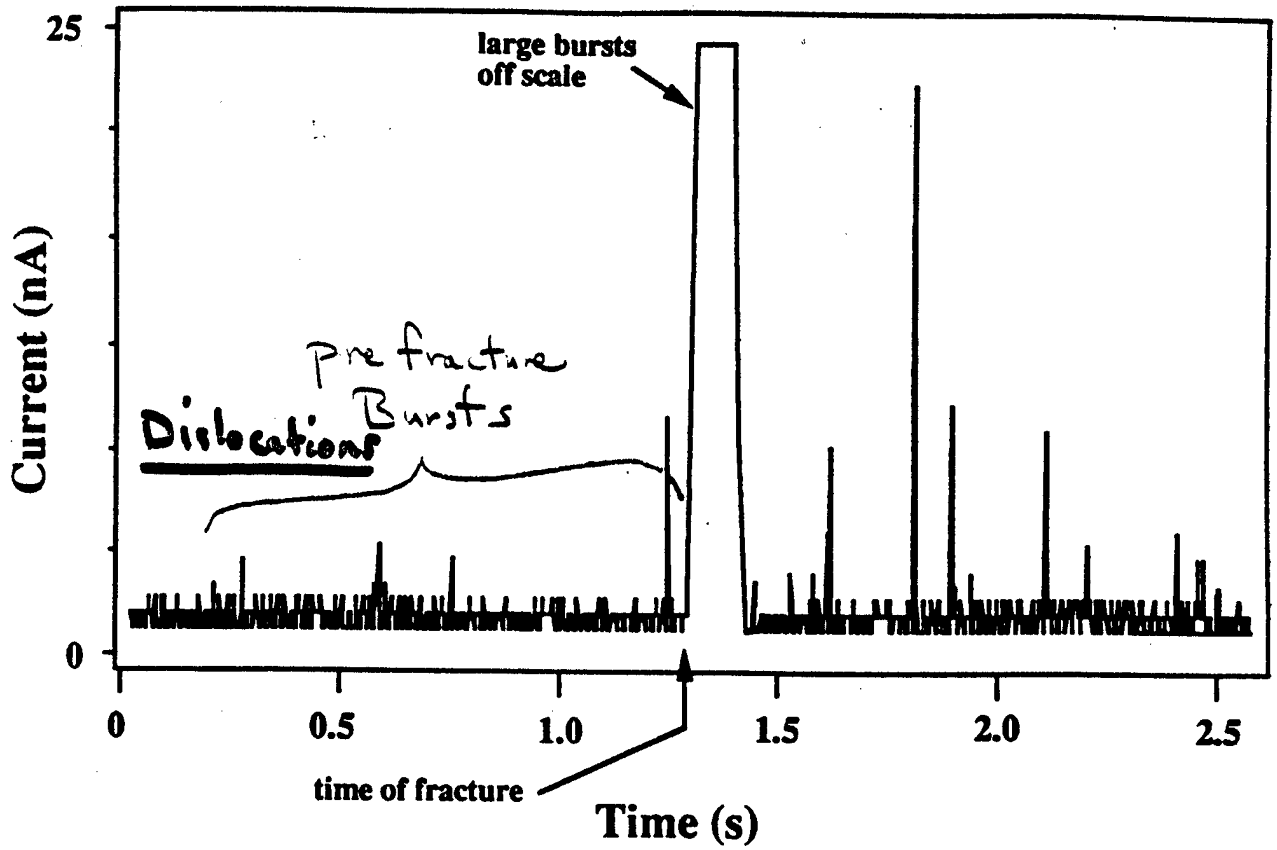

$\langle n_{\text{LARGE BURSTS}} \rangle \sim 4$ / FRACTURE

$\langle$ # of alkali atoms detected $\rangle \sim 10^8$ / Burst

EVIDENCE OF O_2 EMISSION DUE TO MICROCRACKING IN SINGLE CRYSTAL MgO

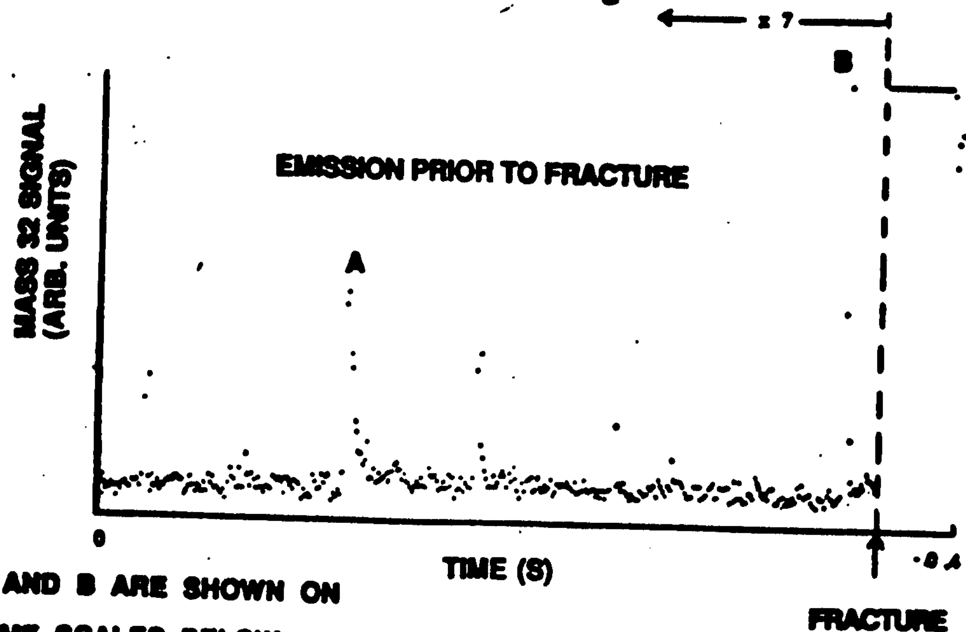

PEAKS A AND B ARE SHOWN ON FASTER TIME SCALES BELOW.

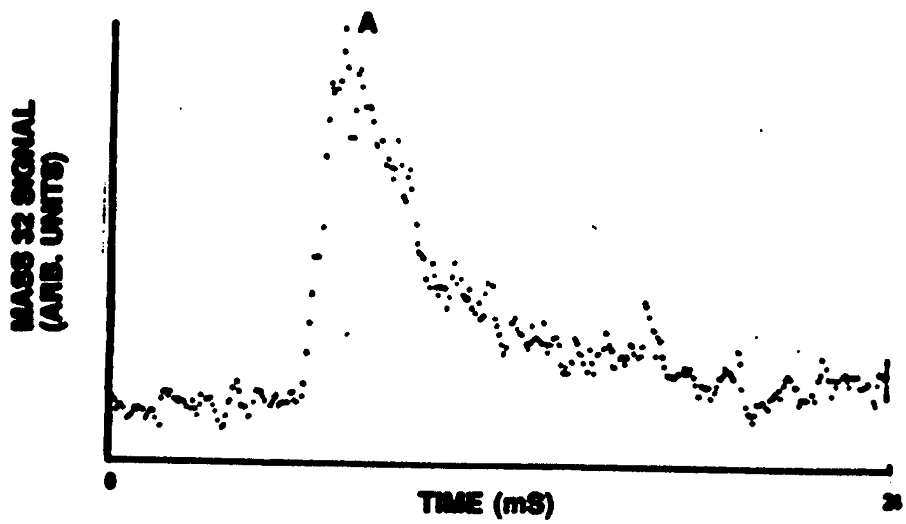

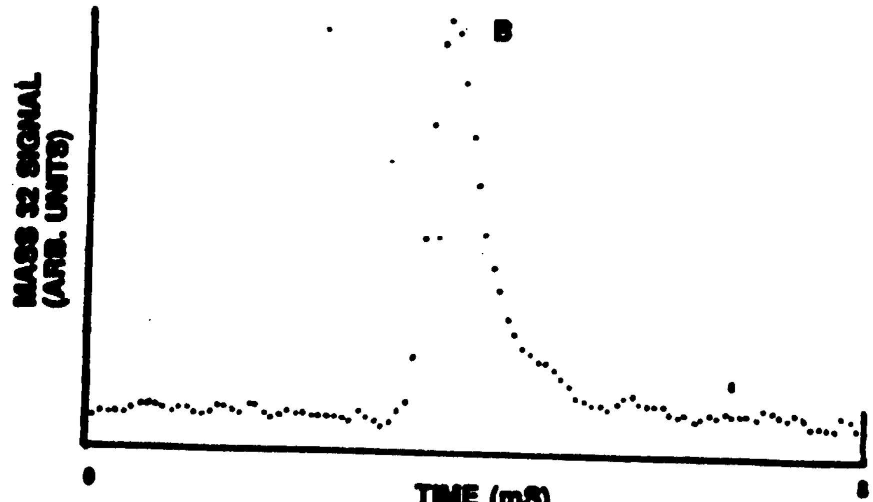

O_2 PRE-CURSORS FROM MgO

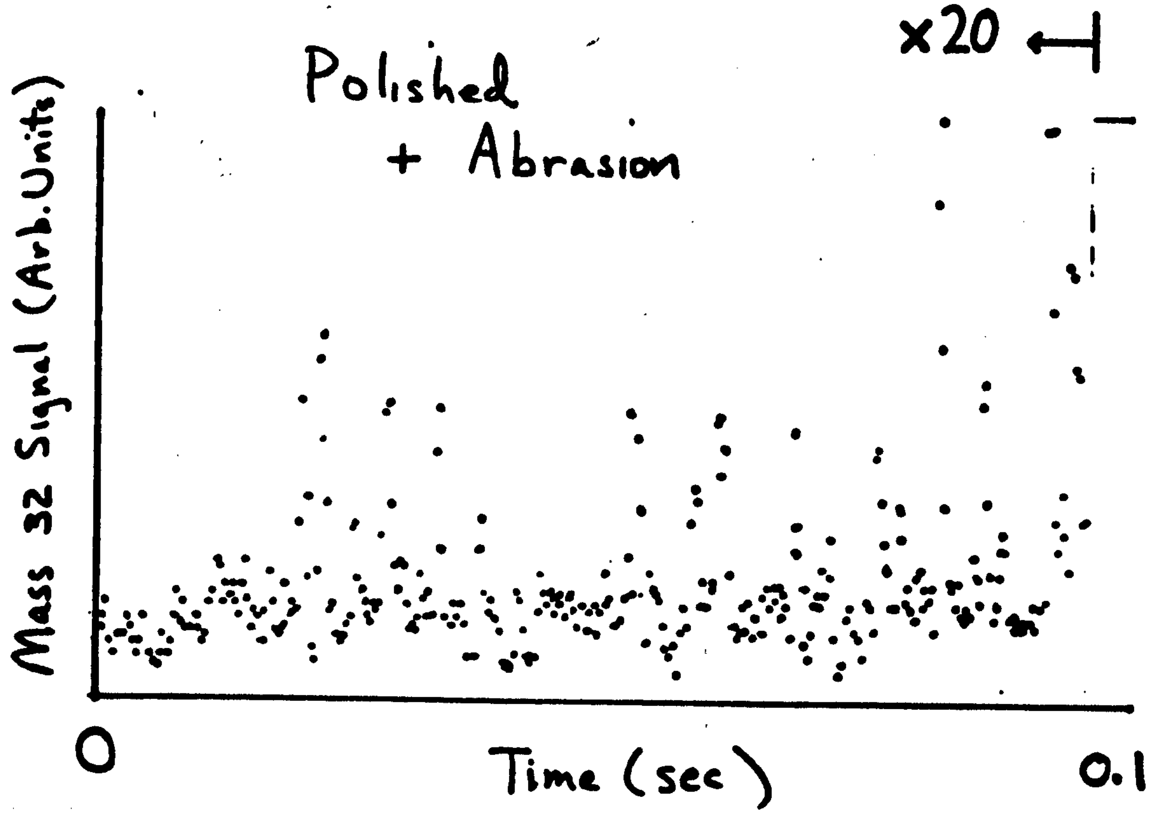

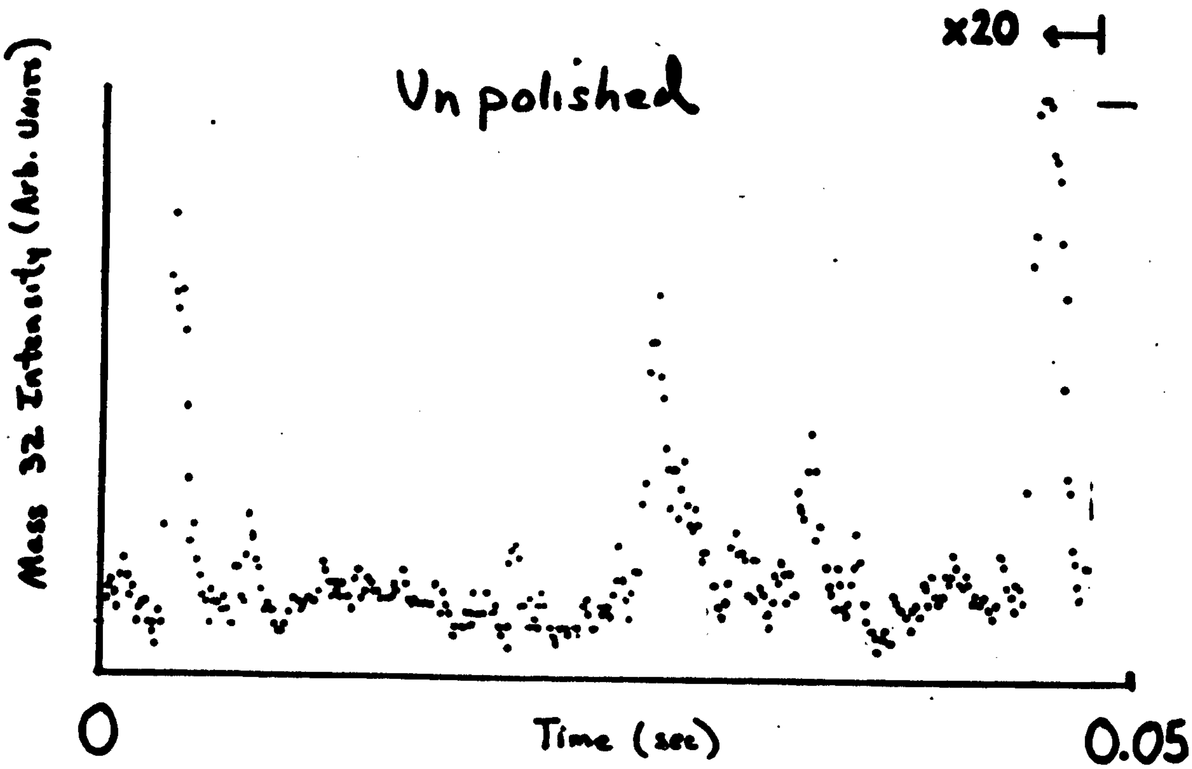

Interfaces

(Evans, Ruhle, Kinloch, Mattox)

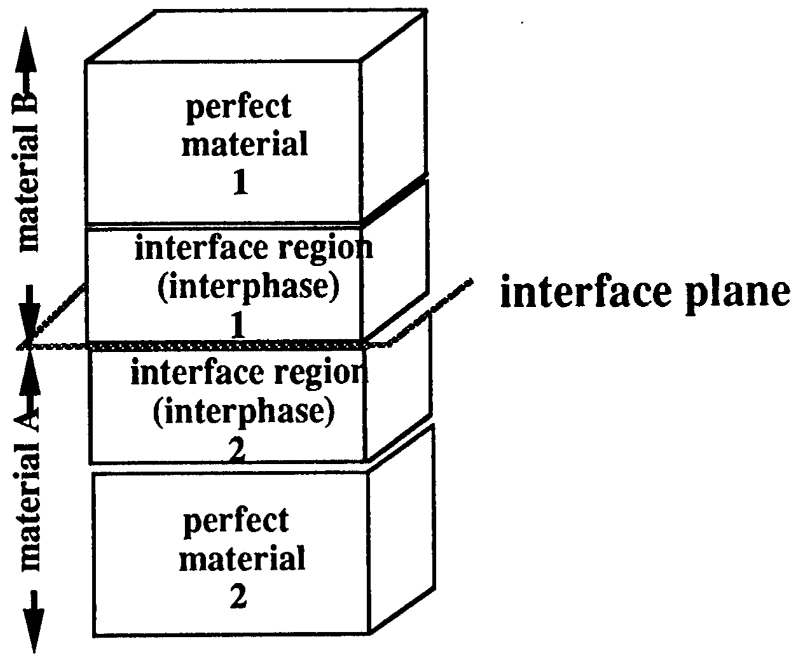

Defects at or near interfaces:

chemical defects	segregation chemical reactions chemical gradients interphases (reaction products)
structural defects	facets, steps misfit dislocations lattice dislocations impurities pores precipitates

Chemical Defects often reduce W_{ad} (Work of adhesion (reversible work/area to separate the bond into two free surfaces)

$$W_{ad} = \gamma_1 + \gamma_2 - \gamma_{12}$$

where γ_1, γ_2 = free energies of relaxed surfaces; γ_{12} = energy of a relaxed interface between the two materials. W_{ad} cannot be measured directly.

In practice use, equilibrium contact angle, θ, measured:

$$W_{ad} = \gamma_1 (1 + \cos\theta)$$

Fracture Resistance, $\Gamma_{interface} > W_{ad}$ (typically 1 J/m^2).

$\Gamma_{interface}$ ~ Metal/ceramic ~ 50-300 J/m^2. Due to dissipative processes: plastic deformation of one or both materials. Important to realize that $\Gamma_{interface}$ usually scales with (provided a strong singularity remains at the crack tip) W_{ad}: i.e., the stronger the adhesion, the more plastic deformation of one or both materials .

Internal Stress: often due to differences in α (thermal exansion).

Phase Transitions in one component.

Issues

1. **Detection and Characterizations of Defects**
2. **Description and Kinetics of Evolution of Damage**
3. **Materials Design to Counter Degradation**
4. **Statistical Physics:**
   - **Concepts:**
     - Fractals
     - Self-Organized
     - Criticality
     - Scaling Phenomena

5. Experimental Advances

- **Sensitivity to "Differences"**
  - Perfect vs. Flaws
  - Defects (t)
- **Surface vs. Interior Phenomena**
- **Probes in Hostile Environments**
  - Temperature
  - Atmosphere/Chemical
  - Radiation

6. Modeling Efforts

- **Global**
- **Atomic**

TECHNICAL PRESENTATION

"Hysteresis and Incremental Collapse of Structures"

A Paradigm for the Fatigue
Strength of Metals

BY

Professor S. A. Guralnick
Dept. of Civil Engineering
Illinois Institute of Technology

OBJECTIVES

- TO CORRELATE FATIGUE AND HYSTERESIS BY RECOGNIZING THE PROCESSES WHICH BEGIN WITH MICRO-IMPERFECTIONS, PROGRESS THROUGH MACRO-IMPERFECTIONS AND CULMINATE IN FATIGUE RUPTURE.

- TO CORRELATE ACOUSTIC EMISSION PHENOMENA WITH THE INCEPTION OF THE DAMAGE GROWTH PROCESS WHICH ULTIMATELY RESULTS IN FATIGUE RUPTURE.

APPROACH

- TO INVESTIGATE THE COMPLETE EVOLUTION OF HYSTERESIS, FROM FIRST CYCLE TO LAST CYCLE, BY MEANS OF EXPERIMENTS PERFORMED UPON STEEL SPECIMENS SUBJECTED TO CYCLIC LOADS ($R = 0$ AND $R = -1$).

STRESS AND CYCLIC STRAIN PARAMETERS

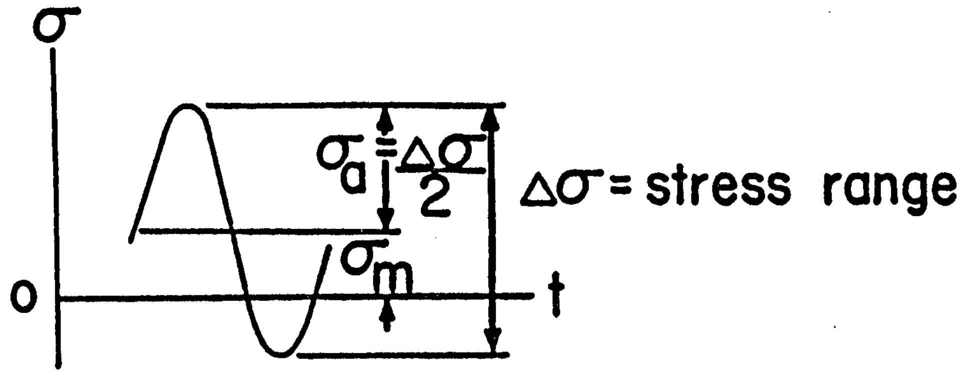

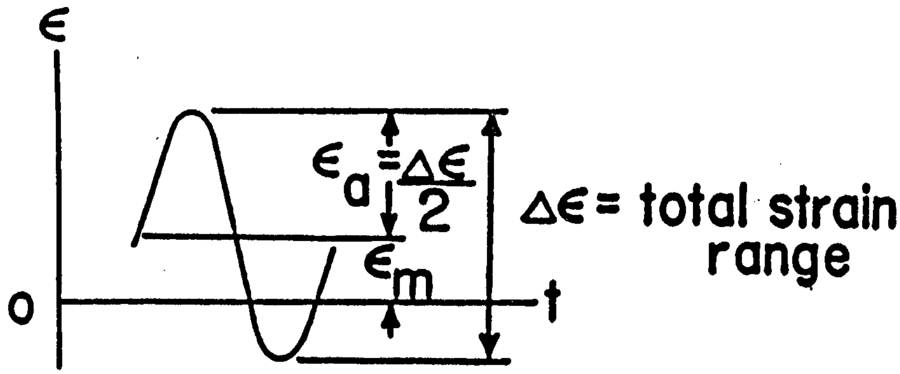

STRUCTURAL SCALE

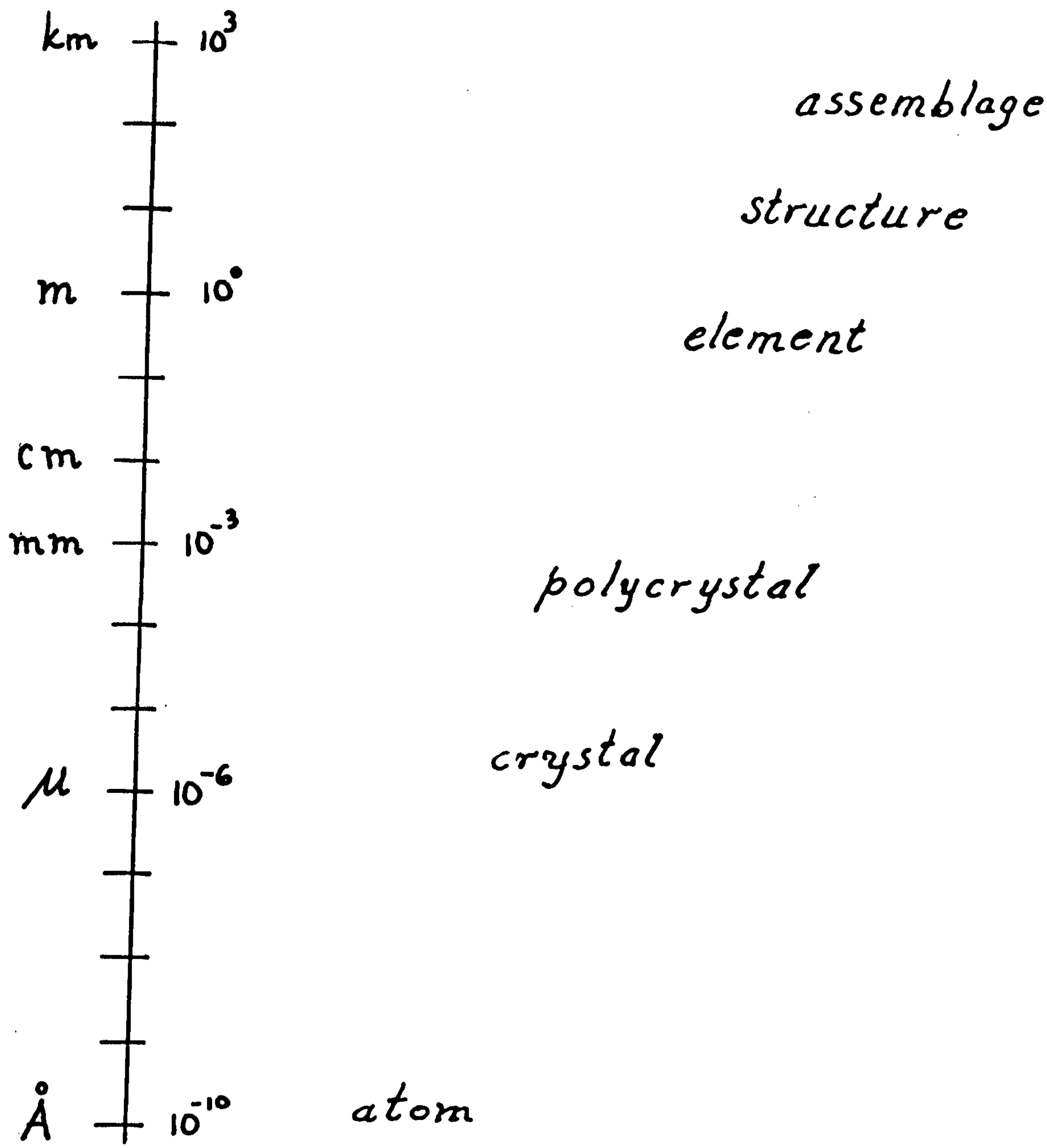

POSSIBLE DEFECTS IN METAL CRYSTALS AND POLYCRYSTALS

CRYSTAL DEFECTS

- POINT DEFECTS
  - ATOMS INSERTED OR SUBSTITUTED IN SOLID SOLUTIONS OR VACANCIES
- LINE DEFECTS (DISLOCATIONS)
  - EDGE DISLOCATIONS
  - SCREW DISLOCATIONS
  - DISLOCATION LOOP OR LINE
- SURFACE DEFECTS (SURFACES OF SEPARATION)
  - DISLOCATION LOOPS
  - TWIN CRYSTAL BOUNDARIES

POLYCRYSTAL DEFECTS

- SURFACE DEFECTS (SURFACES OF SEPARATION)
  - CRYSTAL OR GRAIN BOUNDARIES
  - INTERFACES BETWEEN TWO PHASES (EXOGENOUS AND ENDOGENOUS)
- COHESION DEFECTS
  - MICROCRACKS AT CRYSTAL BOUNDARIES
  - CAVITIES BETWEEN CRYSTALS

POSSIBLE MICROMECHANICAL RESPONSES OF METALS TO CYCLICALLY-VARYING LOADS

ELASTIC DEFORMATIONS (REVERSIBLE)

- VARIATION IN INTERATOMIC SPACING

PLASTIC DEFORMATIONS (IRREVERSIBLE)

- SLIP ALONG CRYSTALOGRAPHIC PLANES OF MAXIMUM ATOMIC DENSITY IN SINGLE CRYSTALS
- PLANAR GLIDE IN SINGLE CRYSTALS
- DEFORMATION TWINNING AND/OR KINKING
- SLIDING OR SLIPPING BETWEEN GRAIN BOUNDARIES

FRACTURE

- INTERGRANNULAR FRACTURE
    - MICROVOID FORMATION
    - MICROVOID COALESCING
    - GRAIN BOUNDARY CRACK AND CAVITY FORMATION
    - DECOHESION BETWEEN CONTIGUOUS GRAINS DUE TO PRESENCE OF IMPURITIES
    - SEPARATION DUE TO INSUFFICIENT NUMBER OF INDEPENDENT SLIP SYSTEMS TO ACCOMMODATE PLASTIC DEFORMATIONS BETWEEN CONTIGUOUS GRAINS
- INTRAGRANNULAR FRACTURE
    - CLEAVAGE FRACTURE

        TRANSCRYSTALLINE FRACTURE ALONG SPECIFIC CRYSTALOGRAPHIC PLANES

INFLUENCE OF NUMBER OF CYCLES OF LOADING UPON MECHANICAL PROPERTIES OF MILD STEEL IN TENSION

(AFTER PUSKAR AND GOLOVIN, 1985)

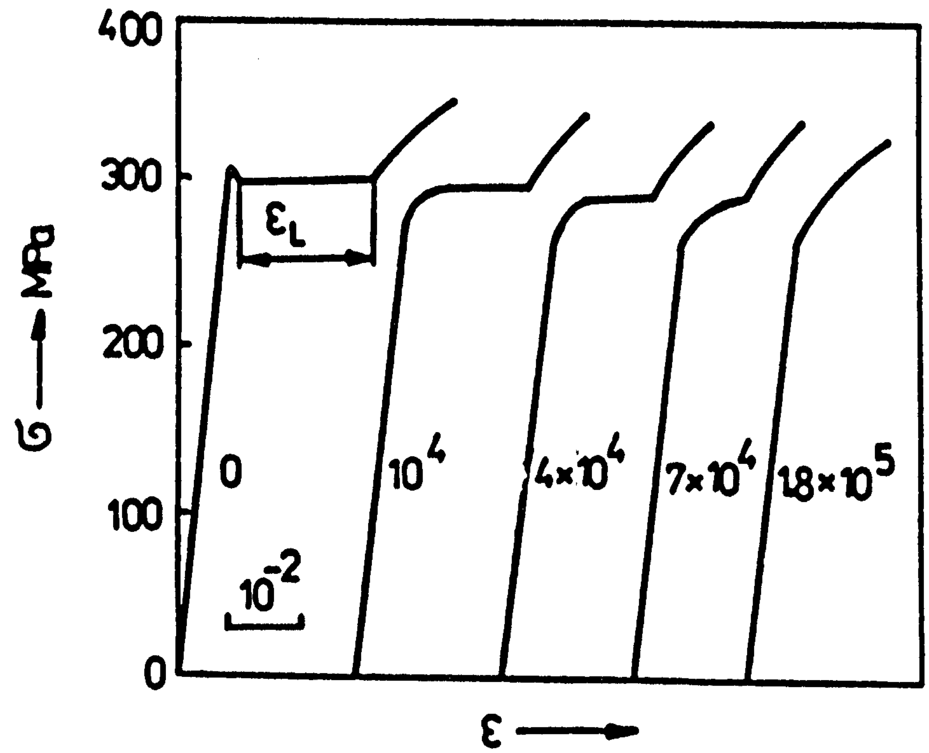

MAXIMUM STRESS VS. CYCLIC LIFE CURVES
(AFTER LEMAITRE AND CHABOCHE, 1990)

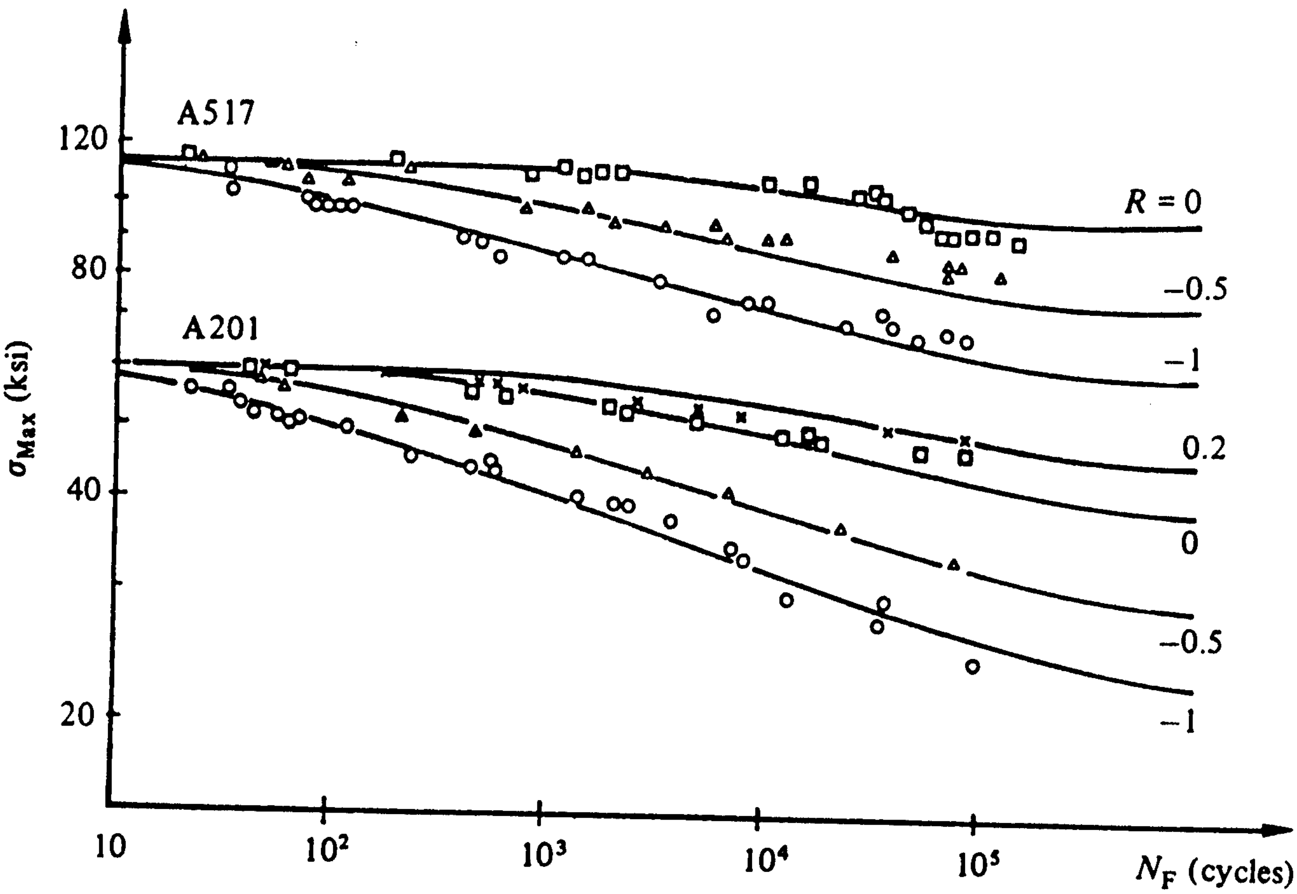

GOODMAN-GERBER DIAGRAM FOR 'SAFE' RANGE OF STRESS

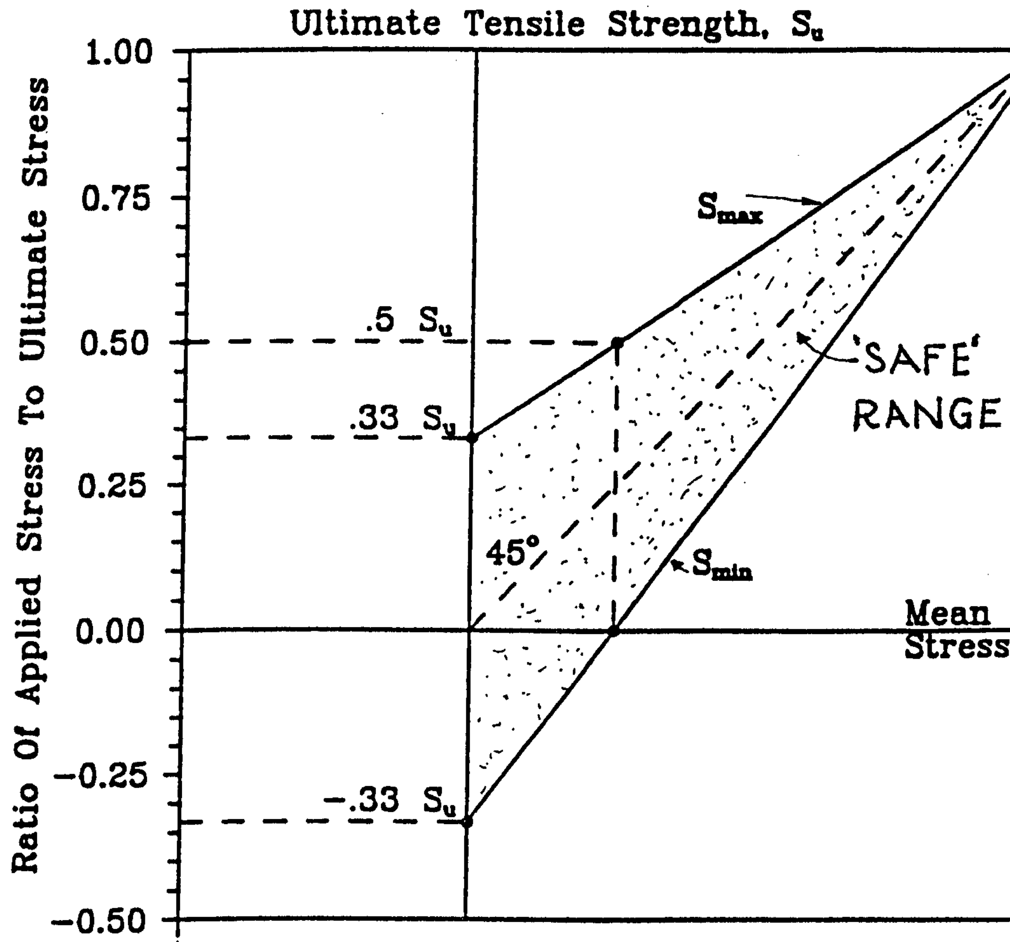

CONVENTIONAL REPRESENTATION OF THE FATIGUE FAILURE PROCESS

(AFTER BANNANTINE, COMER AND HANDROCK, 1990)

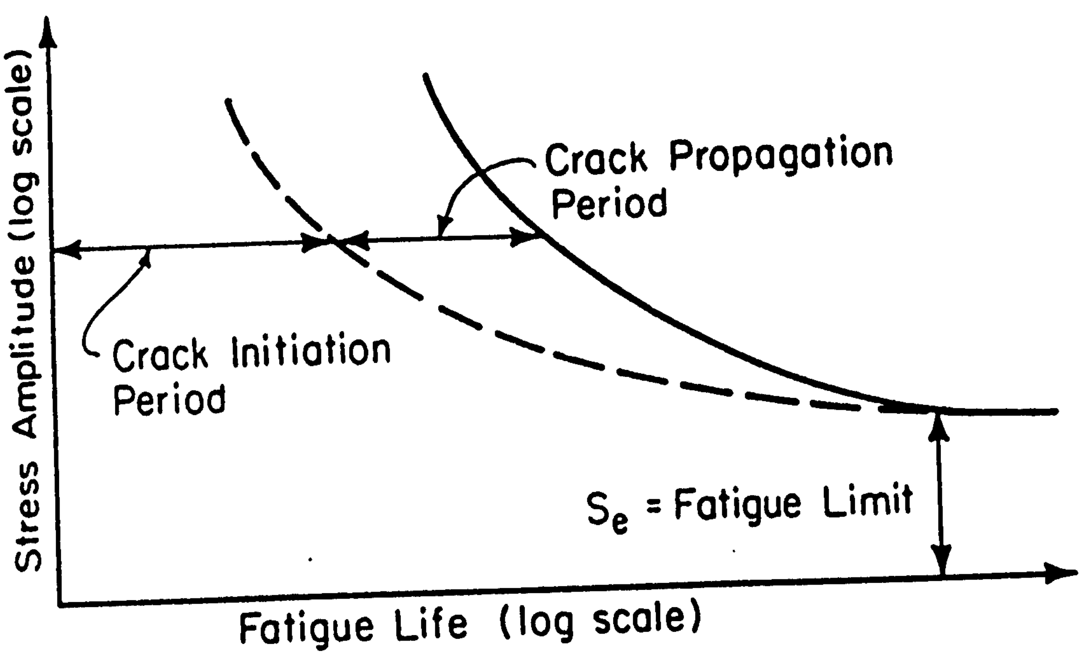

CONSTANT STRESS RANGE CRACK GROWTH VS. NUMBER OF CYCLES
(AFTER ROLFE AND BARSOM, 1977)

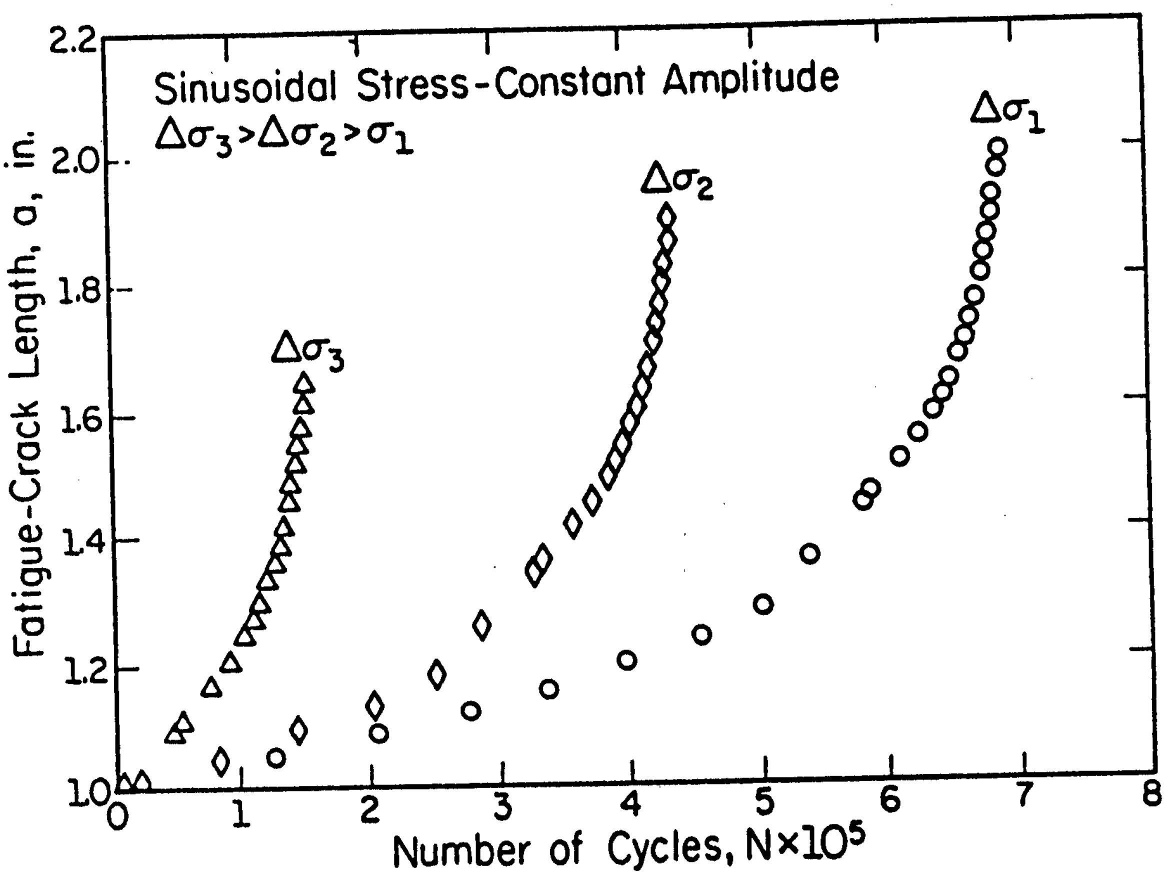

CRACK GROWTH RATE VS. STRESS INTENSITY FACTOR RANGE
(AFTER HERZBERG, 1989)

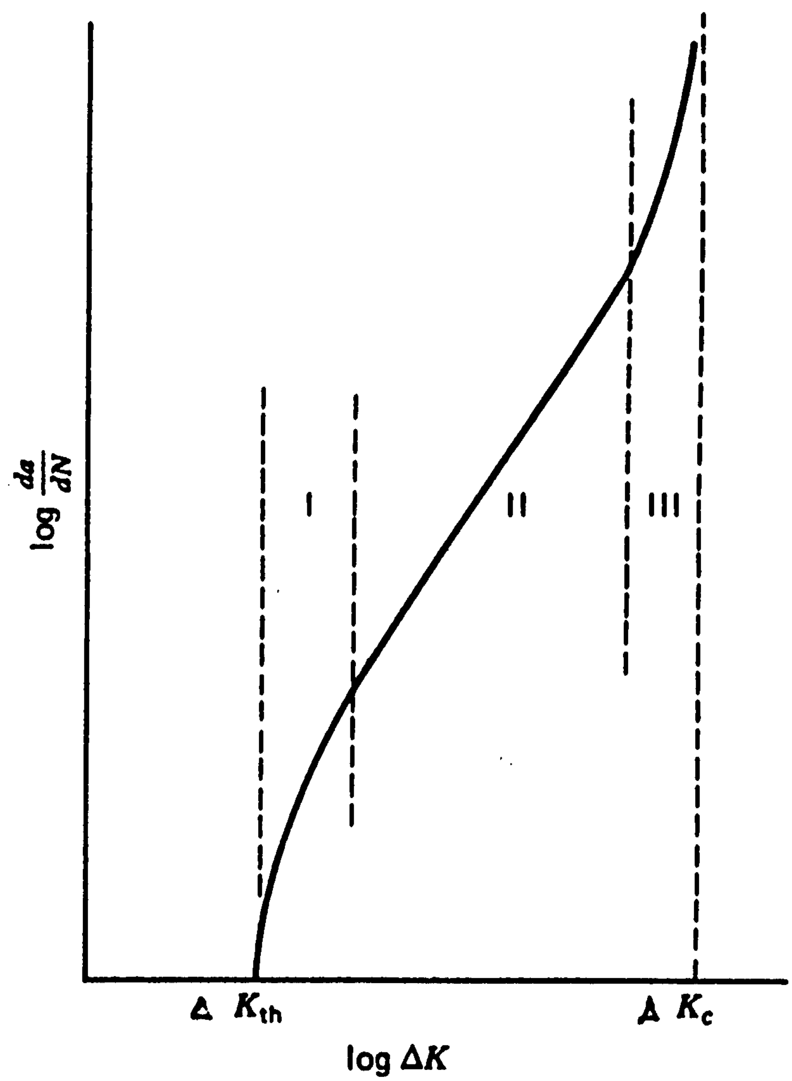

PERCENT OF LIFE TO CRACK INITIATION VS. CYCLIC LIFE
(AFTER LAIRD AND SMITH, 1963)

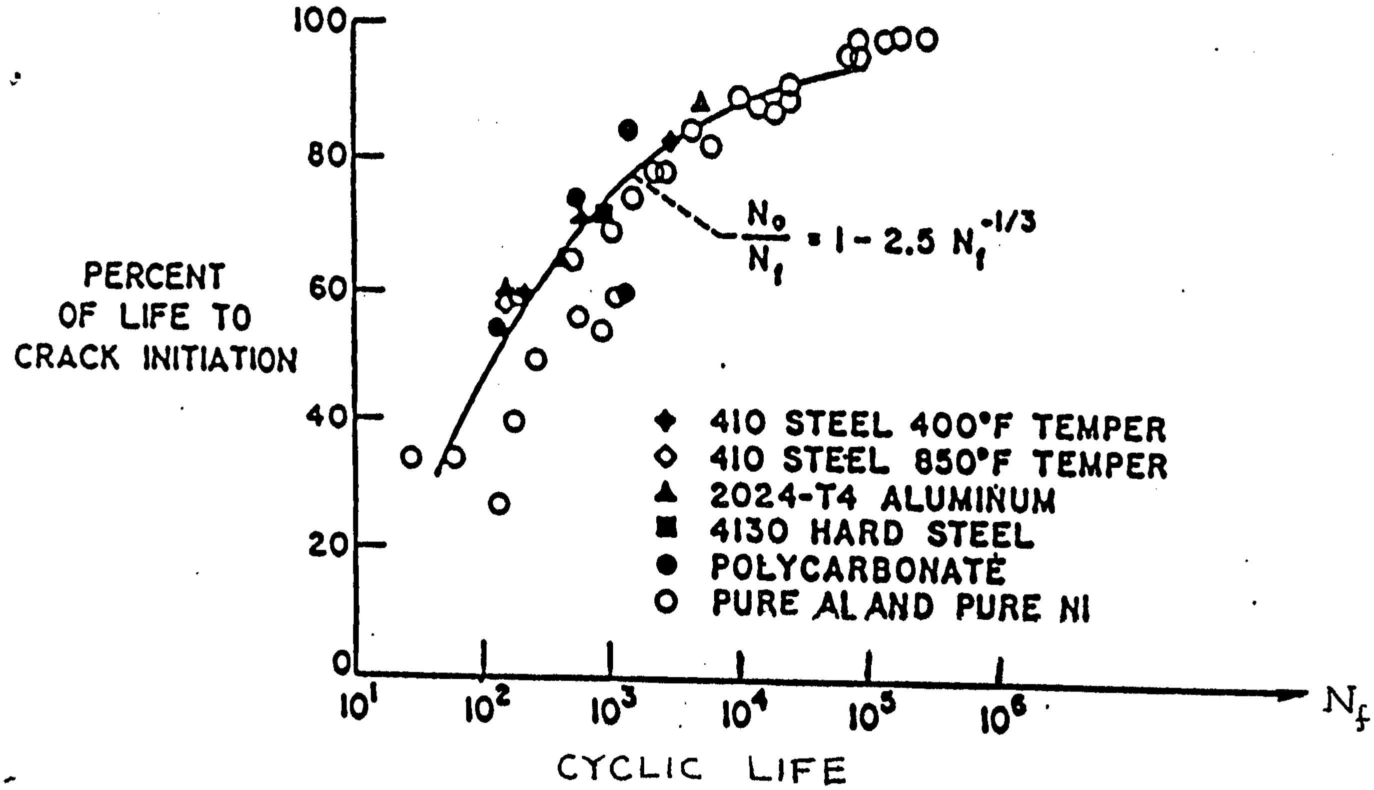

WAVY GLIDE IN HIGH STACKING FAULT ENERGY MATERIAL
(AFTER HERZBERG, 1989)

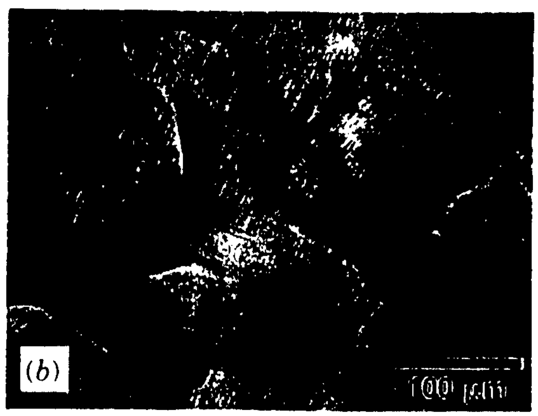

STRIATIONS PRODUCED AT VARIOUS ALTERNATING STRESS LEVELS
(AFTER SANDOR, 1972)

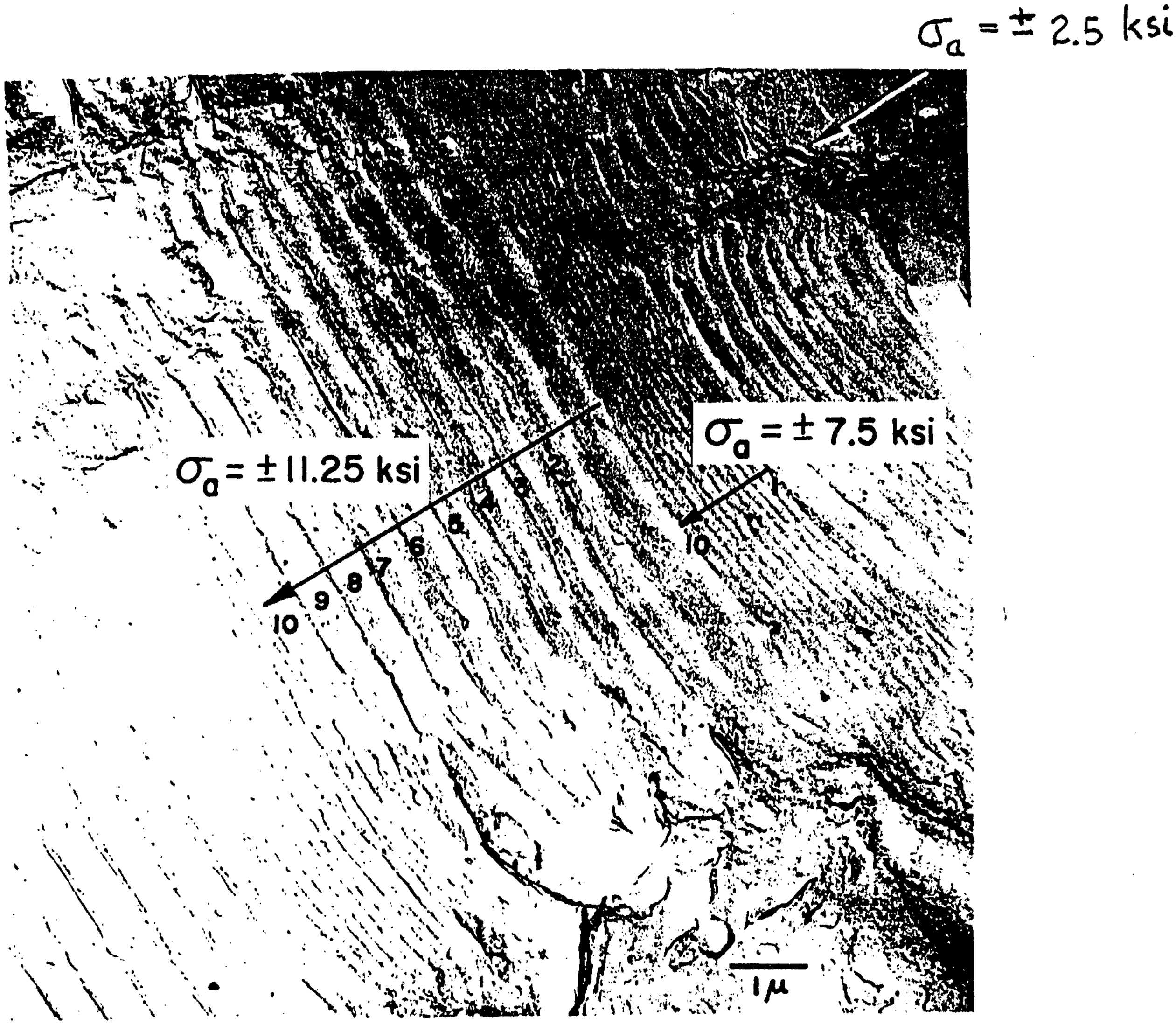

A471 STEEL REVEALING LOCALIZED EVIDENCE OF INTERGRANNULAR FAILURE AS A RESULT OF CYCLIC LOADING
(AFTER HERZBERG, 1989)

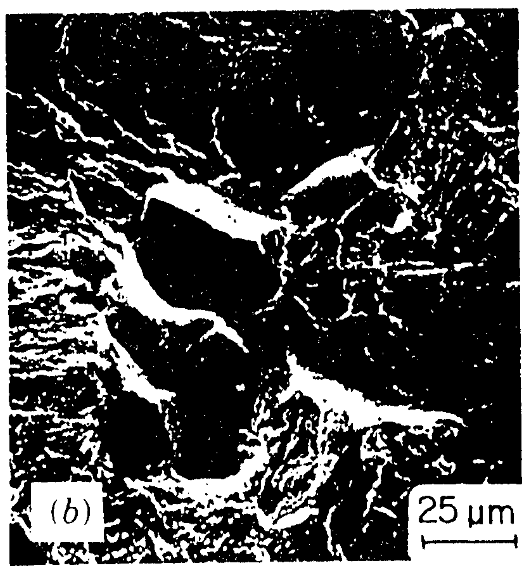

PLASTIC STRAIN-INDUCED SURFACE OFFSETS (A) MONOTONIC LOADING, (B) CYCLIC LOADING LEADING TO EXTRUSIONS AND INSTRUSIONS AND (C) PHOTOMICROGRAPH OF INTRUSIONS AND EXTRUSIONS ON PREPOLISHED SURFACE

(after Herzberg, 1984)

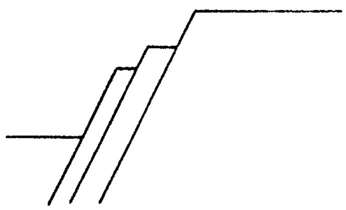

(a)

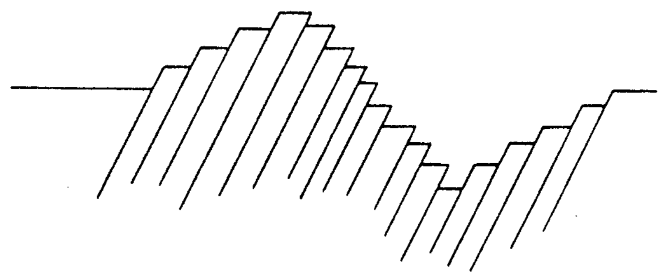

(b)

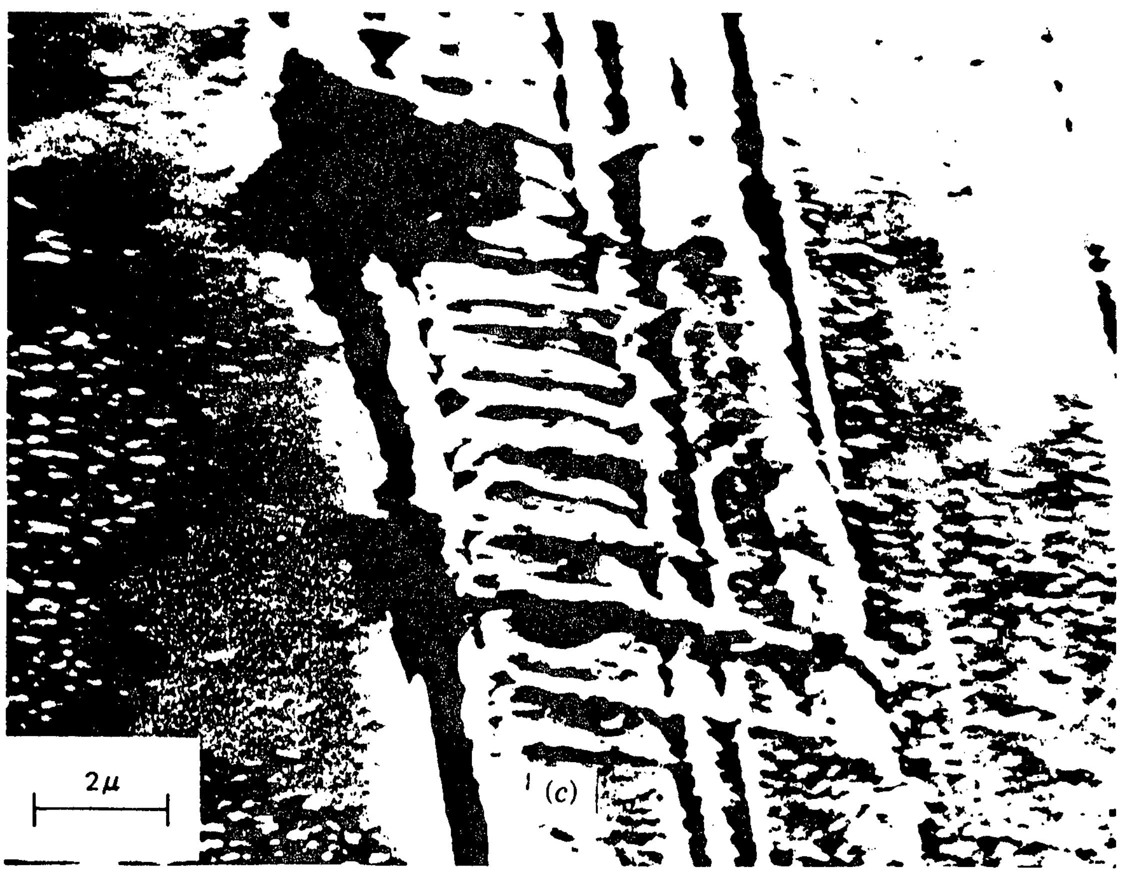

(c)

METALLOGRAPHIC SECTION REVEALING ONSET OF MACROCRACKING
(AFTER HERZBERG, 1989)

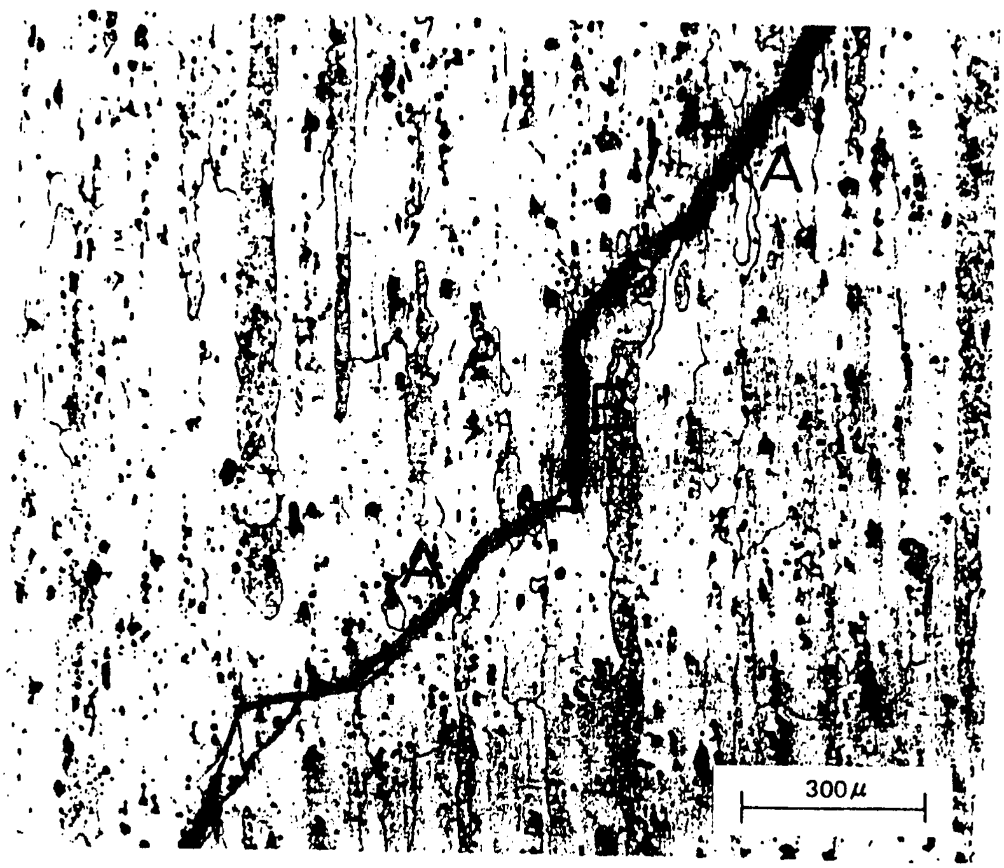

PROGRESSION OF THE FATIGUE PROCESS

(AFTER PUSKAR AND GOLOVIN, 1985)

1. DISLOCATION SEGMENTS BLOCKED BY PRECIPITATES OR BY ATOMS OF ADMIXTURES. LOCAL MOVEMENTS ARE REVERSIBLE, $(0<\sigma<\sigma_{CE})$

2. DISLOCATION SEGMENTS CAN BE DISPLACED BY SHORT SEGMENTS AND LOCALIZED MICROPLASTICITY OCCURS. $(\sigma_{CE} < \sigma < \sigma_{Cc})$

3. ACTIVITATION OF DISLOCATION SOURCES RESULTING IN FINE TRANSITION SLIP LINES. $(\sigma > \sigma_{Cc})$

4. DISLOCATION DENSITY INCREASES AND THEIR DISTRIBUTION CHANGES FROM A STATISTICALLY RANDOM DISTRIBUTION THROUGH THE OCCURRENCE OF CLUSTERS AND TANGLES VIA AN IMPERFECT CELL STRUCTURE TO A PERFECT CELL SUBSTRUCTURE.

5. PERMANENT SLIP LINES AND BANDS FORM. CRACKS BEGIN TO NUCLEATE IN POINTS OF INTRUSIONS.

6. FRACTURES PROPAGATE FIRST IN A CRYSTALLOGRAPHIC AND LATER IN A NON-CRYSTALLOGRAPHIC WAY.

7. FRACTURES ORGANIZE INTO NETWORKS AND COMPLETE RUPTURE ENSURES. $(\sigma \leq \sigma_F)$

PROGRESSION OF THE FATIGUE PROCESS

(AFTER LEMAITRE AND CHABOCHE, 1990)

1. INITIATION STAGE
   - CYCLIC ELASTICITY, NEARLY COMPLETELY REVERSIBLE BEHAVIOR AND 'INFINITE' LIFE. ($0 < \sigma < \sigma_1$)
2. ACCOMMODATION STAGE (OR NUCLEATION)
   - CYCLIC PLASTIC MICRODEFORMATIONS OCCUR WHICH, IN TURN, BLOCK FURTHER SLIP BY VIRTUE OF MULTIPLICATION OF DISLOCATION NODES ($\sigma = \sigma_1 \leq \sigma_{\text{elastic limit}}$)
3. INITIATION PHASE OF MICROCRACKS (STAGE 1)
   - DISLOCATION CLIMBS ACCOMPANIED BY FORMATION OF VOIDS
   - FORMATION OF PERMANENT SLIP BANDS AND DECOHESION
   - INTRUSION-EXTRUSION MECHANISMS
4. GROWTH PHASE OF MICROCRACKS (STAGE 2)
   - ORIENTATION OF MICROCRACKS PERPENDICULAR TO PLANE OF MAXIMUM PRINCIPAL STRESS
   - PROGRESSION OF MICROCRACKS THROUGH SUCCESSIVE GRAINS OR ALONG GRAIN BOUNDARIES. MACROSCOPIC CRACK INITIATION TAKES PLACE.
5. GROWTH PHASE OF MACROCRACKS
   - CYCLIC OPENING AND CLOSING OF CRACKS RESULTS IN ALTERNATING PLASTIC SLIPS AT THE CRACK TIP, WHICH IN DIFFERENT CRYSTALLOGRAPHIC PLANES FORM A RIDGE OF CLEAVAGE AT EACH GROWTH OF THE CRACK.
   - CRACKS GROW UNTIL A CRITICAL SIZE IS REACHED AT WHICH PART BECOMES UNSTABLE.
   - CRACKS PROPAGATE RAPIDLY UNTIL COMPLETE RUPTURE OCCURS ($\sigma = \sigma_F$).

STAGES IN THE PROGRESSION LEADING TO RUPTURE

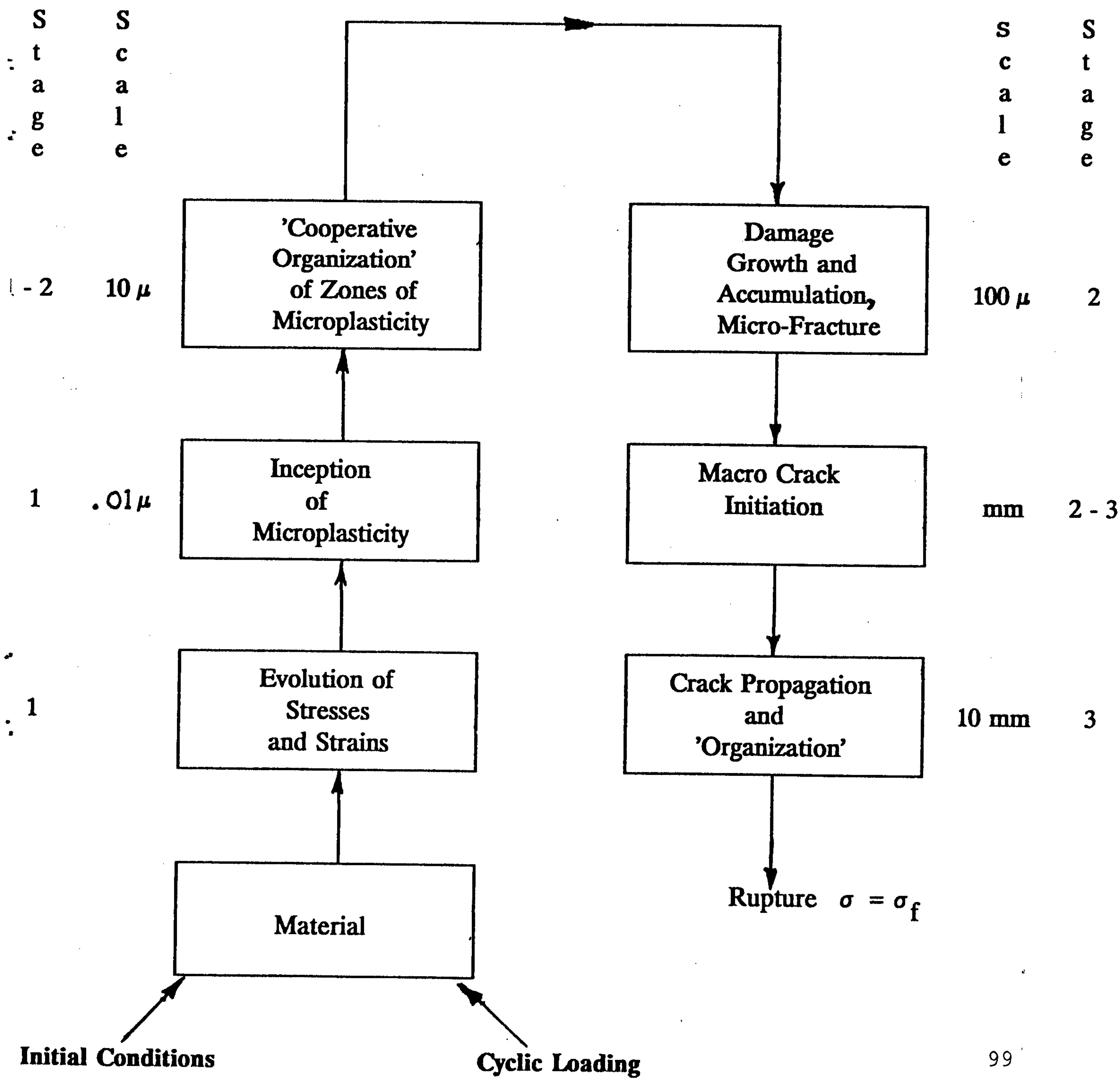

INCEPTION OF MICROPLASTICITY, P, INCEPTION OF MACROCRACKING, F, AND THE S VS. N_f DIAGRAM

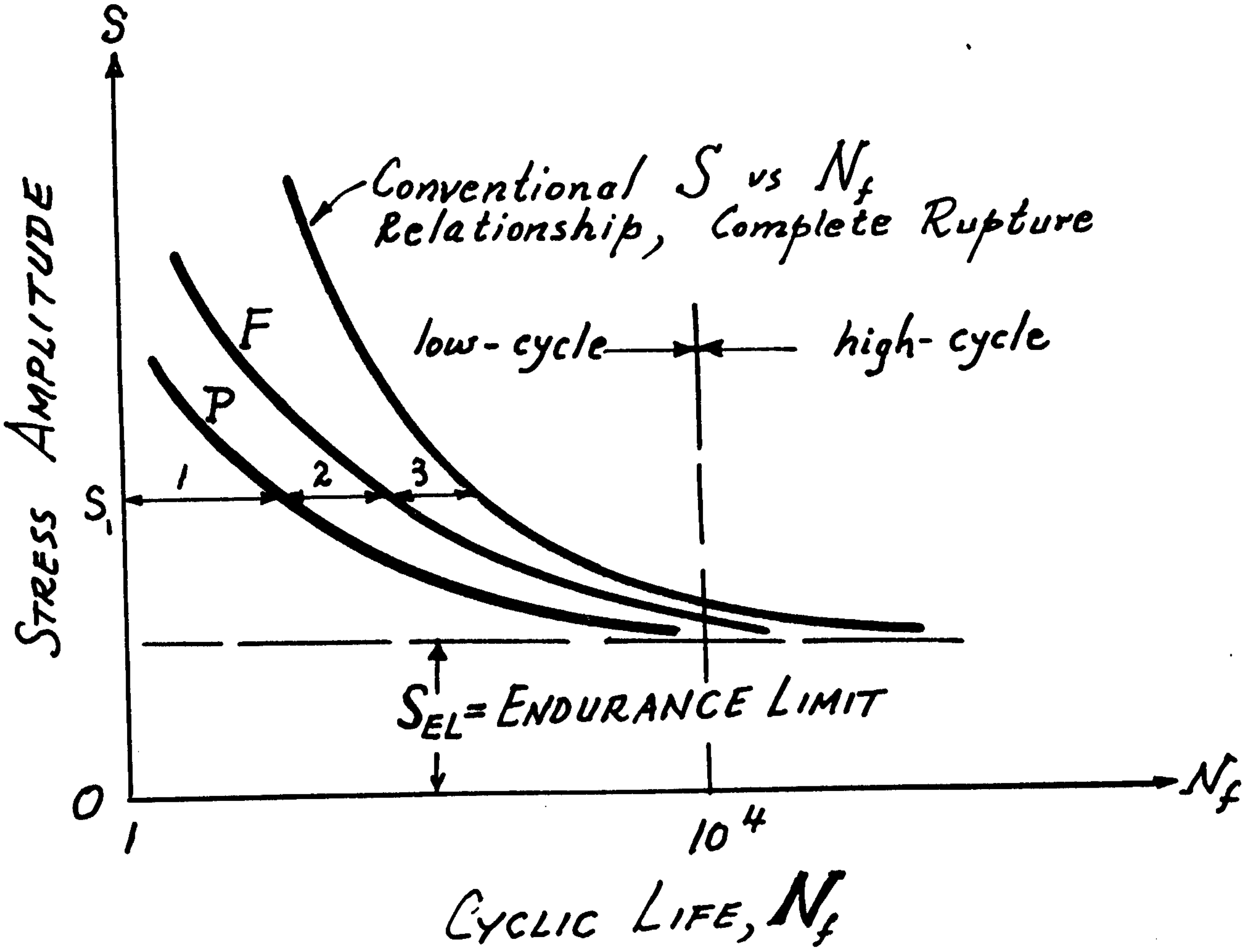

POSSIBLE DIAGNOSTIC TECHNIQUES

1. Analysis of Hysteresis Evolution
2. Magnetic Effects (in steel)
3. Acoustic Transmission and Harmonic Generation
4. Acoustic Emission
5. Acoustic Scattering (Macro-Crack Growth Monitoring)
6. Micro-Mechanical Physical Testing in Conjunction With:
   - a. Scanning Tunneling Microscope
   - b. Scanning Electron Microscope
   - c. Transmission Electron Microscope
   - d. Positron Annihilation
7. Photostimulated Exo-electron Emission
8. Surface Examination
   - a. Optical Holography
9. Eddy Current Probes (Micro-Crack Monitoring)

RESPONSE OF A STRAIN-SOFTENING MATERIAL TO CYCLIC APPLICATIONS OF LOAD UNDER STRAIN CONTROL

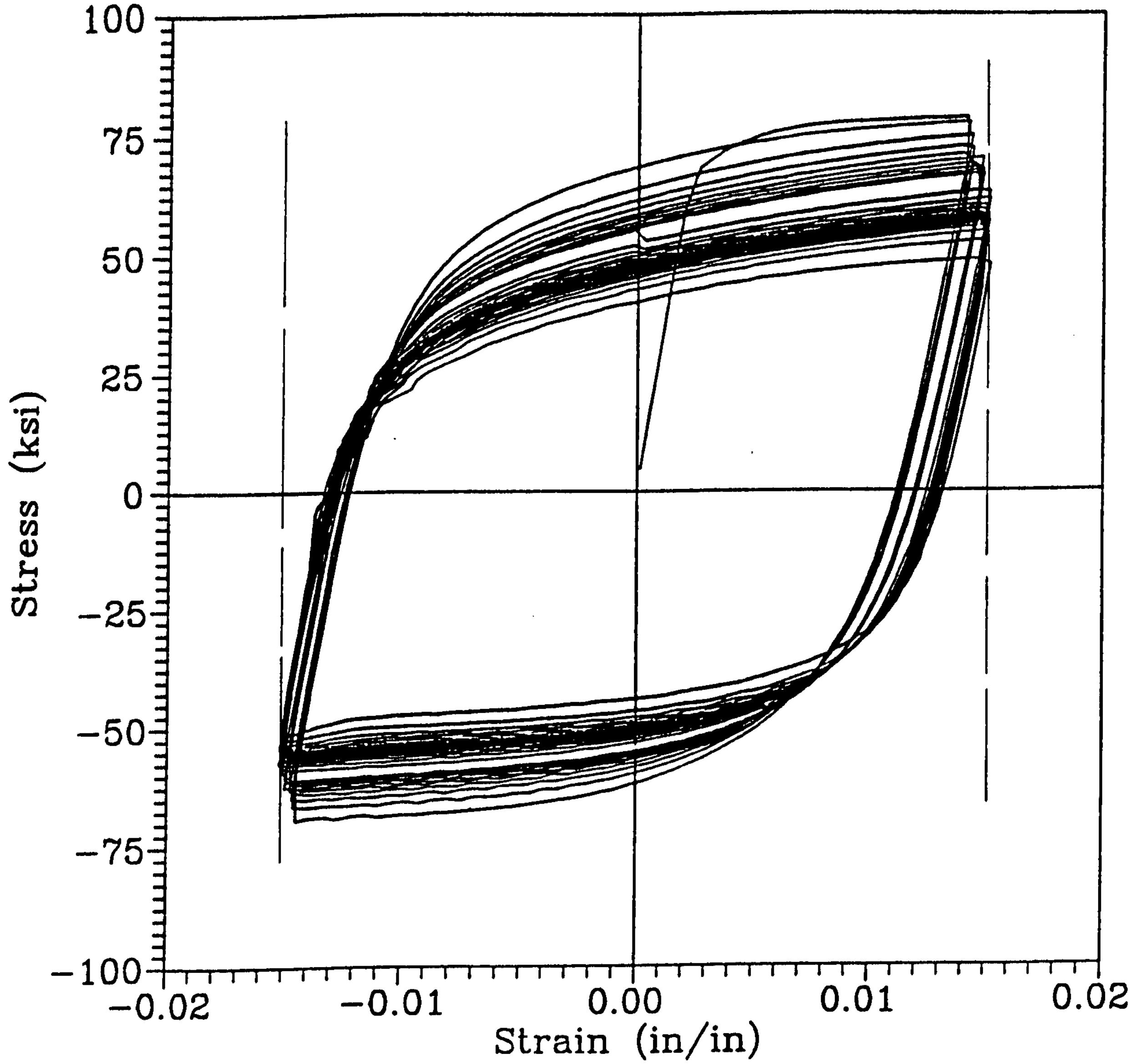

TYPICAL HYSTERESIS LOOP SHOWING ELASTIC-PLASTIC STRAIN DIVISION

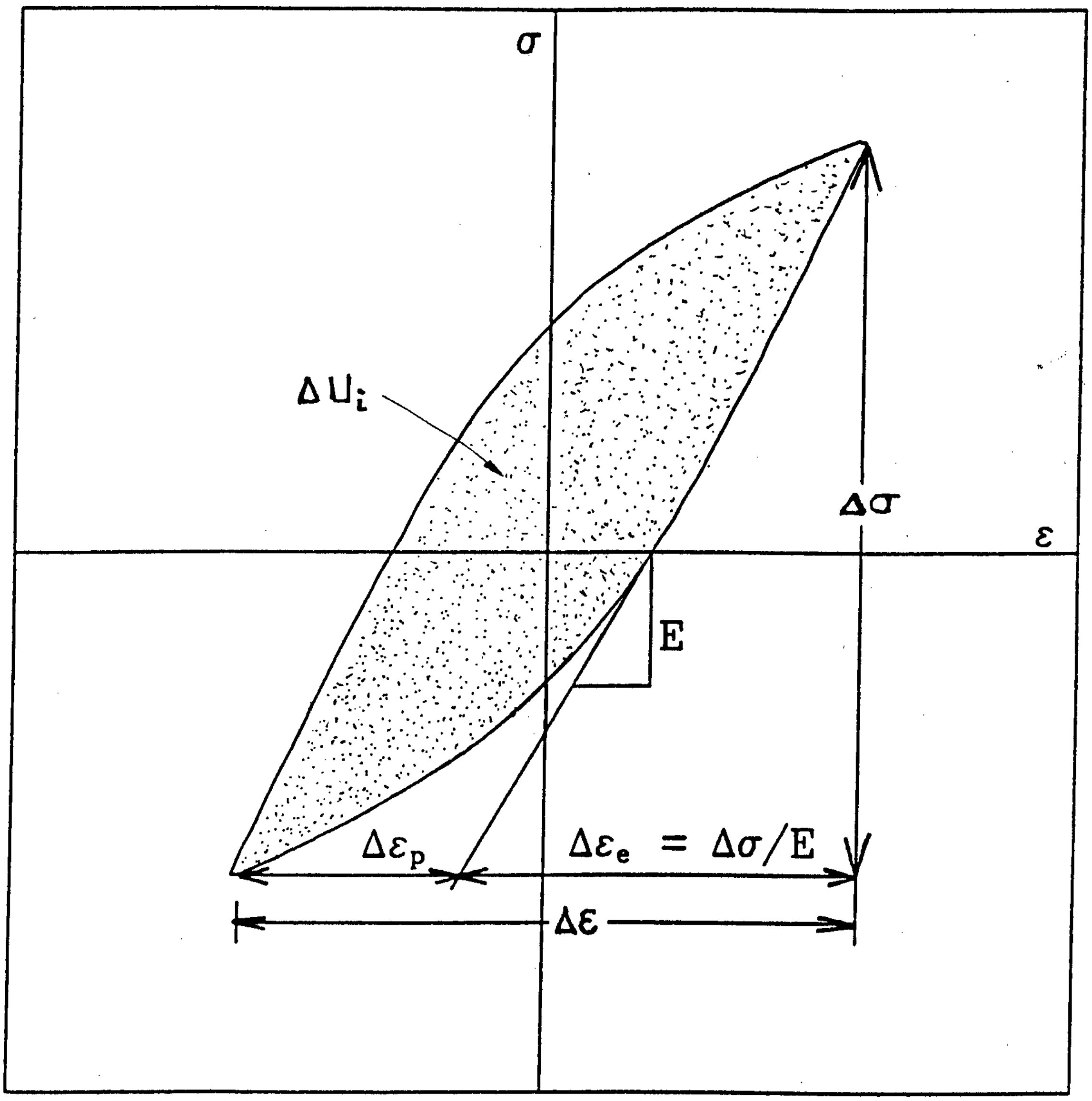

STRESS VS. STRAIN DIAGRAM FOR RIMMED AISI 1018 UNANNEALED STEEL

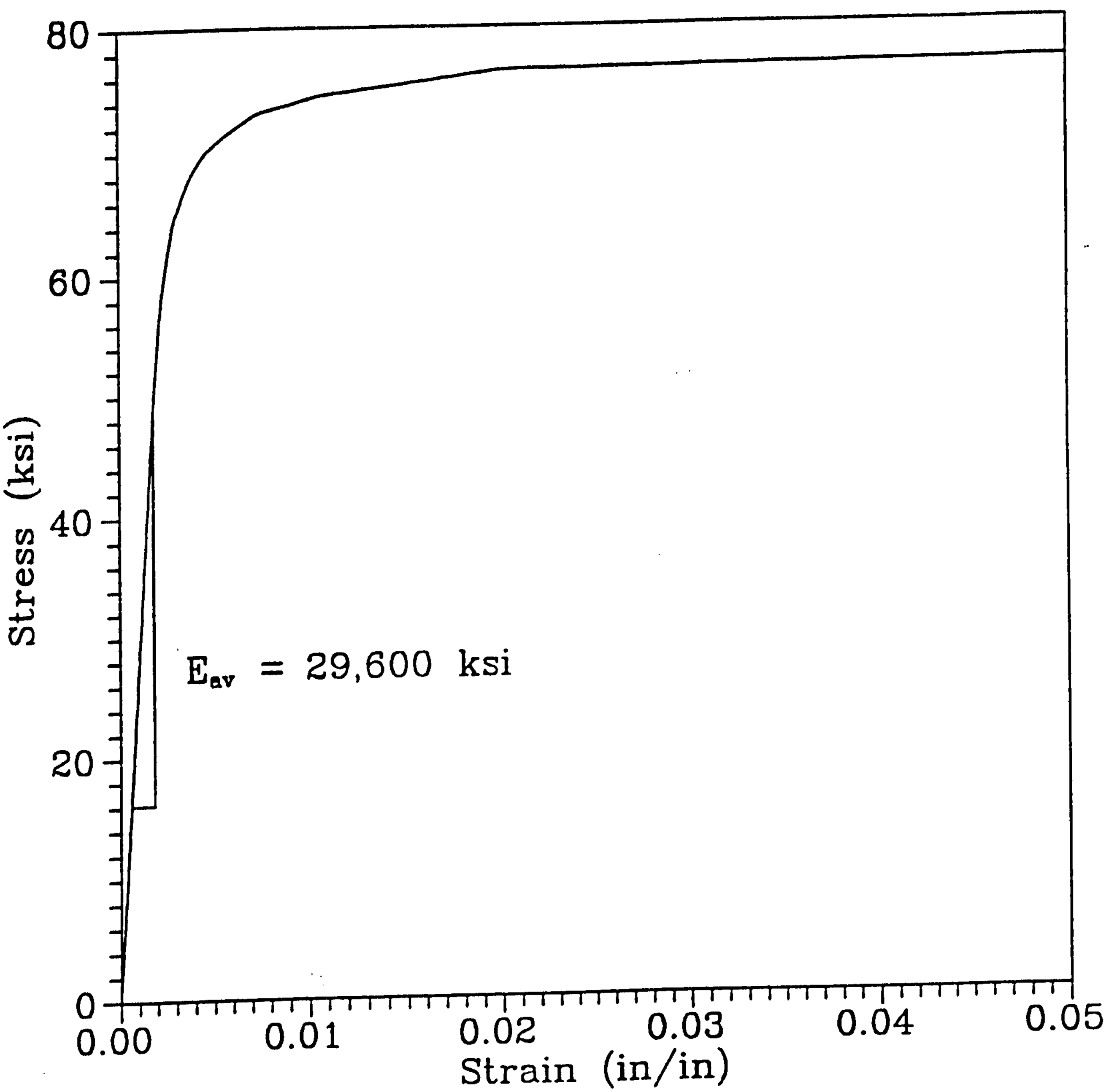

CYCLIC AND MONOTONIC STRESS-STRAIN CURVES

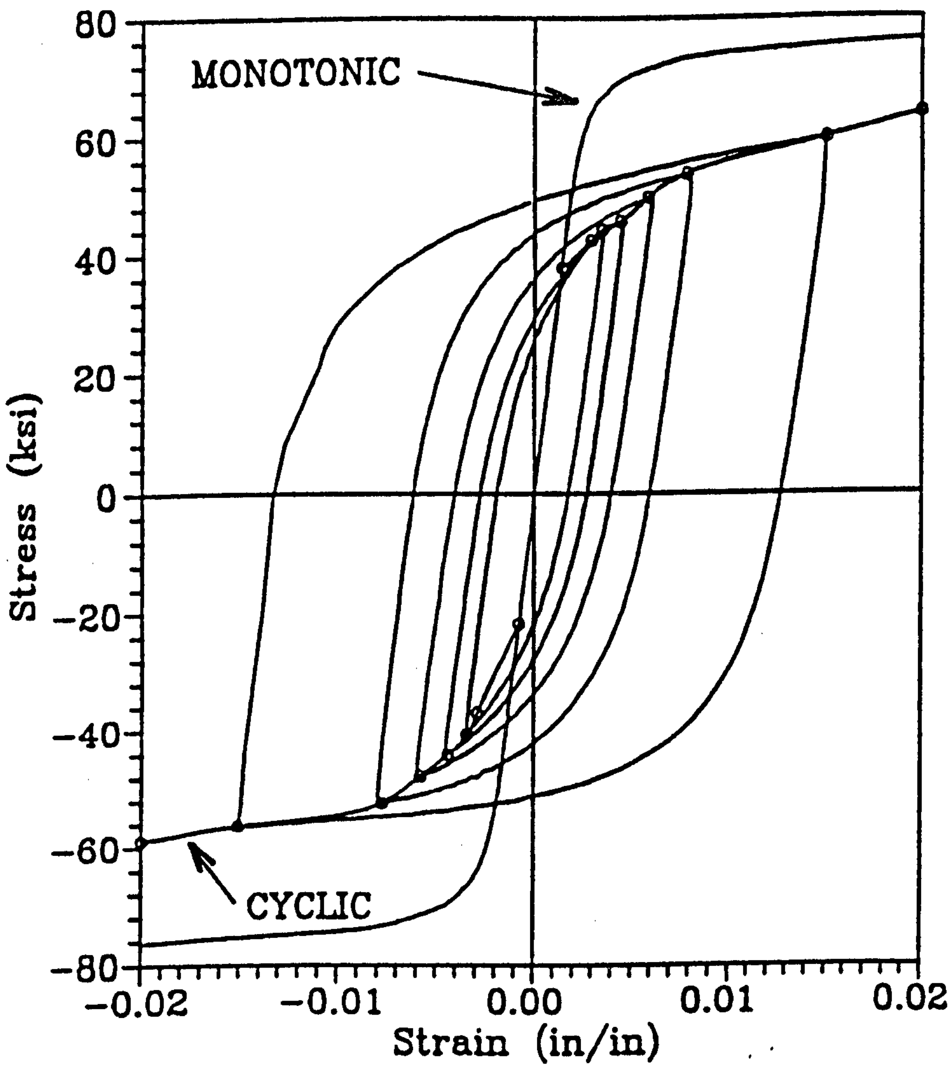

HYSTERESIS LOSS PER CYCLE VS. NUMBER OF CYCLES
($\Delta\ \epsilon/2$ - 0.006 in/in)

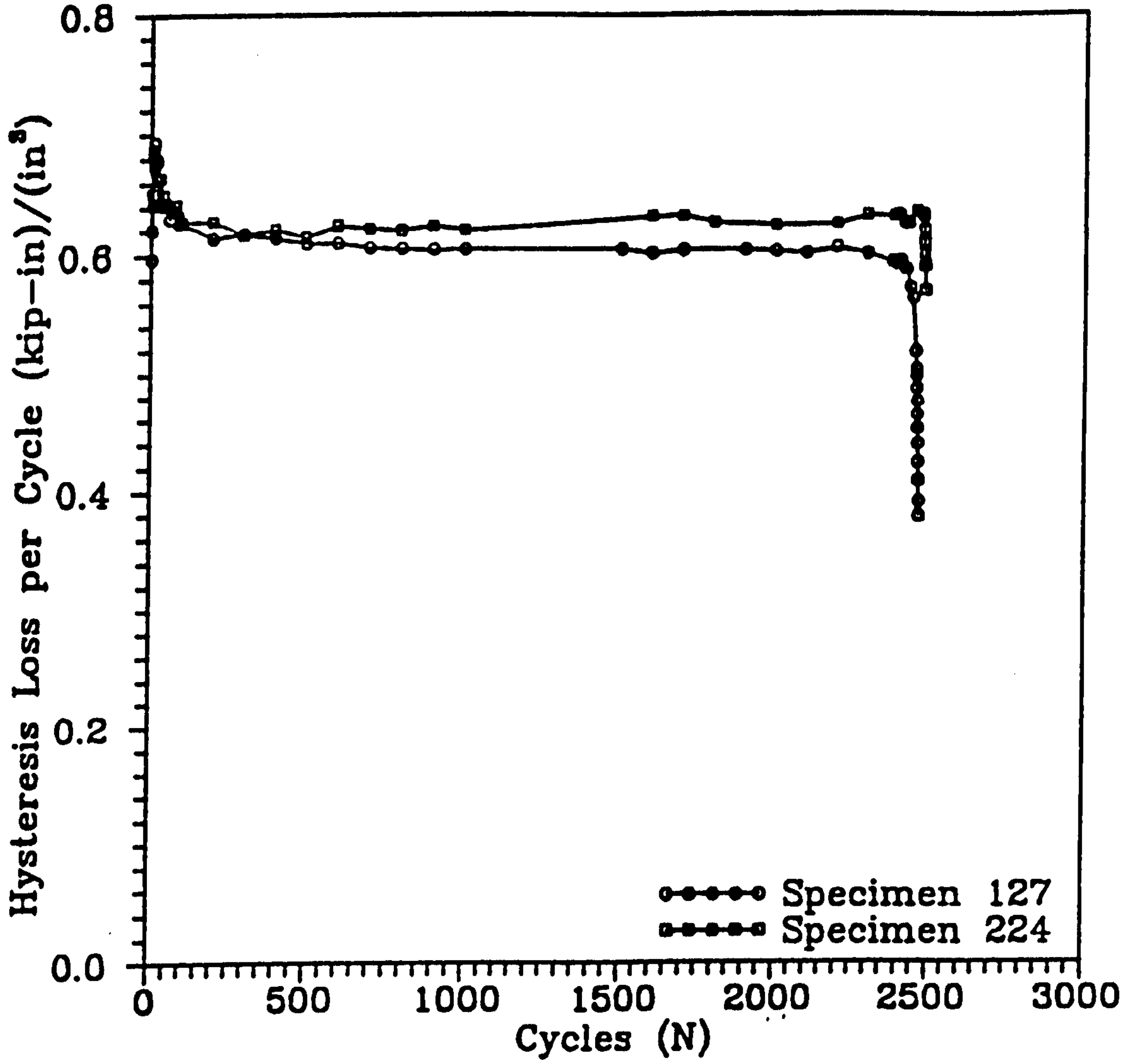

HYSTERESIS LOSS PER CYCLE VS. NUMBER OF CYCLES FOR A SPECIMEN SUBJECTED TO OVERLOADS

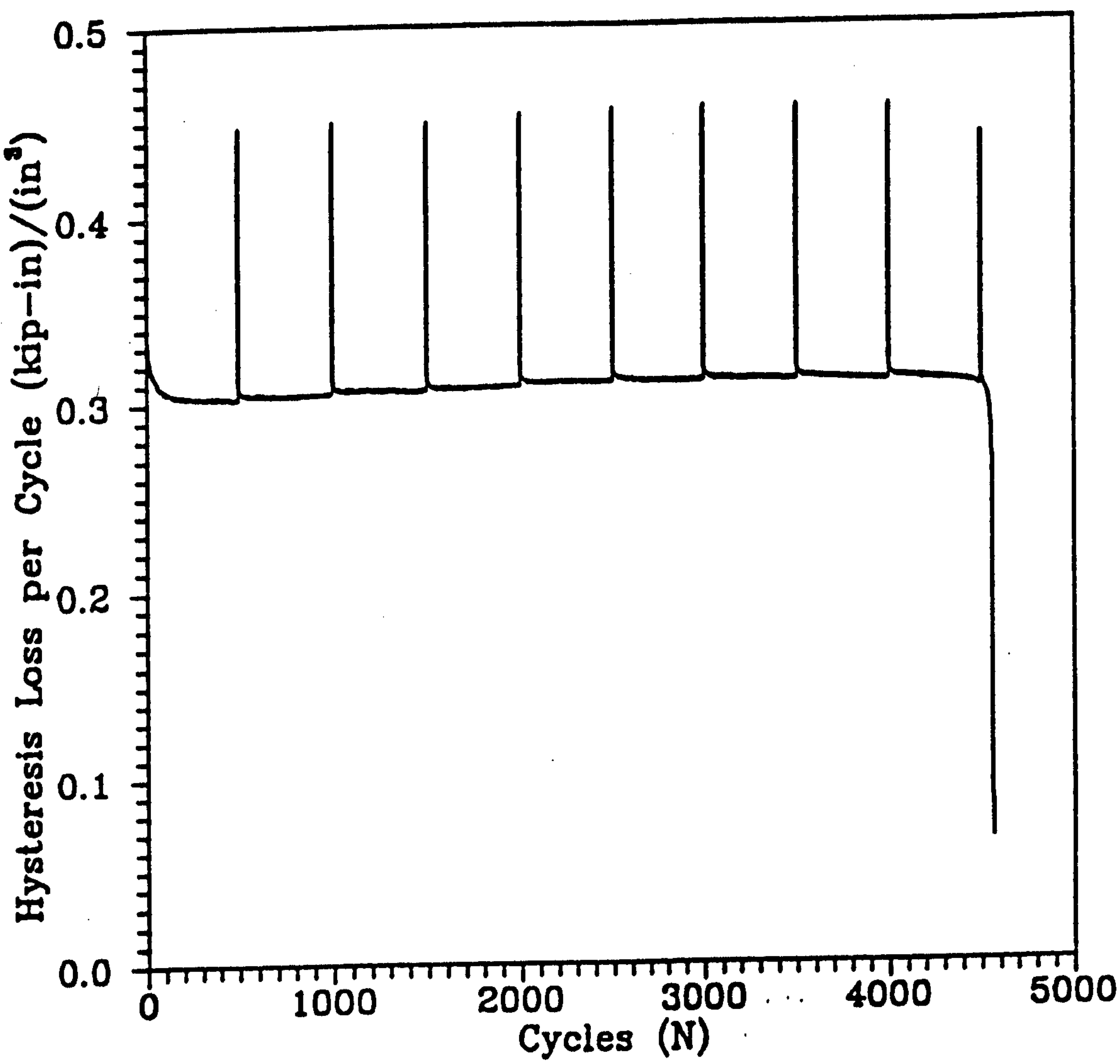

AVERAGE HYSTERESIS LOSS PER CYCLE VS. STRAIN AMPLITUDE

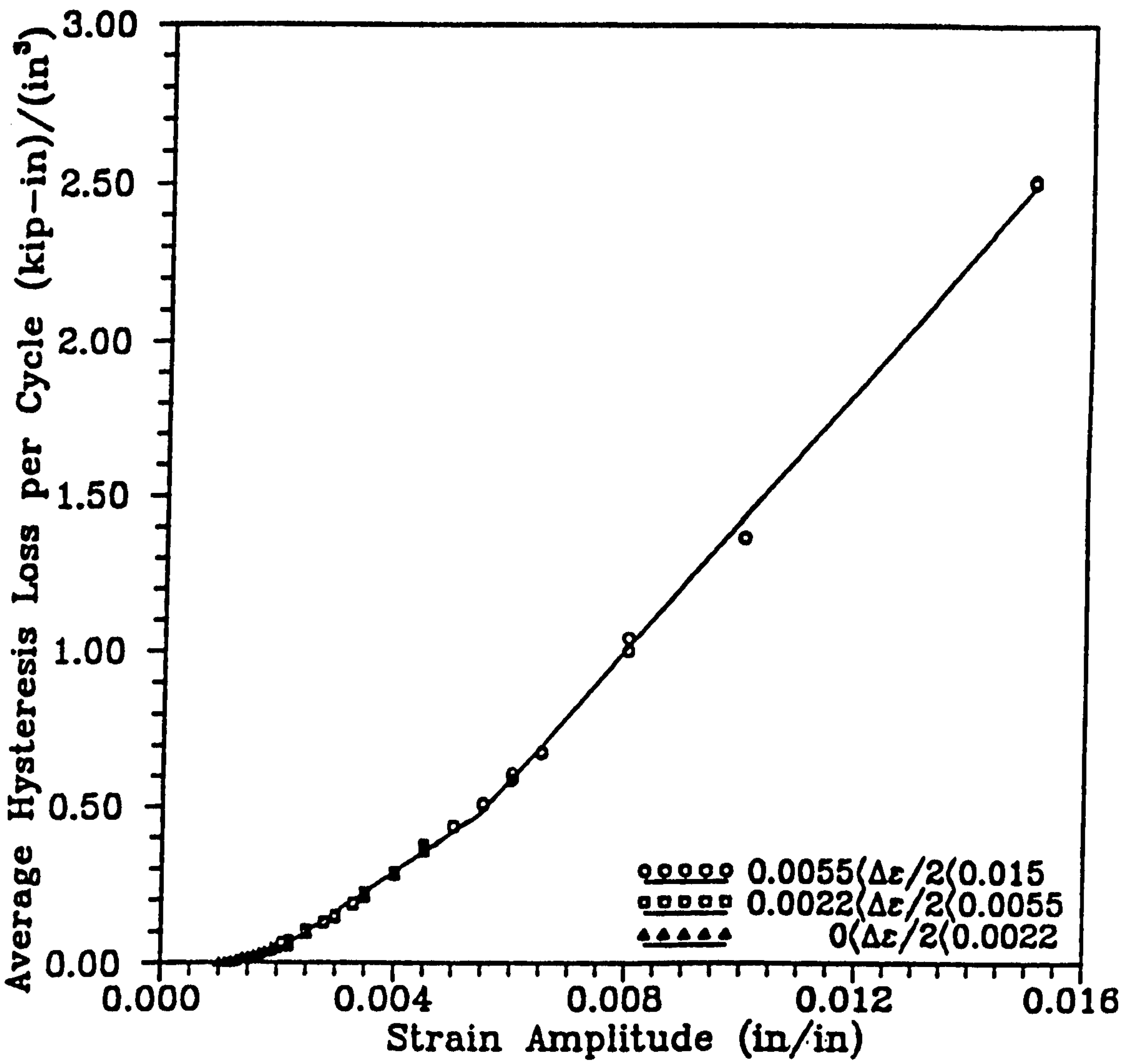

HYSTERESIS LOSS PER CYCLE VS. NUMBER OF CYCLES

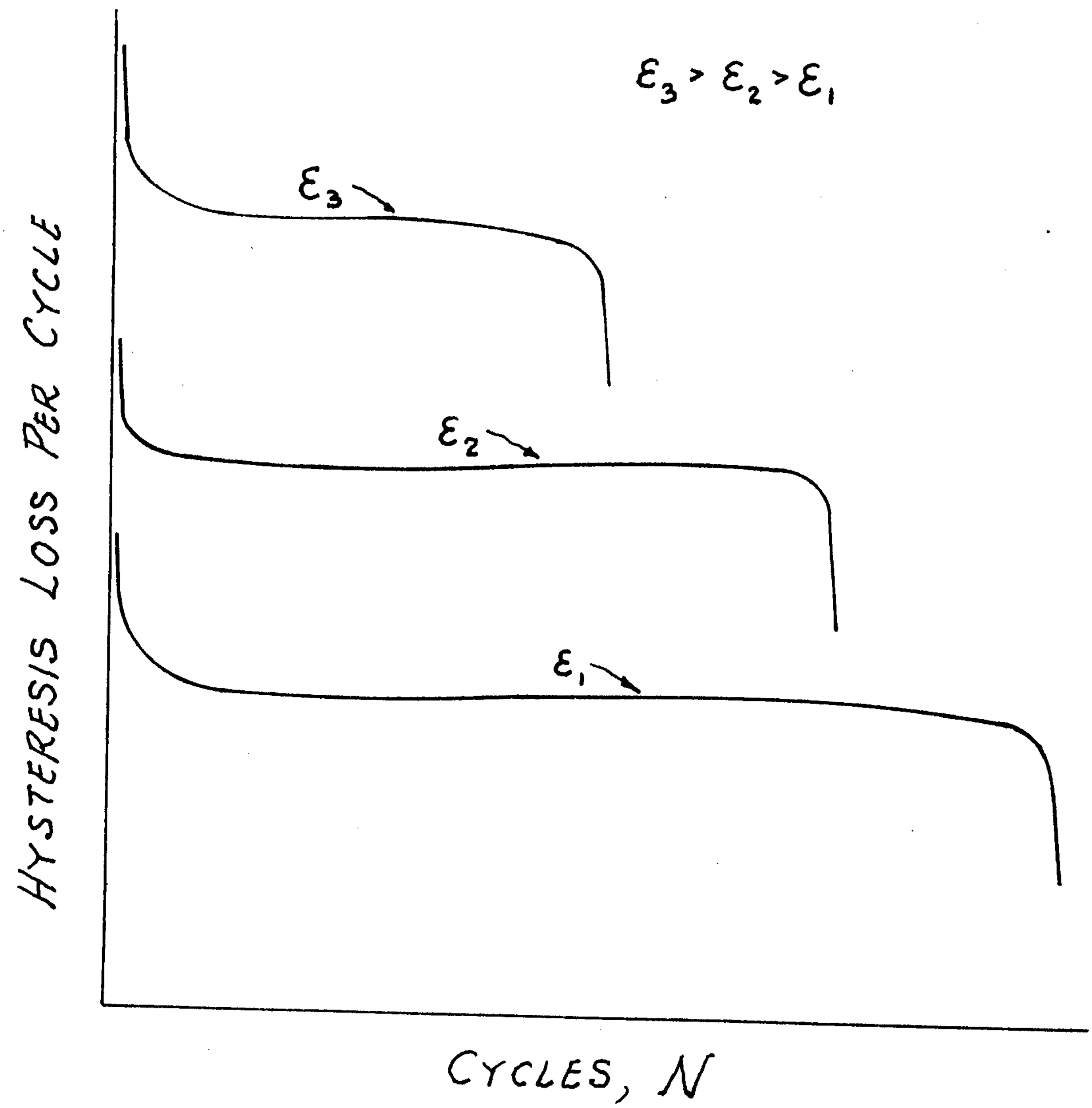

ZONES IN THE EVOLUTION OF HYSTERESIS LOSS PER CYCLE

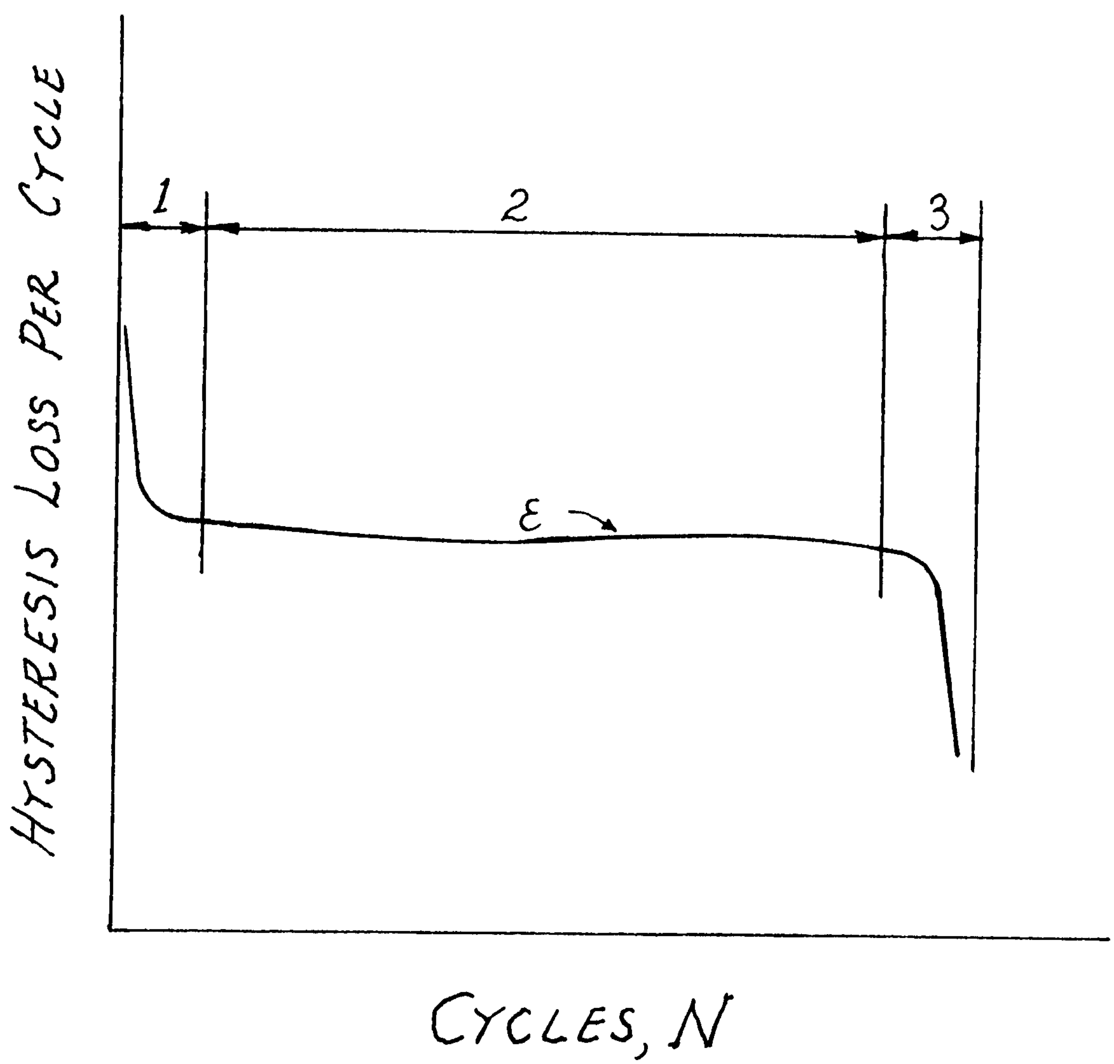

DISSIPATED ENERGY OF PLASTIC DEFORMATION UNTIL FAILURE AND ITS ACTIVE PART, TYPE 316 STAINLESS STEEL AT ROOM TEMPERTURE

(AFTER LEMAITRE AND CHABOCHE, 1990)

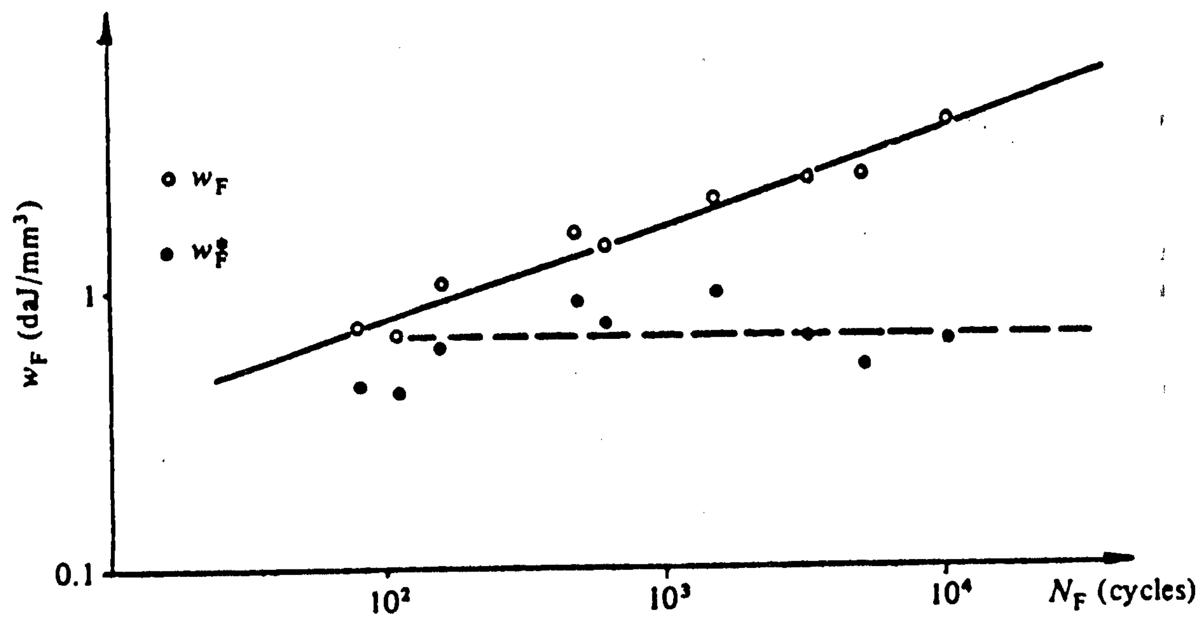

$$w_F = w_F^* + N_F \Delta\Phi = \alpha N_F^{\delta}$$

w_F^* = Damaging Component of the total dissipation energy up to failure = constant

$\Delta\Phi$ = Energy dissipated as heat in each cycle

N_F = Number of cycles to failure

w_F = Total dissipation energy up to failure

THE CONNECTION BETWEEN
CUMULATIVE HYSTERESIS LOSS, U_f,
ENERGY OF DAMAGE, U_d,
STRAIN AMPLITUDE AND NUMBER
OF CYCLES TO FAILURE

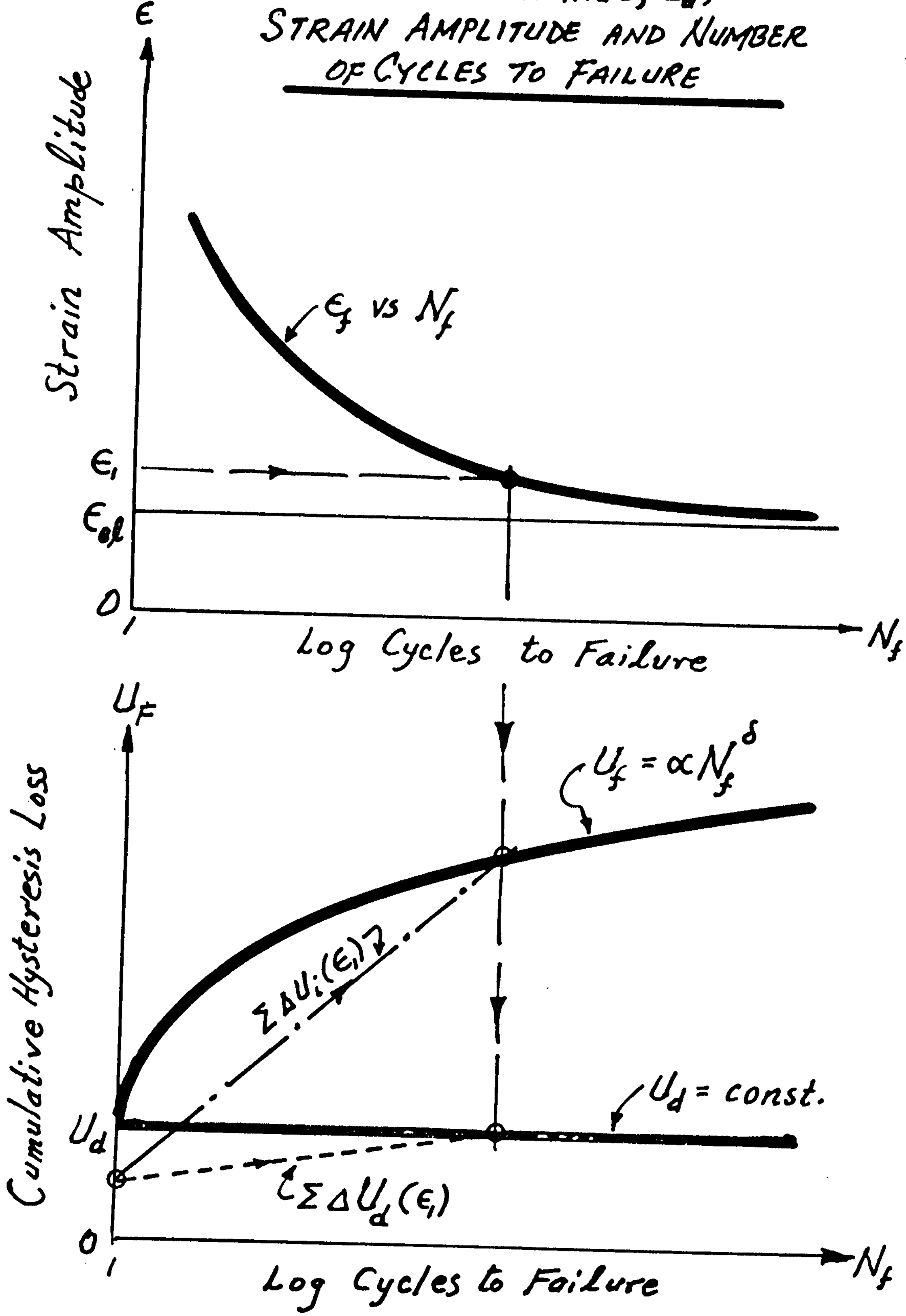

CUMULATIVE DAMAGE AND STRAIN LEVEL

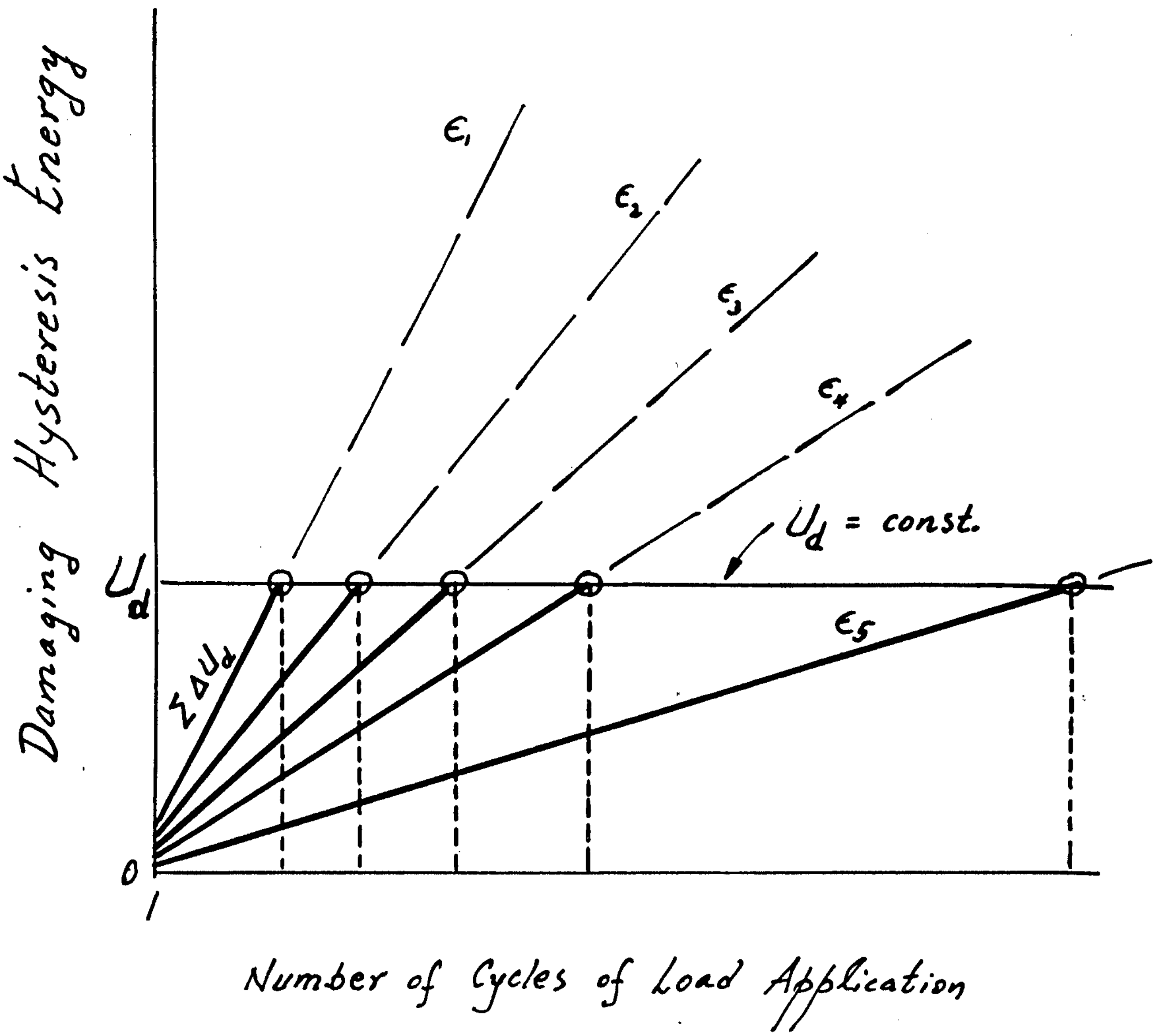

$$\epsilon_1 > \epsilon_2 > \epsilon_3 > \epsilon_4 > \epsilon_5 > \epsilon_{el}$$

THE PALMGREN-MINER LAW

Let

$$\left.\begin{aligned} U_d(\epsilon_1) &= n_1 \Delta U_{d1} \\ U_d(\epsilon_2) &= n_2 \Delta U_{d2} \\ &\vdots \\ U_d(\epsilon_5) &= n_5 \Delta U_{d5} \end{aligned}\right\} \qquad (1)$$

Failure will occur when,

$$U_d(\epsilon_i) = U_d, \text{ a constant} \qquad (2)$$

From Eqs. 1 and 2,

$$N_{F1} \Delta U_{d1} = N_{F2} \Delta U_{d2} = N_{F3} \Delta U_{d3} \cdots = U_d \qquad (4)$$

If a material is subjected to several different strain levels under cyclic loading, then failure due to cumulative damage will occur when,

$$n_1 \Delta U_{d1} + n_2 \Delta U_{d2} + \cdots \leq U_d \qquad (5)$$

in which,

$$n_1 < N_{F1}, \quad n_2 < N_{F2}, \quad n_3 < N_{F3}, \cdots$$

Dividing both sides of Eq. 5 by U_d,

$$n_1 \frac{\Delta U_{d1}}{U_d} + n_2 \frac{\Delta U_{d2}}{U_d} + n_3 \frac{\Delta U_{d3}}{U_d} + \cdots \leq 1 \qquad (6)$$

Substituting for U_d the appropriate value given by Eq. 4 in Eq. 6, one obtains,

$$\frac{n_1}{N_{F1}} + \frac{n_2}{N_{F2}} + \frac{n_3}{N_{F3}} + \cdots \leq 1 \qquad (7)$$

ACOUSTIC EMISSION IN ALUMINUM
(AFTER GRAHAM AND MORRIS, 1975)

1. ACOUSTIC EMISSION BEHAVIOR OF VARIOUS MATERIALS IN DIFFERENT CONDITIONS IS MARKEDLY DIFFERENT

2. AT LEAST FOUR DIFFERENT TYPES OF EMISSION WERE OBSERVED

3. PRIMARY SOURCE OF ACOUSTIC EMISSION IS BRITTLE FRACTURE OF INTERMETALLICS

4. SECONDARY SOURCE OF ACOUSTIC EMISSION IS BRITTLE FRACTURE OF MATRIX MATERIAL

5. TERTIARY SOURCES OF ACOUSTIC EMISSIONS ARE:
   - GRAIN BOUNDARY SEPARATION
   - DELAMINATION ALONG GRAIN BOUNDARIES
   - MATRIX CLEAVAGE

6. GROSS PLASTIC DEFORMATION OF THE ALUMINUM MATRIX YIELDS VERY LITTLE MEASURABLE ACOUSTIC EMISSION

THE FOUR DISTINCT TYPES OF ACOUSTIC EMISSION OBSERVED FOR INDIVIDUAL ACOUSTIC EMISSION EVENTS

(AFTER GRAHAM AND MORRIS, 1975)

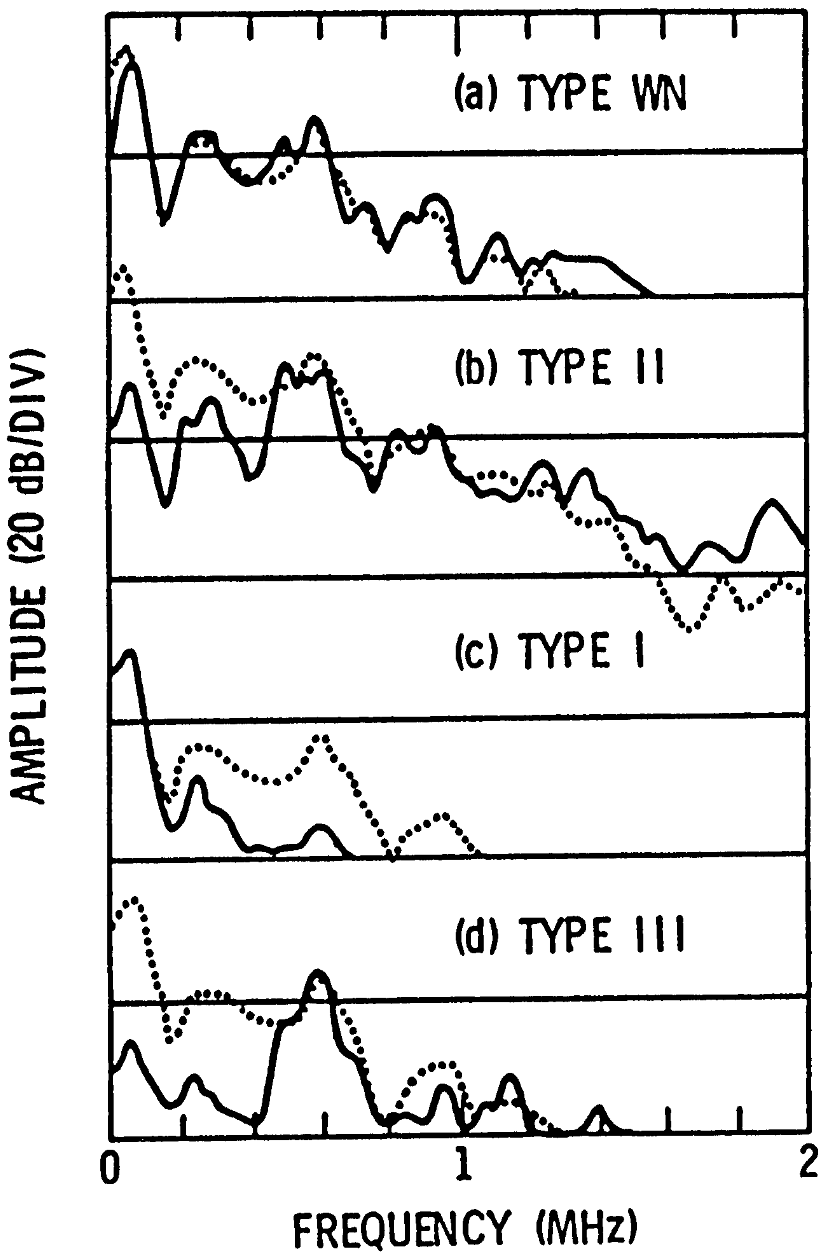

MOST LIKELY SOURCES PRODUCING THE FOUR TYPES OF ACOUSTIC EMMISSION
(AFTER GRAHAM AND MORRIS, 1975)

TYPE	FREQUENCY CONTENT	LIKELY SOURCE
WN	WHITE NOISE	MOSTLY BRITTLE FRACTURE OF INTERMETALLICS; SOME BRITTLE MATRIX FRACTURE
II	HIGH FREQUENCY	SAME AS FOR TYPE WN
I	LOW FREQUENCY	DELAMINATION ALONG GRAIN BOUNDARIES
III	PEAKED	SOURCE UNDETERMINED

PRELIMINARY CORRELATION OF METALLURGICAL STATE WITH ACOUSTIC EMISSION RATE

	Scale	Stage	Acoustic Emission
• Inception of Microplasticity	.01 μ	1	Kaiser Effect Occurs
• Cooperative Organization of Microplasticity	10 μ	1 - 2	Non-Vanishing counts, Felicity Effect
• Damage Growth and Assumulation, Micro Fracture	100 μ	2	
• Macro Crack Initiation	mm	2 - 3	
• Macro Crack Propagation and Organization	10 mm	3	
Rupture	> 10 mm		

RESULTS OF MECHANICAL (HYSTERESIS) EXPERIMENTS

ULTIMATE TENSILE STRENGTH, $\sigma_u = 77.72$ ksi

- YIELD STRENGTH (0.2% OFFSET), $\sigma_y = 70.77$ ksi

- PROPORTIONAL LIMIT, $\sigma_{pl} = 48.00$ ksi

PERCENT ELONGATION = 18.2 %

PERCENT REDUCTION IN AREA = 61.05%

MODULUS OF ELASTICITY, $E = 29{,}600$ ksi

- ENDURANCE LIMIT, $S = \Delta\sigma = \underline{\underline{32.63 \text{ ksi}}}$
  ($\sigma_{min} = 0$)

PRELIMINARY ACOUSTIC EMISSION RESULTS

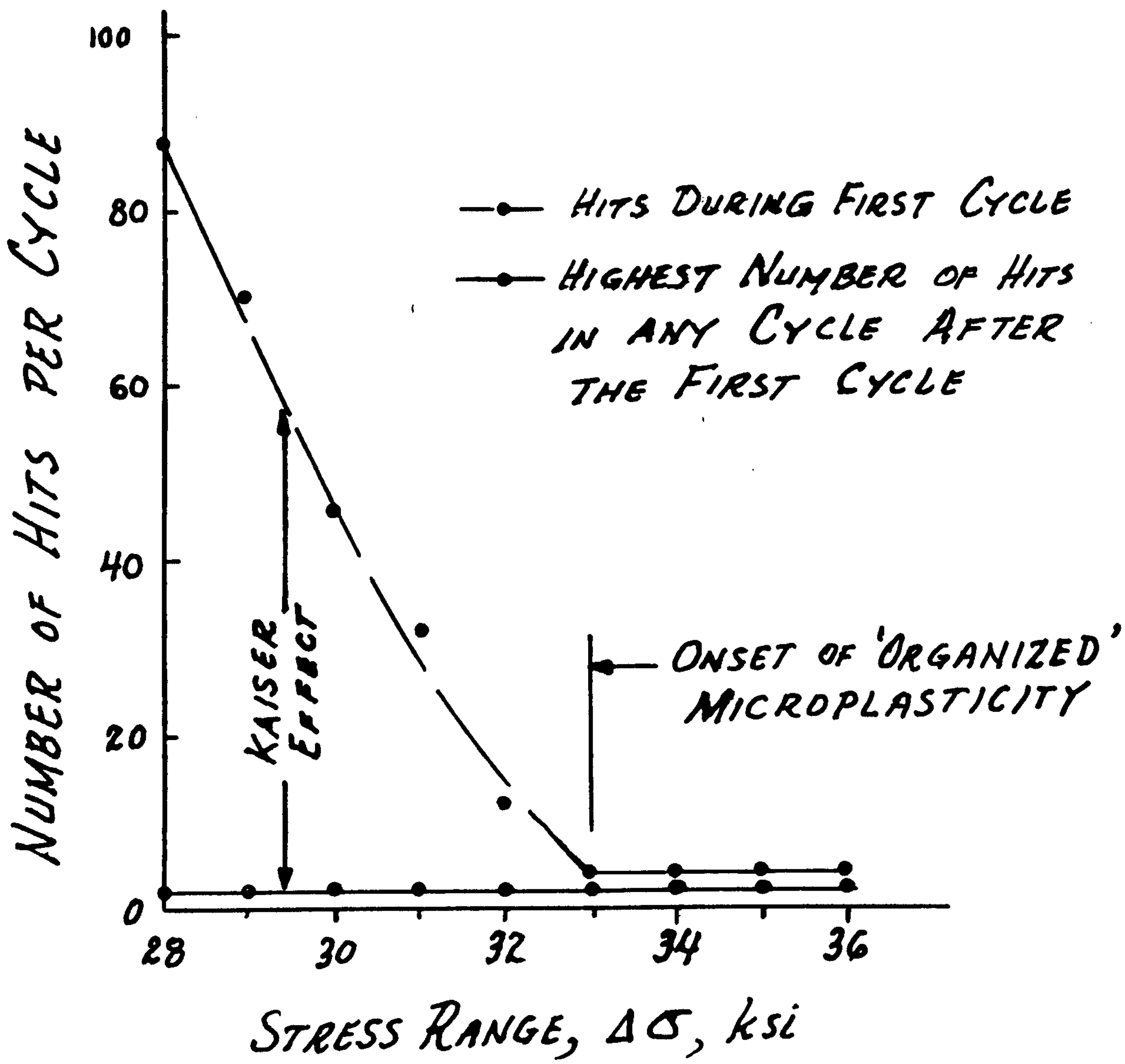

PRELIMINARY ACOUSTIC EMISSION RESULTS

(Adjusted Slow Loading)

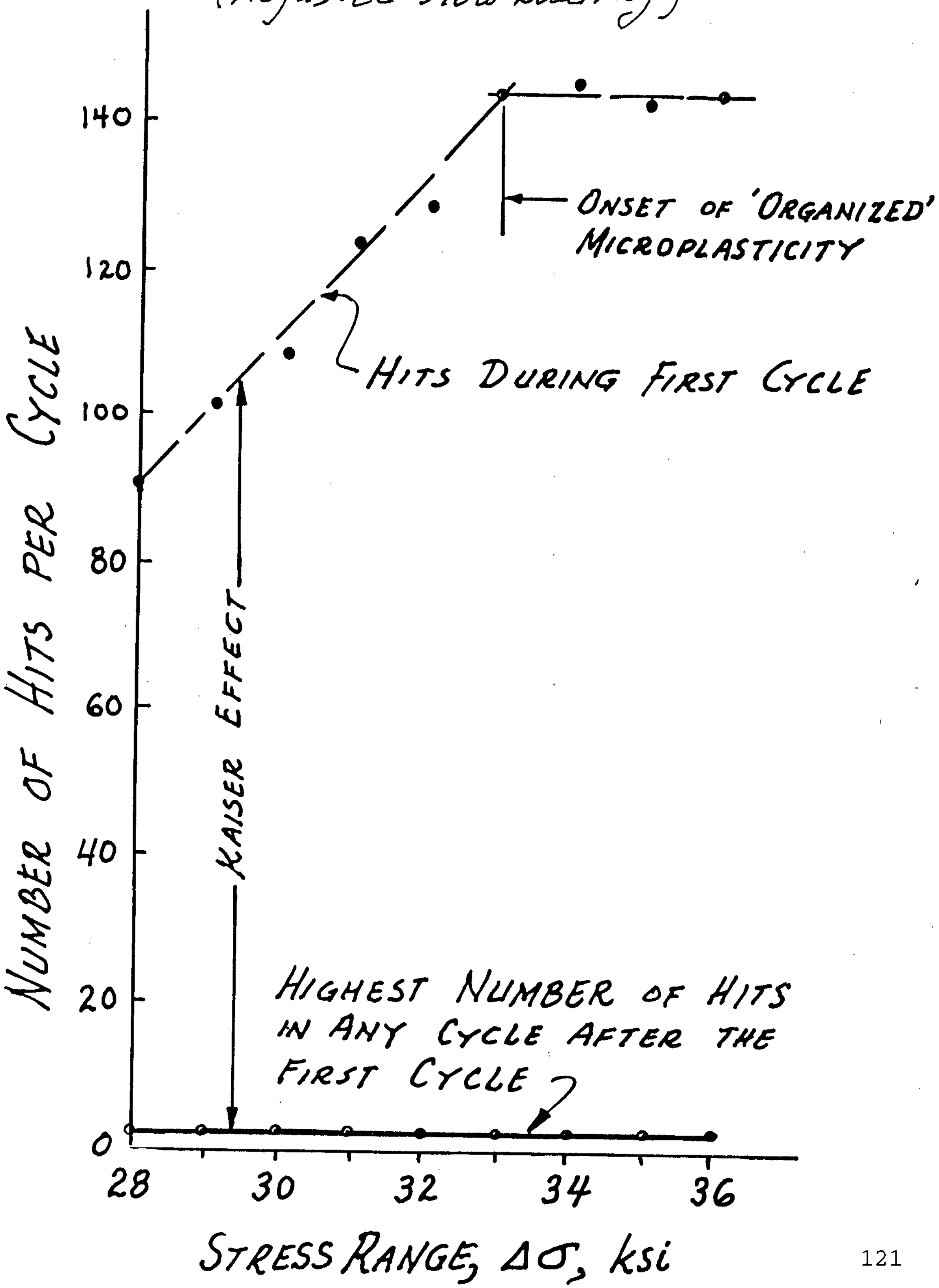

CONCLUSIONS

- BY SEPARATING HYSTERESIS INTO TWO COMPONENTS -- ONE DUE TO HEATING AND THE OTHER WHICH CAUSES DAMAGE -- IT IS POSSIBLE TO CONSTRUCT THE FULL S VS N_f DIAGRAM AS WELL AS THE GOODMAN-GERBER DIAGRAM WITH A MINIMUM OF TESTS.

- WHEN THE TOTAL ENERGY OF DAMAGE, U_d, IS A CONSTANT, THEN THE PALMGREN-MINER LAW FOR CUMULATIVE DAMAGE IS APPLICABLE. CONVERSELY, IF THE PALMGREN-MINER LAW IS FOUND TO BE VALID FROM THE DATA, THEN IT IS EVIDENT THAT THE TOTAL ENERGY OF DAMAGE, U_d, IS A CONSTANT.

- AE APPEARS PROMISING AS A MEANS TO DIAGNOSE THE ONSET OF MICROPLASTICITY 'ORGANIZATION.'

DIRECTIONS FOR FUTURE RESEARCH

1. Correlation of Acoustic Emission Data With Actual Metallurgical States Using SEM Observations
2. Observation of Fatigue Progression on a Micro-Mechanical Scale Using a Micro Tester in Conjunction With The TEM
3. Correlation of Hysteresis Data With Actual Metallurgical States Using SEM Observations
4. Correlation of Magnetic Field Evolution With Progression of Fatigue Process (in Cooperation With NRL)
5. Investigation of Inception of Microplasticity By Hysteresis Measurements With STM (In Cooperation With C. Teague of NIST)

REFERENCES

- Anon, 1978, "Fatigue and Microstructure", Paper presented at the 1978 ASM Materials Science Seminar, American Society for Metals, Metals Park, Ohio.

- Bannantine, J.A., Comer, J.J., and Handrock, J.L., 1990, "Fundamentals of Metal Fatigue Analysis", Prentice-Hall, Inc., Englewood Cliffs, New Jersey.

- Hertzberg, Richard W., 1989, "Deformation and Fracture Mechanics of Engineering Materials", Third Edition, John Wiley and Sons, New York, N.Y.

- Lemaitre, J. and Chaboche, J., 1990, "Mechanics of Solid Materials", Cambridge University Press, New York, N.Y.

- Parker, A.P., 1981, "The Mechanics of Fracture and Fatigue", E. and F.N. Spon, in association with Methuen, Inc., New York, N.Y.

- Puskar, A., and Golovin, S.A., 1985, "Fatigue in Materials: Cumulative Damage Processes", Elsevier Science Publishing Co., Inc., New York, N.Y.

- Sandor, B.I., 1972, "Fundamentals of Cyclic Stress and Strain", The University of Wisconsin Press, Madison, Wisconsin.

- Suresh, S., 1991, "Fatigue of Materials", Cambridge University Press, New York, N.Y.

TECHNICAL PRESENTATION

"The Microscopic Origin of Inelastic Behavior"

BY

Dr. Harold Weinstock

AFOSR

Bolling Air Force Base

OBJECTIVE:

Develop techniques using magnetometric methods for the study of deformation and corrosion.

APPROACH:

Use SQUID, with three orthogonal axes, to monitor magnetic fields changes associated with change in deformation and corrosion processes.

Design and construct non-magnetic load frame to isolate deformation induced magnetic field changes.

Scan specimen to study effects of specimen geometry and localized stress.

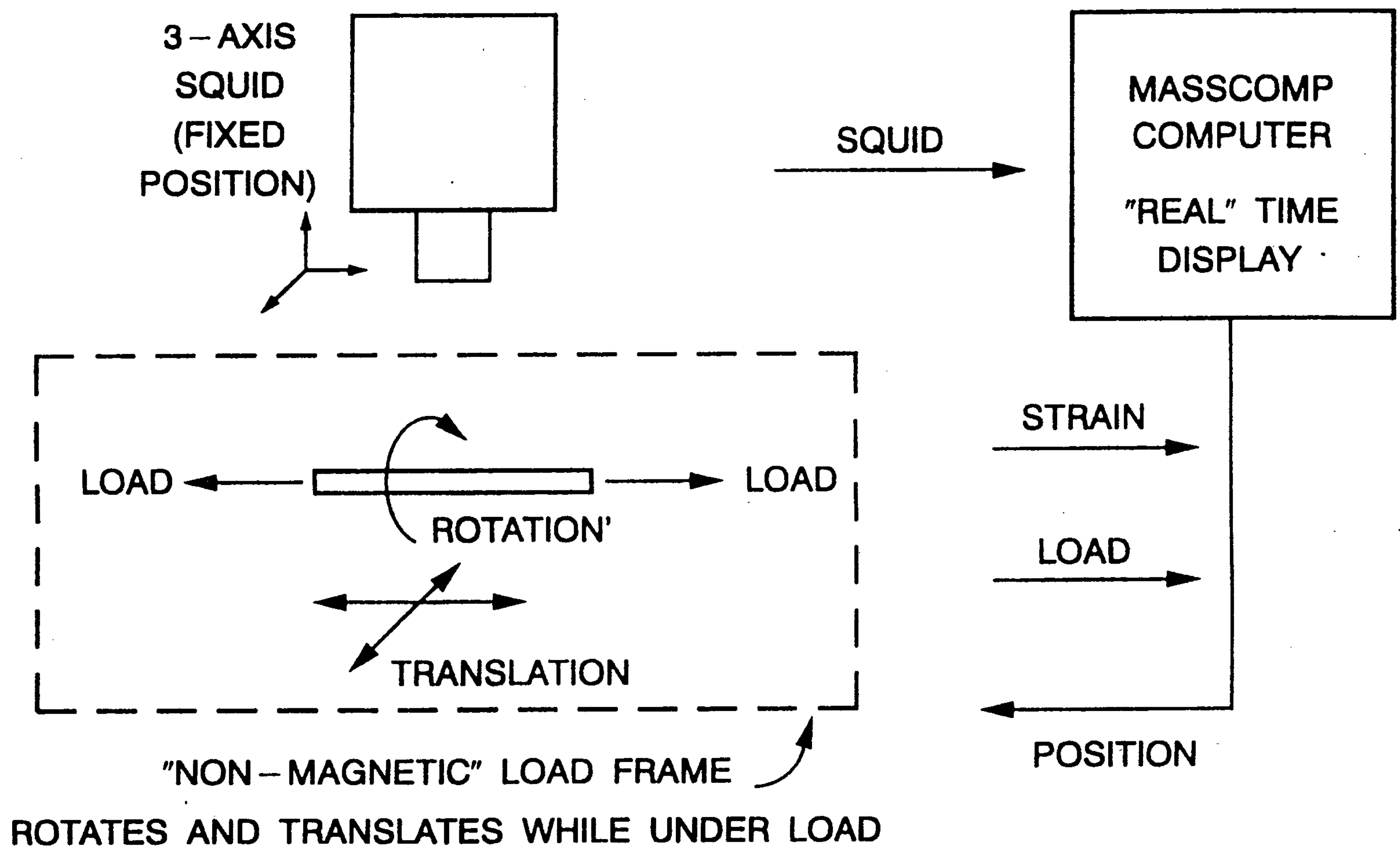

3-AXIS
SQUID
(FIXED
POSITION)
SQUID
MASSCOMP
COMPUTER
"REAL" TIME
DISPLAY
LOAD
LOAD
ROTATION'
TRANSLATION
STRAIN
LOAD
POSITION
"NON-MAGNETIC" LOAD FRAME
ROTATES AND TRANSLATES WHILE UNDER LOAD

ORIGIN OF IMPERFECTIONS
INITIATION OF ATOMIC DISPLACEMENT

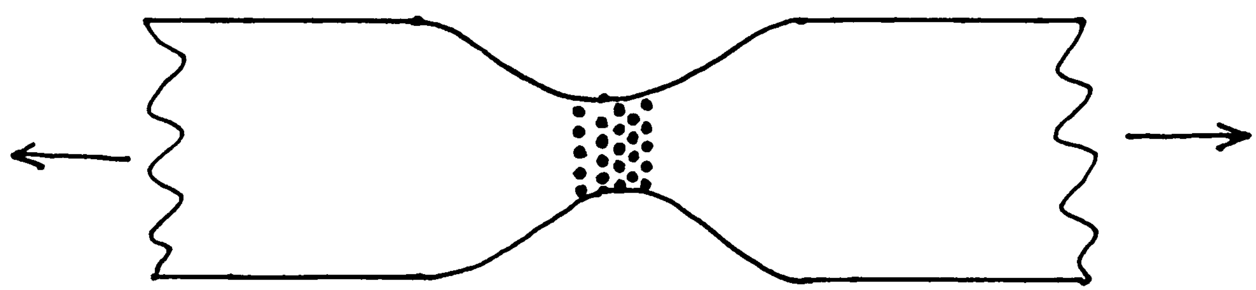

VIEW SURFACE WITH SPECIAL STM
E. C. TEAGUE, NIST
M^3 = MOLECULAR MEASURING MACHINE

Schematic of Experimental Arrangement

Magnetic field-free environment
Magnetic field coil in transverse direction
SQUID magnetic gradiometer

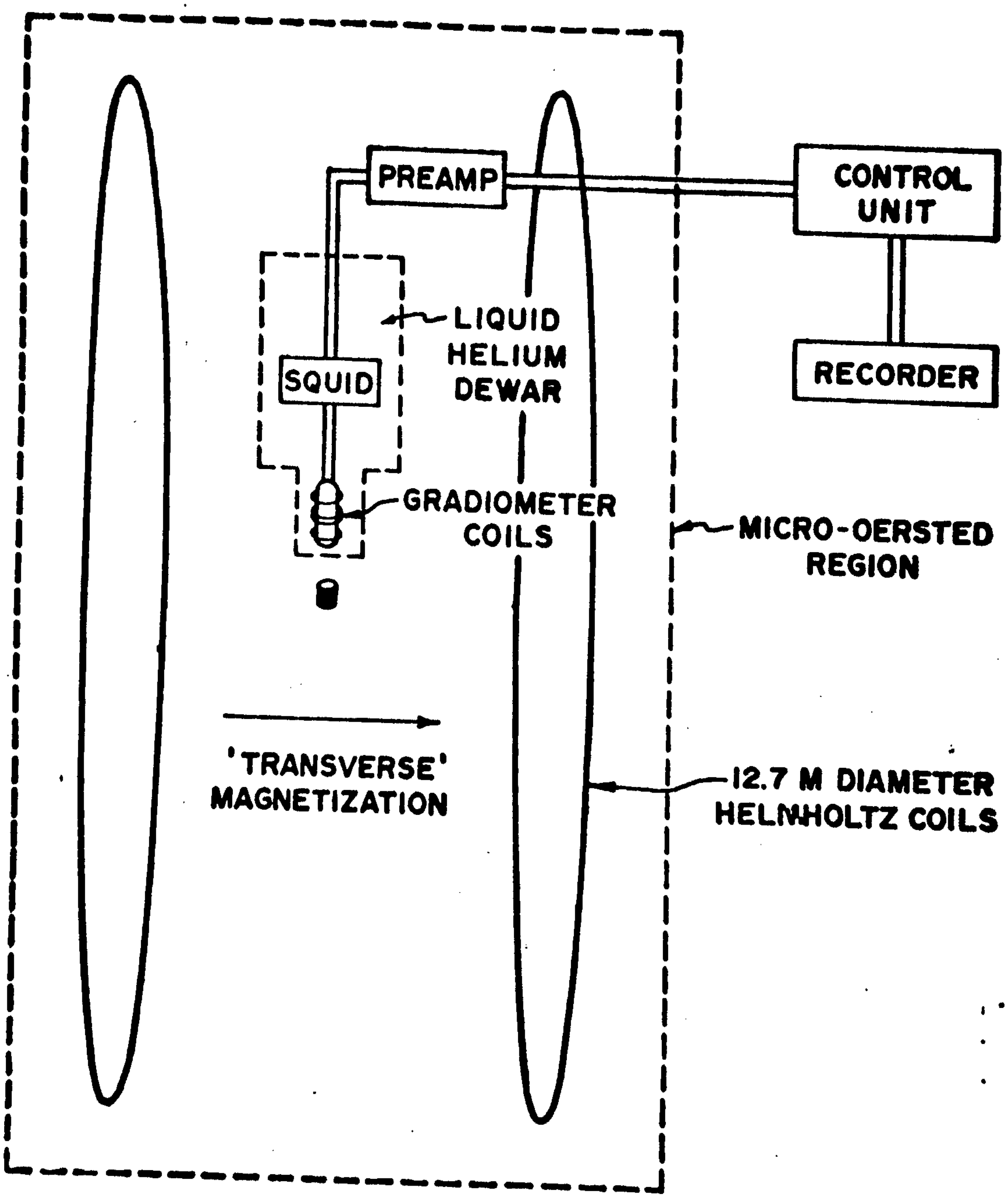

Stress + Magnetic Response to Strain for a Steel Bar

REVERSIBLE REGIME

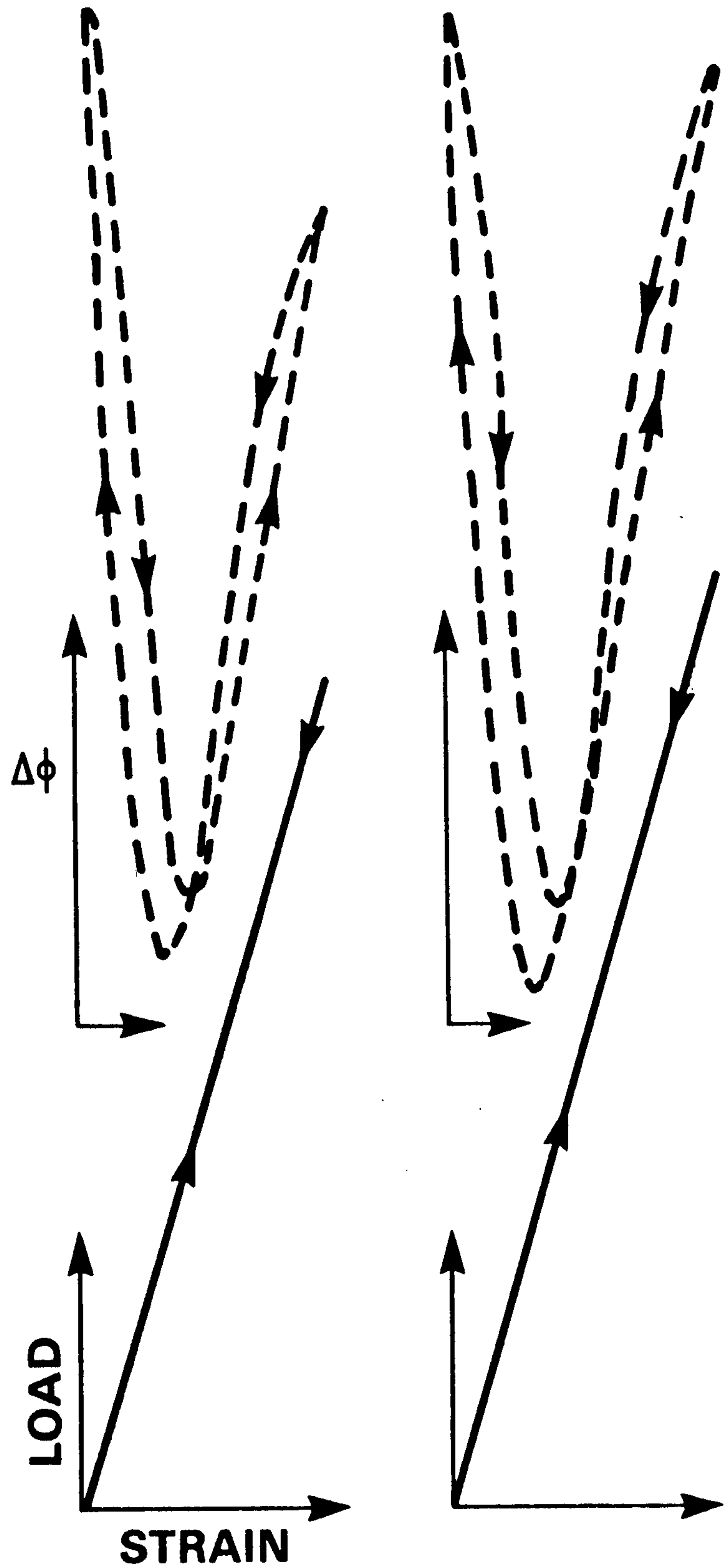

Stress and Magnetic Response as a Function of Strain for a Steel Bar

Feb 22 14:42:22 1991		Testid	Ins Type	Location	Dig_Rate (Hz)	Key
D633	Units Conversion	squid13		load *20	10	
D635	Scalar Multiply	squid13		bz *1	10	

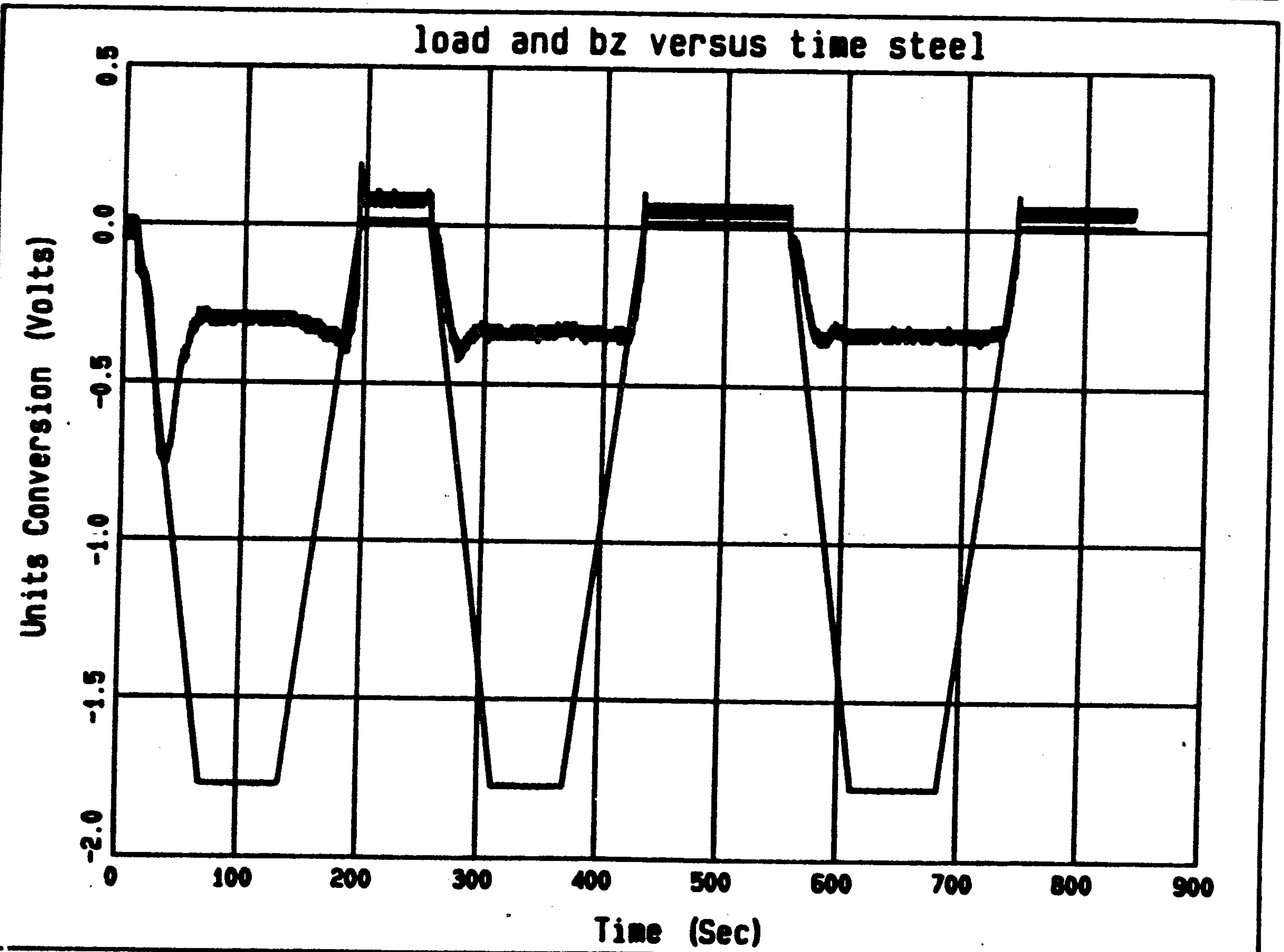

Stress and Magnetic Response to Strain for a Steel Bar

PLASTIC FLOW REGIME

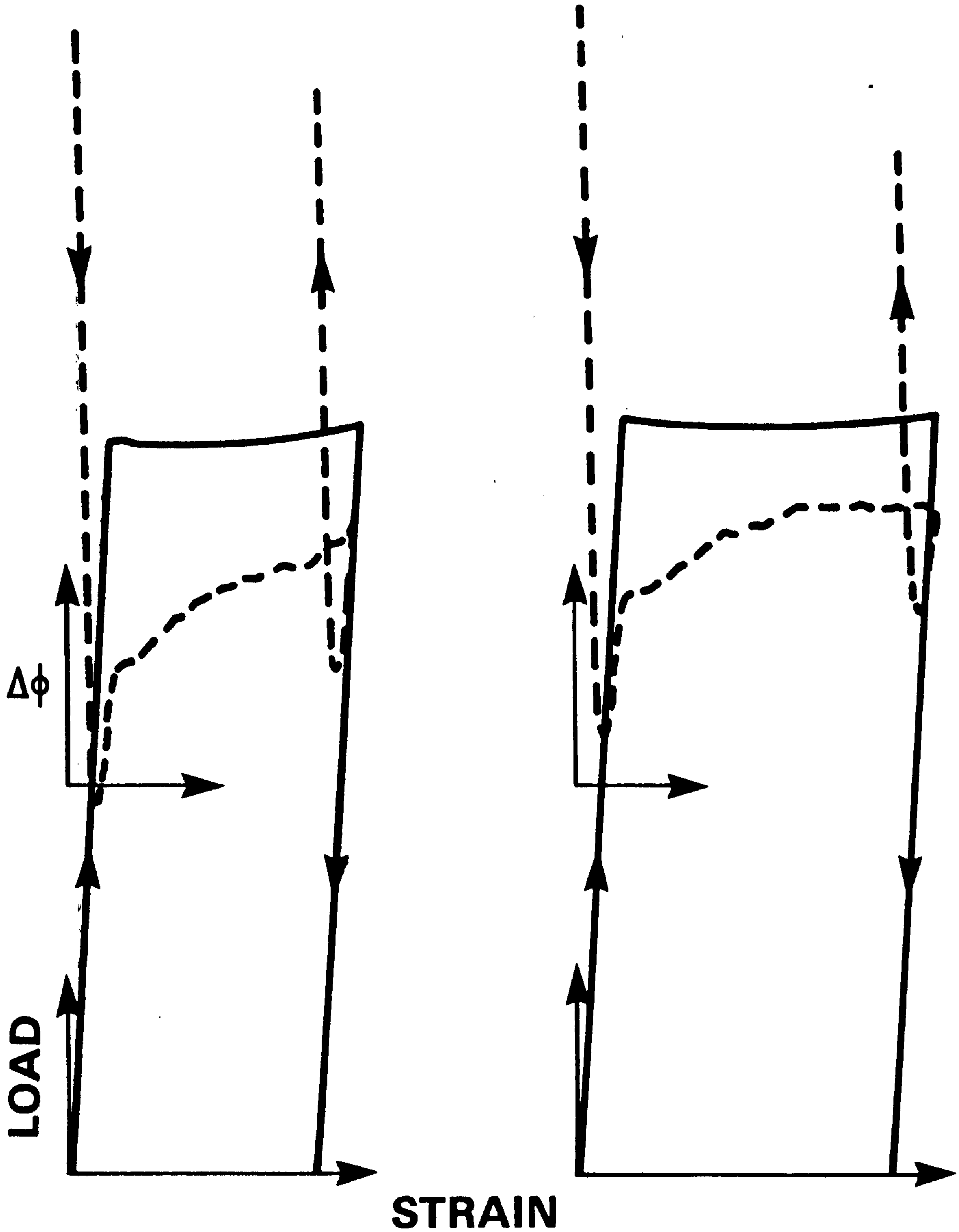

Acoustic Emission vs. Stress in NbTi

NbTi

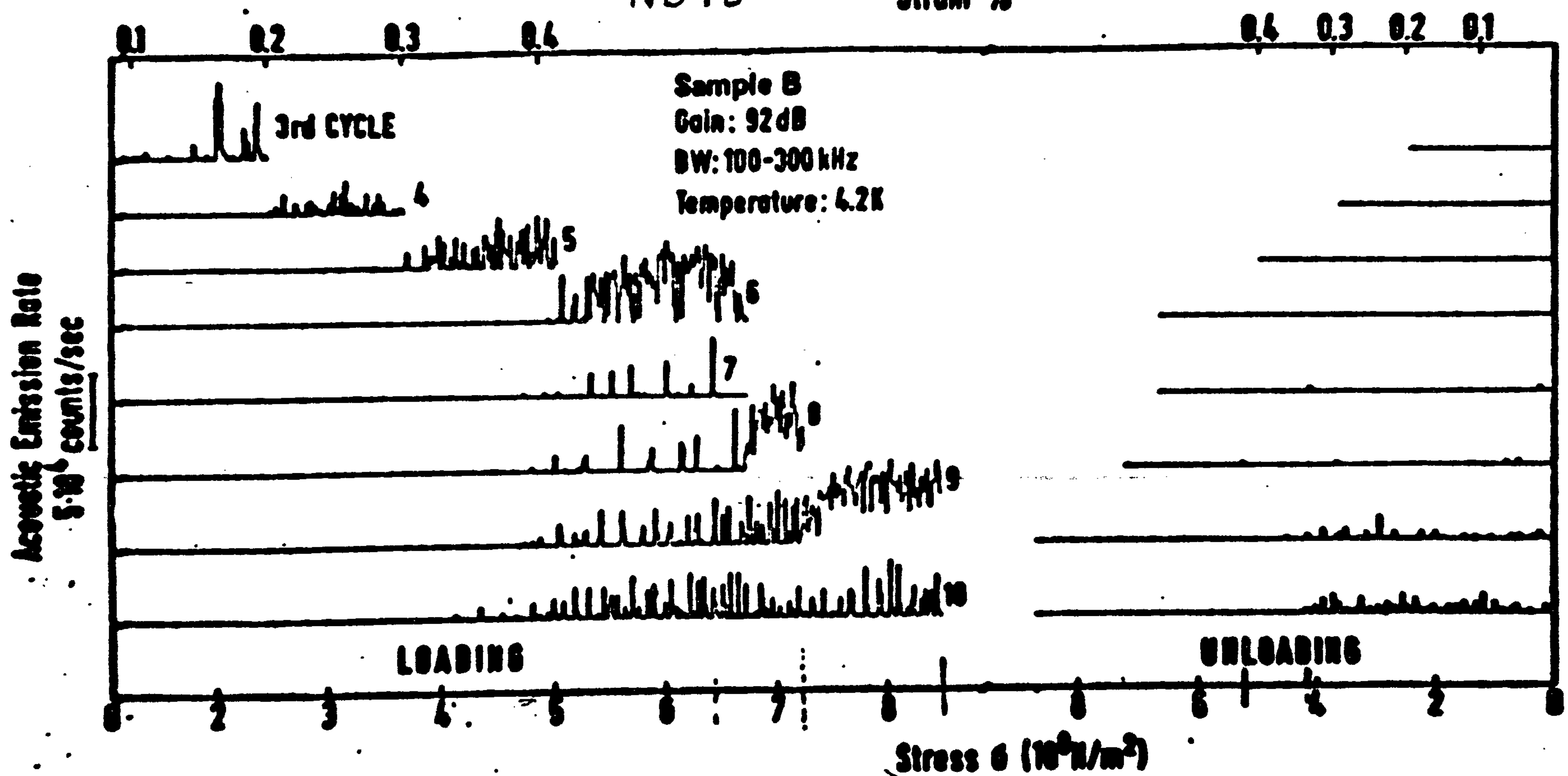

Pasztor + Schmidt J.A.P. 49, 886 (1978).

FERROMAGNETIC SAMPLES IN AN APPLIED FIELD
BARKHAUSEN NOISE

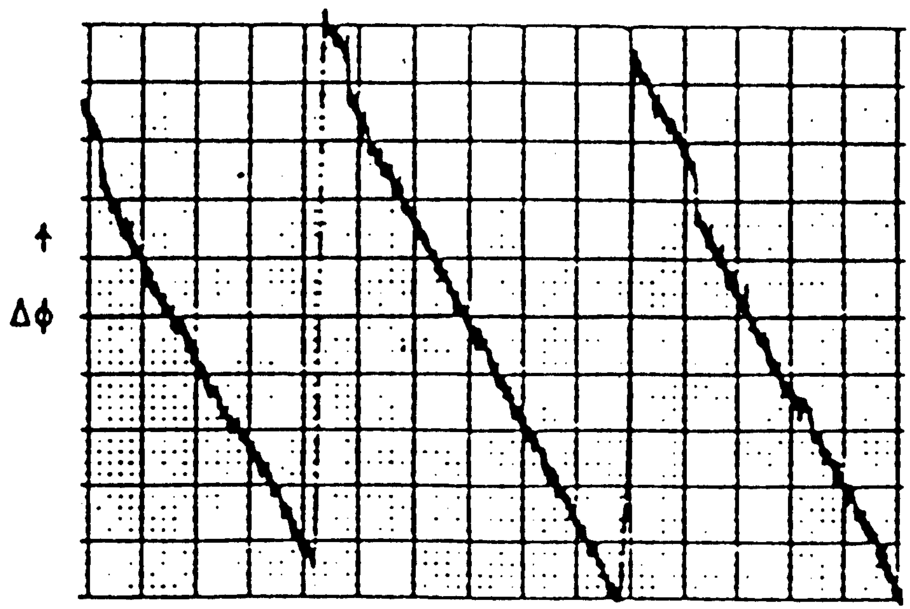

- Polycrystaline iron samples
- Field ramped (Increasing from right to left)
- Appearance of Barkhausen jumps corresponds to the transition from reversible to irreversible magnetization, i.e. the onset of hysteresis.
- Repeated field cycles at threshold remove jumps and extend the range of reversible magnetization.

"Threshold of Barkhausen emission and onset of hysteresis in iron," H. Weinstock, T. Erber, and M. Nisenoff," *Physical Review B*, **31** 1535–1553 (1985).